STATISTICAL ANALYSIS OF MAPPED SPATIAL POINT PATTERNS

By

SANI IBRAHIM DOGUWA

A thesis submitted to satisfy the requirements of the degree of Doctor of Philosophy (Ph.D) in the Department of Mathematics, University of Essex.

May, 1988

To

My parents :

HADIZA ABUBAKAR SULAIMAN

SULAIMAN IBRAHIM DANTEBUR,

Uncle and Aunt:

NUHU KAWU BAKINKWADO,

ADAMA INNA BAKINKWADO.

ACKNOWLEDGEMENTS

I would like to express my profound gratitude to my supervisor, Dr Graham J. G. Upton for suggesting an original idea and for his invaluable guidance and help in the course of this study, without which this work would not have been possible.

I would like to extend my gratitude to Mr Michael J. Fryer, my temporary supervisor for the encouragement accorded me in the course of this study, and to Dr David Fremlin for his invaluable advice on some aspects of measure theory.

I owe a special debt of thanks to the Commonwealth Scholarship Commission in the United Kingdom for awarding me the Commonwealth Scholarship to study at Essex University. I am also very grateful to the Royal Commission for the Exhibition of 1851 for awarding me the Rutherford Foundation Scholarship, even though I was unable to take up the offer. I also wish to thank, Ahmadu Bello University, Zaria, Nigeria for giving me a study fellowship and for releasing me during the period of this study.

I wish to express my sincere gratitude to my wife, Habiba who was a constant source of encouragement throughout my study and to my son, Fahd who missed me a lot during the course of this study.

Finally, I am grateful to Mrs. Sandra Davies for her most efficient secretarial assistance in the preparation of some aspects of this thesis.

ABSTRACT

The object of this study is to examine the various methods which deal with tests of randomness for univariate mapped point patterns. Some of these methods are extended to multitype patterns. Particular attention is paid to the bounded nature of the pattern being studied, and the complications that thereby arise in the implementation of the various methods.

Edge corrections are reported for the mean and variance of the average distance between a sampling point and the nearest object, X, for the case of a regular grid of sampling points. Using these corrections the point-object analogue of the Clark-Evans statistic is found to be a powerful detector of departures from randomness in the clustered direction.

A new edge-corrected estimator is proposed for the second moment cumulative function K(t), introduced by Ripley for the study of spatial point processes. This new estimator is compared by simulation methods with existing edge-corrected estimators in the context of L(t) function which is used to study point patterns. The result of the simulation study suggests that the new estimator provides almost unbiased estimate of L(t) and has a smaller mean squared error than its predecessors.

A new method is proposed for estimating G(w) and F(x), the distribution functions of the object-to-object and point-to-object nearest neighbour distances respectively. The new method makes more complete use of the information available and has a smaller mean squared error than the existing alternatives. The method appears equally effective with random, clustered and regular patterns.

Programs for statistical analysis were written in FORTRAN and run on a DEC system - 1.0/99 computer of the University of Essex. The graphs were plotted on the versatec-plotter of the University using SIMPLE PLOT MARK2.

Contents

		Page
1.0	INTRODUCTION	1
1.1	Spatial point patterns	1
1.2	Objective of statistical analysis	6
1.3	The Poisson process	7
1.4	Some clustering models	8
1.5	Some inhibition models	9
1.6	Some soft core models	11
1.7	The selection of the study region D	14
1.8	Monte Carlo tests	15
2.0	THE AVERAGE NEAREST NEIGHBOUR METHODS IN CIRCULAR SAMPLING WINDOWS	21
2.1	Introduction	21
2.2	Clark and Evans Statistic CE	22
2.2.1	Edge corrections for CE	27
2.3	Analogue of the CE Statistic: M	28
2.4	Edge corrections for M	30
2.5	Examples	38
3.0	THE AVERAGE NEAREST NEIGHBOUR METHODS IN SQUARE AND RECTANGULAR WINDOWS	43
3.1	Introduction	43
3.2	Edge corrections for M	43
3.3	Analysis of Japanese black pine saplings, Biological cells and redwood seedlings	54
3.4	Alternative statistics to CE and M	57

		Page
3.4.1	Quadrat count index of dispersion	57
3.4.2	Quick tests using small distances	60
3.4.3	Squared nearest neighbour distances	62
3.5	Power study	66
4.0	THE SECOND ORDER METHODS	71
4.1	Introduction	71
4.2	The estimators of K(t)	73
4.2.1	The naive estimator	73
4.2.2	Border edge correction	75
4.2.3	Ripley's estimator	76
4.2.4	Ohser's estimator	78
4.2.5	Ohser and Stoyan's estimator	79
4.2.6	Vere-Jones's estimator	81
4.2.7	The new estimator	82
4.3	Theoretical values of K(t)	84
4.4	Error Analysis - bias and mse of the estimators	89
4.5	Graphical analysis	95
4.5.1	Analysis of the two alternative patterns	98
4.5.2	Analysis of Waterstriders data	98
4.5.3	Analysis of the cellular process	100
4.6	The second order neighbourhood function $S_i(t)$	102
4.7	Comparative study	105
4.7.1	Tests based on the $\hat{K}(t)$ function	106
4.7.2	Tests based on the $\hat{S_i}(t)$ function	106
4.7.3	Jolivet, Liebetrau and Rothman's statistics	106
4.7.4	Hermans, Rasson and Weverbergh's statistic	107
5.0	'REFINED' NEAREST NEIGHBOUR METHODS	110
5.1	Introduction	110

		Page
5.2	The existing estimators of G(t)	112
5.2.1	Diggle's estimator	113
5.2.2	Hanisch's estimator	113
5.2.3	The new estimator of G(t)	114
5.3	Estimators of F(t)	117
5.3.1	Ripley's estimator	117
5.3.2	Hanisch's analogue	118
5.3.3	The new estimator	118
5.4	G(t) and F(t) for a Poisson process	119
5.5	G(t) and F(t) for a clustered process	123
5.6	G(t) and F(t) for a regular process	131
5.7	Graphical analysis	136
5.7.1	Analysis of Redwood seedlings	138
5.7.2	Analysis of Waterstriders data	140
5.7.3	Analysis of the cellular process	140
6.0	METHOD FOR ANALYSING MULTITYPE SPATIAL POINT PATTERNS ..	143
6.1	Introduction	143
6.2	Multitype spatial point processes	144
6.2.1	Processes displaying repulsion	144
6.2.2	Processes displaying attraction	146
6.3	Conditional Monte Carlo tests	149
6.4	Quadrat counts method	150
6.5	The average nearest neighbour distance method	154
6.6	'Refined' nearest neighbour method	157
6.6.1	Estimators of $G_{ij}(t)$	159
6.6.2	Estimators of $F_{oj}(t)$	160
6.6.3	Estimators of $F_{o}(t)$	161
6.6.4	Graphical analysis	162
6.7	The second order methods	167

Page

6.7.1 The estimators of $K_{ij}(t)$ and $K_{ji}(t)$ 168

6.7.2 Graphical analysis 172

7.0 SUMMARY AND CONCLUSIONS 173

REFERENCES 177

CHAPTER I

Introduction

1.1 Spatial point patterns

A spatial point pattern is a configuration of objects $\mathcal{U} = \{u_i \in D,\ i = 1, 2, \ldots, n\}$, for some designated planar region D. These types of data sets occur in a suprisingly wide variety of scientific disciplines. Examples include studies of the structure of biological cells, the evolution of galaxies or the settlement patterns revealed by archaeological excavations. Furthermore, Ripley(1981) writes:

> "Foresters and Agricuturalists need to investigate plant competition and account for soil variations in their experiments. _ _ _ _ _ _. Rocks, metals, and tissue and blood cells are all studied at a microscopic level"

ABDULLAHI ARABIYAM LIBRARY AHMADU BELLO UNIVERSITY ZARIA, NIGERIA.

However, the common features of the objects studied are that the individual observations can be located as points. Of course none of these is actually a point, but in each case the sizes of the objects are so small compared with the distances between them that their physical size can sometimes be ignored. This spatial attribute is, in many cases, a highly revealing piece of information concerning the causal processes and mechanisms operating amongst the data.

We refer to these locations as objects so as to distinguish them from sampling points in the region of interest. We shall also assume throughout that our raw data are a map, or a list of coordinates, giving the locations of all objects within a sampling window D, typically a rectangle of sides $a < b$ perimeter P, area A and diagonal d; although most of the ideas discussed extend at least in principle to other spaces.

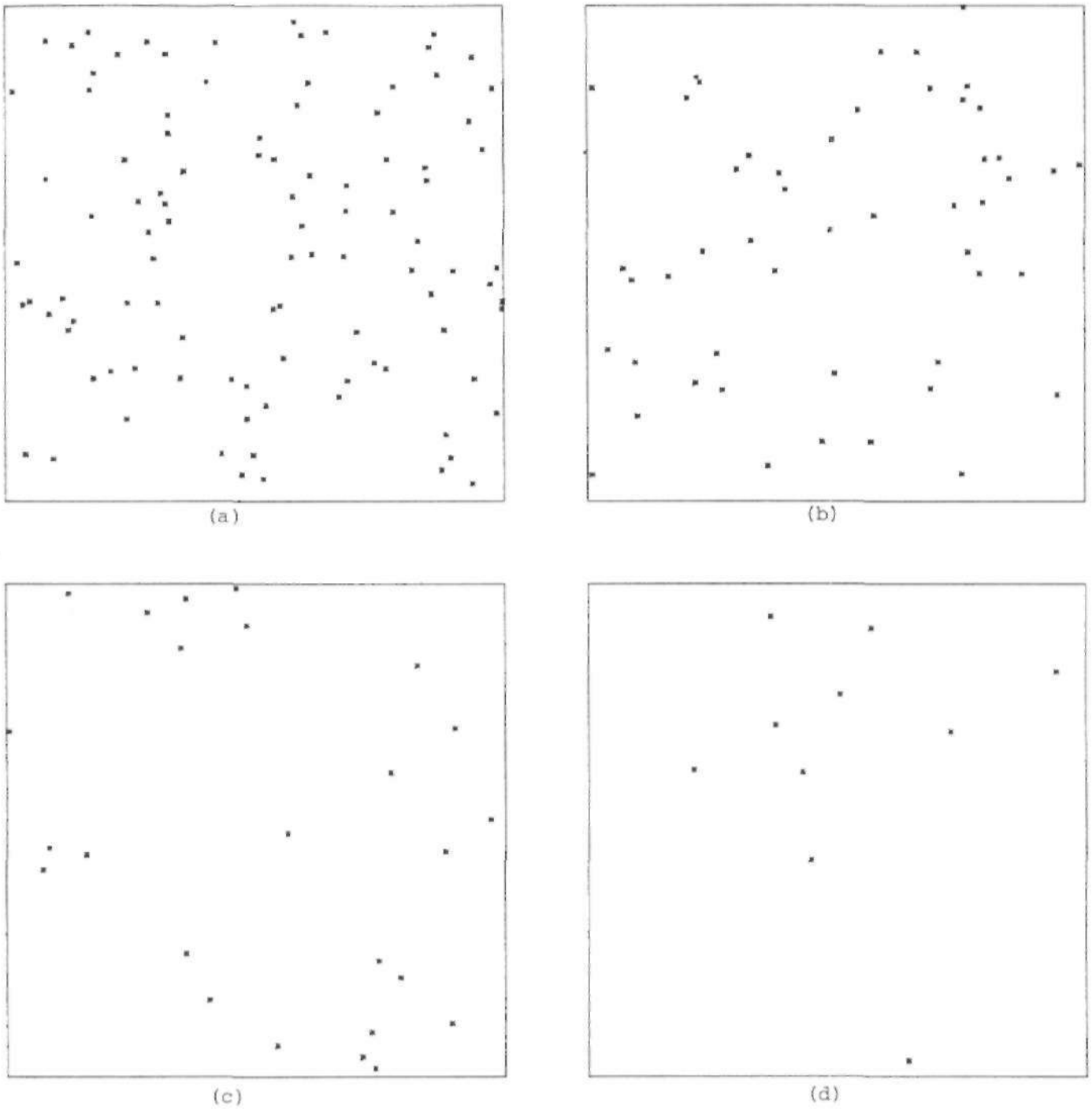


FIGURE 1.1 : Realization of a Poisson process, in a unit square window, with (a) n = 100, (b) n = 50, (c) n = 25 and (d) n = 10. [See section 1.3]

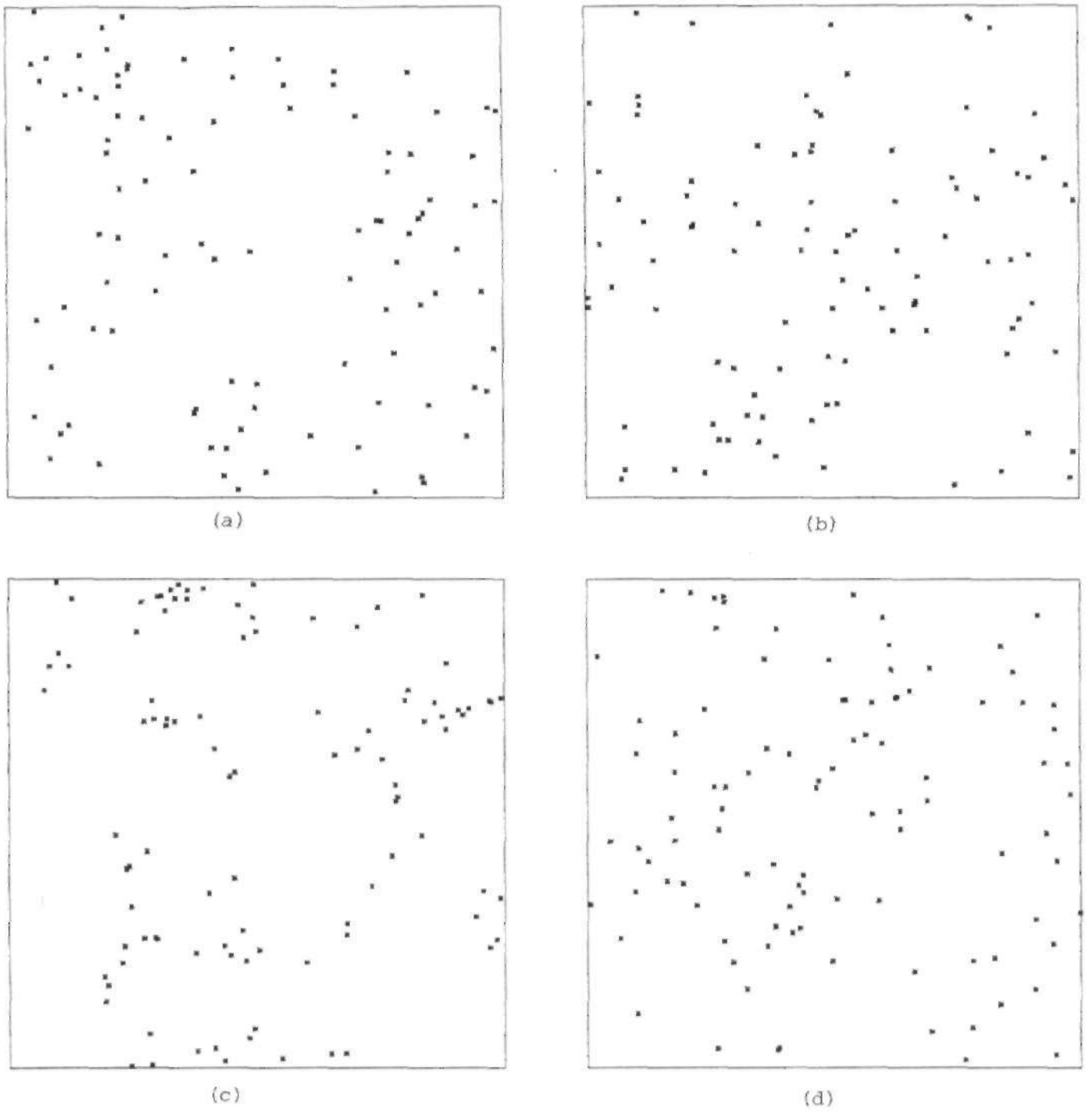


FIGURE 1.2 : Simulations of 100 objects from (a) cluster process with 25 parents and cluster radius 0.05, (b) cluster process with 25 parents and cluster radius 0.10, (c) cluster process with 25 parents and dispersion parameter $\sigma = 0.05$, (d) cluster process with 25 parents and dispersion parameters $\sigma = 0.10$. [See section 1.4]

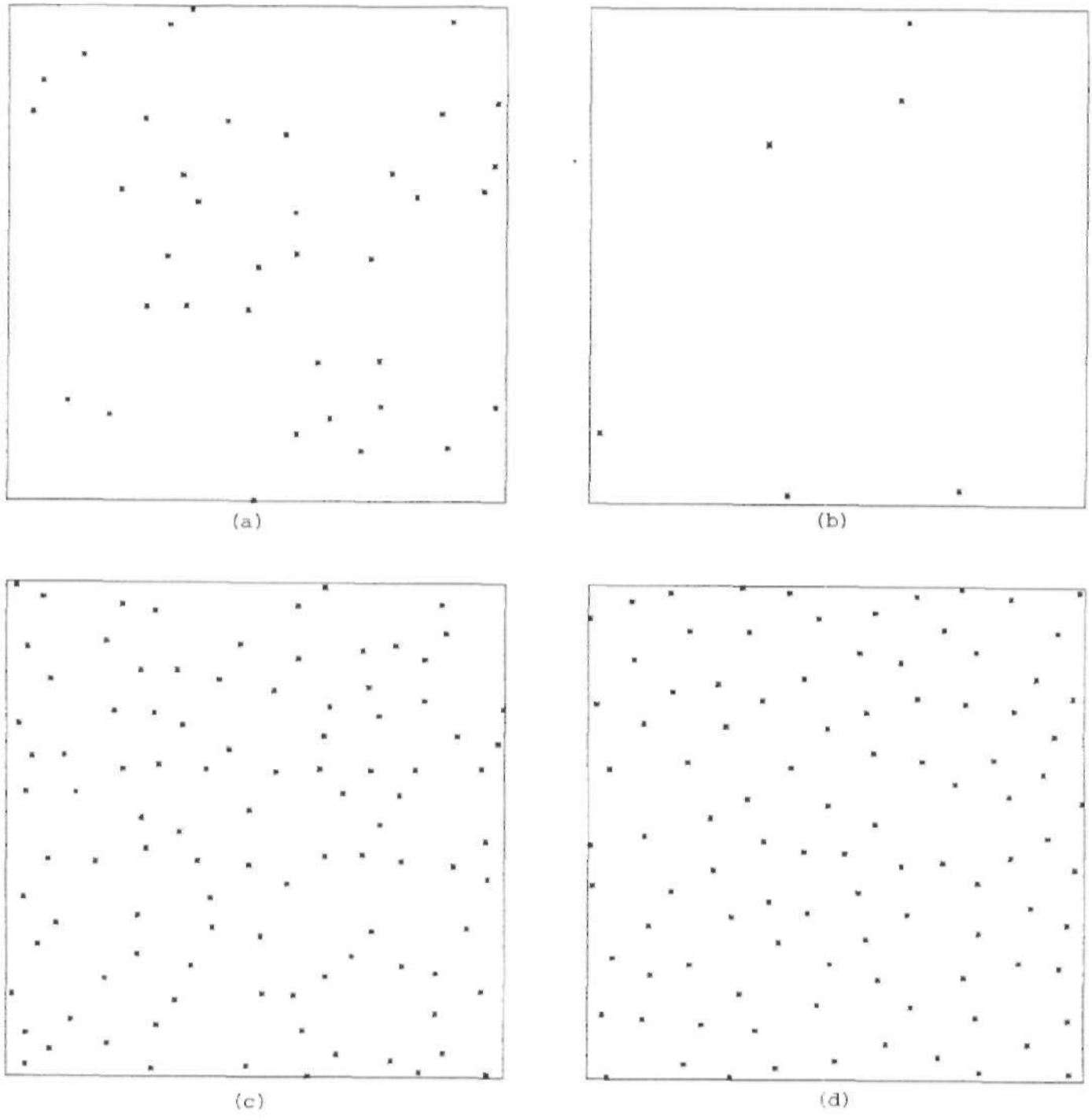


FIGURE 1.3 : Partial realization of (a) Matern static process with $\sigma = 0.05$, (b) Matern static process with $\sigma = 0.10$, (c) simple sequential inhibition process with $\tau = 0.25$, $n = 100$, (d) simple sequential inhibition process with $\tau = 0.50$, $n = 100$. All realizations are in the unit square. [See section 1.5]

Figures 1.1 to 1.3 illustrate a broad classification of point patterns. All are computer simulations of the processes detailed in the caption. Figure 1.1 is a realisation of a Poisson process (or Poisson forest). Conditional on the number of objects n in D, the objects are independently and uniformly distributed. By independence, we mean that there is no interaction between the objects in D.

Figures 1.2a and b are realisations of a cluster process with an average of 25 clusters and cluster radius 0.05 and 0.10 respectively. Figures 1.2c and d are realisations of a cluster process with an average of 25 clusters and with dispersion paramaters 0.05 and 0.10 respectively.

Figures 1.3a to d represent realisations of processes with inhibition between the objects, which we will call regular patterns.

Diggle(1983) noted that the nature of the pattern generated may be affected by the physical scale on which the process is observed. This is because, at a sufficiently large scale, most natural environments exhibit heterogeneity, which may tend to produce aggregated patterns. However, at a small scale, environmental variation will be less pronounced and the major determinant of pattern may be the nature of the interactions amongst the objects themselves.

As regards the classification of patterns, Diggle(1983) writes:

> "Our classification of pattern as regular, random or clustered is therefore an over simplification, but a useful one especially at the early stage of analysis. At a later stage however, this simplistic approach maybe abandoned in favour of a more detailed and essentially multidimensional description which can be obtained either by identifying different scales of pattern or by formulating an explicit model of the underlying process."

1.2 Objective of Statistical Analysis

Most people have been using maps and so have been studying spatial point patterns for years, yet the need to reduce such information to numbers is rather recent. Ripley(1981) noted that "the human eye and brain form a marvellous mechanism with which to analyze and recognize patterns, yet they are subjective, likely to tire and so to err."

Spatial data analysis of mapped point patterns includes the reduction of such patterns to a few clear and useful summaries. These summaries can then be compared with what might be expected from theories of how the pattern might have originated and developed.

In most cases, we may have only a single observation of a particular pattern, rather than the many replications of measurements found in most experimental sciences. In order to obtain some idea of the variability of such data, we have to make some assumptions of stationarity of the underlying mechanism that generated the pattern. However Ripley(1981) noted that such an assumption has often been called to question, particularly in the geographic literature. However the validity of such an assumption may entirely depend on the type of questions being asked. For example, if we are looking at the population density of an area, we may wish to know whether we need to consider the topography, which might suggest non-stationarity, to explain the observed variation in the population density of that area.

Patterns that do not vary in a systematic way from one place to another are said to be homogeneous (opposite heterogeneous). These patterns can sometimes exhibit preferred directions in which case they are called anisotropic (opposite isotropic). We shall assume that the data have been divided into sufficiently small units, to permit us to make the assumption of homogeneity or isotropy or both.

The books by Diggle (1983), Ripley (1981) and Upton and Fingleton (1985) among others, have put together the abundance of recent research in many fields into the analysis of spatial point patterns.

1.3 The Poisson process

The homogeneous planar Poisson process, or Poisson forest, is the cornerstone on which the theory of the spatial point process is built. The Poisson process is conveniently defined by the following properties:

(i) For some $\lambda > 0$, and any finite planar region D of area A, the number of objects in D has a Poisson distribution with mean λA.

(ii) Given the number n of objects in D, the n objects form an independent random sample from the uniform distribution in D.

The parameter λ is the intensity of the process, defined as the mean number of objects per unit area. Diggle(1983) shows that the self consistency of (i) and (ii) imply that the number of objects in any two disjoint regions are independent.

The Poisson process represents an idealized standard which, if strictly unattainable in practice, may nevertheless be tenable as a convenient first approximation. Most analyses begin with a test of a Poisson process. A pattern for which the Poisson process is not rejected scarcely merits any further formal statistical analysis. Furthermore, the Poisson process acts as a dividing hypothesis to distinguish between patterns which are broadly classifiable as regular or clustered.

Figure 1.1 a to d show partial realizations of the Poisson forest in a unit square window with parameters λ = 100, 50, 25, and 10 respectively.

1.4 Some clustering models.

The cluster models represent a move from the Poisson process towards a pattern having a more uneven intensity of objects with local peak at clusters. The most commonly used cluster models are the Poisson cluster process models of Neyman and Scott (1952), Warren (1971) and Matern (1971). These models incorporate an explicit form of spatial clustering, and as such provide a more satisfactory basis for the modelling of aggregated mapped point patterns. The general Poisson cluster process model consists of:

(i) parent objects located at random, forming a Poisson process with intensity ρ .

(ii) a number of offspring for each parent, these being independent observations from some specified distribution (e.g Poisson) and

(iii) the locations of each offspring relative to the position of its parent being independent observations from some specified distribution (e.g bivariate normal).

The third component simply specifies where the offspring are likely to be in relation to their parents. Relatively simple cases occur when the offspring are known to be at a fixed distance from the parent, and when the offspring are distributed at random over the region immediately surrounding the parents location.

Figures 1.2a and b show simulated realizations, in a unit square, of a type of Poisson cluster process known as a Matern cluster process. The simulations arise by generating a Poisson number of cluster centers, mean $\rho = 25$, then assigning the daughter objects to a cluster at random and distributing them uniformly within a disc, radius $R = 0.05$ ($R = 0.10$ for Fig 1b), centred on the parent object. The region D is considered as a torus by identifying opposite edges. Note that the smaller

the values of (ρ ,R) the more aggregated the pattern.

Figure 1.2c and d show different realizations of another Poisson cluster process for which the numbers of offspring per parent is a random variable with mean μ , the spatial distribution of each offspring about its parent is symmetric radial normal with dispersion parameters $\sigma = 0.05$, and $\sigma = 0.10$ respectively, and the parents are retained in the final pattern. To condition this process to produce $n = 100$ objects in D, we first distribute $\rho = 25$ parents completely at random in D, then assign the 75 offspring randomly among the parent objects. Finally, the position of each offspring relative to its parent is determined by an independent realisation from the symmetric radial normal, with the region D converted into a torus to avoid edge-distortion in the simulated pattern. The apparent redundant specification of μ is implicit in the equation,

$$\mu = \begin{cases} 3 & \text{if parents are retained} \\ 4 & \text{if parents are not retained} \end{cases} \qquad (1.1)$$

1.5 Some inhibition models.

We shall consider modelling regular patterns that arise from natural causes. Two natural mechanisms suggest themselves, one being static and the other dynamic. We first consider the static mechanism. Upton and Fingleton (1985) give the following example:

> "Imagine a flower bed in which have been sprinkled at random, the seeds of some choice annual flower. The flower bed is kept free of weeds, the seeds germinate, and the small plants begin to grow. However, quite apart from the effects of genetic variation, the plants do not grow equally well. Some plants quickly become sturdy bearers of masses of flowers while others languish, the difference being due to the differing amounts of inter-plant competition."

Matern (1960) suggested that this type of situation could be modelled by

first generating a Poisson forest of intensity ρ and then eliminating all pairs of plants that are found to be less than a distance σ apart. The quantity σ is simply the diameter of the circle of influence of a mature plant. Examples of such patterns are given in Figure 1.3 a and b. Figure 1.3a is a partial realisation of the Matern static process in which a Poisson forest of intensity $\rho = 100$ is generated in a unit square and then all pairs of objects that are within $\sigma = 0.05$ units of each other are deleted from the pattern. Similarly Figure 1.3b is another realization, with pairs removed from the Poisson forest of intensity $\rho = 100$, if they are within $\sigma = 0.1$ units of each other.

For the dynamic regular pattern Upton and Fingleton (1985) write:

> "Suppose a number of migrant birds arrive one after another to a nesting site in springtime. Each bird in turn selects its nesting site from which it will repulse any other rival bird. The territories so claimed form invisible regions about the central nesting sites; with these nesting sites having been established sequentially rather than simultaneously."

Matern (1960) varied his static model by suggesting that a Poisson forest be generated sequentially, with objects being discarded if they lie within a distance σ of any previously generated object. Diggle et al (1976) have suggested what appears to be a more natural variation to this procedure wherein objects are only discarded if they lie within a distance σ of any retained object. They call this process the simple sequential inhibition and it is parameterised most naturally by its packing intensity,

$$\tau = \rho\pi\sigma^2 / 4 \qquad (1.2)$$

Thus τ is the proportion of the plane covered by non-overlapping circles of diameter σ, or the expected proportion of coverage for a finite region D, and ρ is the intensity of the process.

Figure 1.3c and d show partial realisations of this process in a unit square window with $\rho = 100$ and $\tau = 0.25$ and $\tau = 0.50$ respectively. Note that for ρ fixed, the pattern becomes more regular as the parameter τ increases.

1.6 Some soft-core models

Many regular patterns require a more flexible description than can be provided by a strict simple inhibition rule. For example, competitive interactions between plants may make it unlikely, but not impossible, that two individual plants can survive in close proximity to each other. In contrast to simple inhibition models, here the interaction between plants is such that the inhibitory forces decrease continously with increasing inter-plant distances. This provides a motivation for the class of Markov point processes introduced by Ripley and Kelly (1977). These point processes have a finite number of objects in a bounded region D. Interactions between these objects are determined by a symmetric, reflexive relation on D which specifies whether or not each pair of objects in D are 'neighbours'. Isham (1984) noted that in many applications, objects will be neighbours if they are within some critical distance r_o of each other.

A spatial point process satisfies the Markov property if the conditional intensity of the process at a point x, say, given the realization of the process in the remainder of the region D, depends only on the existence or otherwise of objects within a distance r_o of x.

A Markov point process is defined on an arbitrary, but fixed finite region D. Each process is characterised by its likelihood ratio f(.) with respect to a Poisson process of unit intensity. Thus if $\mathcal{U} = \{u_1, \ldots, u_n\}$ denotes any finite set of object locations in D, then $f(\mathcal{U})$ indicates in an intuitive sense how much more likely is the configuration of objects $\mathcal{U}$ for the particular process than for the Poisson forest of unit intensity.

Particular examples of Markov point processes include Strauss processes, for which

$$f(\mathcal{U}) = \alpha\beta^{n}\gamma^{s} \qquad , \beta > 0, \quad 0 \leq \gamma \leq 1 \qquad (1.3)$$

where s is the number of distinct pairs of neighbours in $\mathcal{U}$ (u_i and u_j in D are neighbours if the distance between them is less than r_o, for $r_o > 0$), α is a normalising constant, β reflects the intensity of the process and γ describes the strength of interactions between neighbours. The case $\gamma = 1$ gives a Poisson process, whilst $\gamma = 0$ gives a simple inhibition process. Intermediate values of γ represent a form of non-strict inhibition or soft-core. The restriction to $\gamma \leq 1$ is needed to avoid an explosion of the process, with an infinite number of objects in D.

More generally, the class of pairwise interaction processes is defined by,

$$f(\mathcal{U}) = \alpha\beta^{n} \prod_{i\neq j}^{n} h\{ d(u_i , u_j) \}, \quad \beta > 0 \qquad (1.4)$$

where α and β are as in (1.3), h(d) is non-negative in d and d is the distance between the two objects u_i and u_j. The function h(d) describes the strength of interaction between pairs that are exactly d apart. This function h(d) is bounded and in many cases $h(d) = 0$ for $d < \sigma$. This automatically limits the number of objects in D by imposing a minimum permissible distance σ between any two objects. Suppose we want to simulate the process, conditional on the number of objects n in D. We let $\mathcal{U}_1 = \{u_1, \ldots, u_{n-1}\}$ be any set of n-1 objects in D, and consider the possible addition of an object y. Under (1.4),

$$f(\mathcal{U}_1 \cup y) = \alpha\beta^{n} \prod_{i\neq j}^{n-1} h\{ d(u_i , u_j)\} \prod_{i=1}^{n-1} h\{ d(u_i , y) \}$$

and

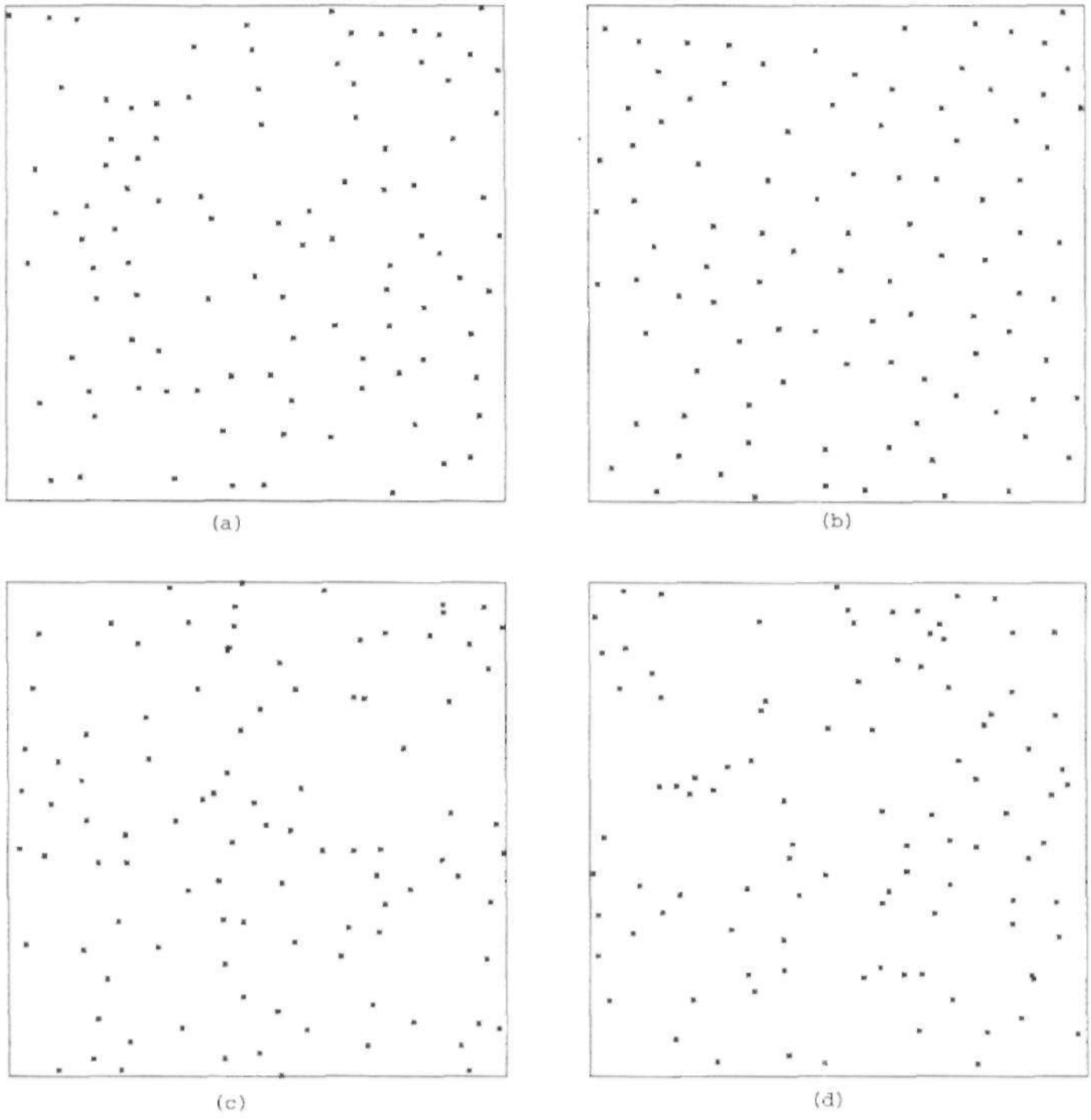


FIGURE 1.4 A realization of each of four pairwise interaction processes (Strauss process) (a) $h(d) = 0.0$, $r = 0.05$, (b) $h(d) = 0.0$, $r = 0.07$, (c) $h(d) = 0.5$, $r = 0.05$ and (d) $h(d) = 0.5$, $r = 0.07$. See text for complete definition of $h(d)$.

$$f(\mathcal{U}_1 \cup y) \;/\; f(\mathcal{U}_1) \;\propto\; \prod_{i=1}^{n-1} h\{ d(u_i , y) \} \qquad (1.5)$$

Since h(d) is bounded above, $h(d) \leq b$, then

$$P(y) \;=\; [\, \prod_{i=1}^{n-1} h\{ d(u_i , y)\}] \;/\; b^{n-1} \qquad (1.6)$$

lies between 0 and 1. This process defined by the alternate deletion and replacement of objects according to (1.6) is shown by Ripley (1977) to converge to the Markov point processes defined by (1.4), but conditioned to produce *n objects in D.*

Consider any set of n objects in D to constitute an initial realisation of the process and delete one of the n objects at random to produce the set $\mathcal{U}_1$ of (1.5). Now generate an object y distributed uniformly in D and accept y with probability P(y), otherwise reject, and repeat until one such object is accepted. Ripley(1979b) gives a FORTRAN subroutine and suggests that provided the initial realisation is a Poisson forest, 4n deletions and replacements are adequate in practice.

Figure 1.4 a to d show simulated realizations of the Strauss processes consisting of 100 objects in the unit square, considered as a toroid, and a range of parameter values. These simulations are performed using the algorithm of Ripley(1979b). Note that,

$$h(d) = \begin{cases} 0 & \text{if } d \leq r \\ b & \text{if } d > r \end{cases} \qquad (1.7)$$

where $b > 0$, for figures 1.4 a and b, and these correspond to hard core models with minimum permissible distance $r = 0.05$ and $r = 0.07$ respectively. However,

$$h(d) = \begin{cases} 0.5b & \text{if } d \leq r \\ b & \text{if } d > r \end{cases} \qquad (1.8)$$

for figures 1.4 c and d and this suggest a soft core model, where the object y is accepted with probability P(y).

1.7 The selection of the study region D

A spatial point pattern, as we have noted, is a configuration of objects $\mathcal{U} = \{u_i \in D,\ i=1, 2, \ldots, n\}$, for some designated planar region D. Typically D is a sampling window within a much larger region E and it is reasonable to regard $\mathcal{U}$ as a partial realisation of a planar point process, the objects consisting of all points of the process which fall within D.

The selection of the study region D, merits some special mention. In some applications, D is objectively determined by the problem in hand, and inferences are required in terms of a Process defined on D itself. One example of this would be a map of all the nesting sites of birds on an island.

More commonly D is selected from some much larger region. The selection of D may then be made according to a probability sampling scheme, or it may simply reflect the experimenter's view that D is in some sense a representative view of the larger region. In either case, inferences drawn from an analysis will carry much greater conviction if consistency over replicate data sets can be demonstrated.

1.8 Monte Carlo tests.

The Monte Carlo test introduced by Barnard (1963) has attracted considerable attention recently, particularly as regards to the analysis of spatial point patterns (Besag and Diggle, 1977; Ripley, 1977). This is largely because even simple stochastic models for spatial point patterns lead to intractable distribution theory. In order to test models against data we have to make use of Monte Carlo tests.

The method is straightforward. Quite generally, let b be the observed value of a statistic B and let b_j, j = 2, 3,...,s, be the corresponding values generated by independent random sampling from the distribution of B under the simple hypothesis H_o. Let $b_{(k)}$ denote the k^{th} largest, amongst b_k , k = 1, 2,...s. Then under H_o,

$$P\{ b_1 = b_{(j)} \} = 1/s , \qquad j = 1, 2,....., s \qquad (1.9)$$

and rejecting of H_o on the basis that b_1 ranks r largest or higher (or r smallest or lower) gives an exact one sided test of size $\alpha = r/s$. The test is exact in the sense that the type I error is precisely α .

The test assumes that the values of $b_{(j)}$ are all different, so that the ranking of b_1 is unambiguous. If B is a discrete random variable, tied values are possible and we then adopt the conservative rule of choosing the least extreme rank for b_1 . For a two sided Monte Carlo test, r is chosen such that,

$$\alpha = 2 r / s \qquad (1.10)$$

Hope (1968) gives some examples to show that the loss of power resulting from a Monte Carlo implementation is small, so that s need not be very large. For a one-sided test at the conventional 5% level, s equals 100 is assumed to be adequate. The effect of the Monte Carlo approach is that the critical region is not of the usual form: A classical test would surely reject H_o if b_1 lay in some well defined critical region, whereas for a Monte Carlo test, there is a range of values of b_1 over which there is a varying probability of rejecting H_o.

This blurring of the critical region leads to a loss of power, which has been investigated by Hope (1968) and recently by Marriott(1979). Clearly this blurring effect could be reduced to a negligible proportion,

by taking s sufficiently large, but this could involve very heavy computing.

The simplest approach to the question of an acceptable value of s is to consider the probability of accepting or rejecting H_o when the conventional significance level takes certain values. This probability can be calculated and involves no assumption about the alternative hypothesis. Suppose p is the probability that b_1 exceeds an arbitrary value from the distribution of B based on H_o. Then if 1-p is less than α, a classical test would reject H_o. The probability that a Monte Carlo test would reject H_o is,

$$P\{ \text{reject } H_o | b_1 \} = \sum_{x=0}^{r-1} \binom{s-1}{x} p^{s-x-1} (1-p)^x \qquad (1.11)$$

For a classical test, represented here by the limit $s \to \infty$, or $(r \to \infty)$,

$$P\{ \text{reject } H_o | b_1 \} = \begin{cases} 1 & \text{if } p > 1 - \alpha \\ 0 & \text{otherwise} \end{cases} \qquad (1.12)$$

For the Monte Carlo test, the effect of blurring introduced, is measured by $P\{ \text{reject } H_o | b_1 \}$ defined in (1.11). This is presented in Table 1.1 for α = 0.1, 0.05, 0.02 and 0.01 and is also produced as Figure 1.5. From this Figure we can see clearly that the extent of blurring depends primarily on r, so that if s = 100 (r = 10) is judged to be acceptable for a test at the 10% level, then s = 200, 500 and 1000 corresponding to (r = 10) should be aceptable at the 5%, 2% and 1% levels respectively.

In practice random sampling will be replaced by pseudo-random sampling when using the Monte Carlo technique. In most of what follows, we have used the generator G05CBF(I), supplied by the NAG (1977) subroutine library.

An inherent weakness of the Monte Carlo approach is its restriction to the simple hypothesis H_o. A composite hypothesis can be tested if pseudo-random sampling is made conditional on the observed values of sufficient statistics for any unknown parameters. A principal advantage however, is that one need not be constrained by known distribution theory, but rather can and should use informative statistics of one's own choosing.

When asymptotic distribution theory is available, a Monte Carlo test provides an exact alternative for small samples and a useful check on the applicability of the asymptotic theory. If the results of a classical and a Monte Carlo test are in substantial disagreement, the explanation is usually that the classical test uses an inappropriate distributional assumption.

Table 1.1a: Values of P{ reject $H_o \mid b_1$ } for α = 10%.

α = 0.1						
	p					
r	0.750	0.800	0.850	0.900	0.950	0.990
1	0.075	0.134	0.232	0.387	0.630	0.914
3	0.013	0.052	0.168	0.435	0.825	0.997
5	0.003	0.021	0.123	0.450	0.903	1.000
7	0.001	0.009	0.091	0.458	0.943	1.000
10	0.000	0.003	0.056	0.465	0.974	1.000
12	0.000	0.001	0.045	0.468	0.984	1.000

Table 1.1 b: Values of P{ reject $H_o | b_1$ } for α = 5%, 2% and 1%

			α = 0.05			
			P			
r	0.875	0.900	0.925	0.950	0.975	0.990
1	0.079	0.135	0.227	0.377	0.618	0.826
3	0.017	0.057	0.171	0.429	0.817	0.979
5	0.004	0.025	0.128	0.445	0.897	0.997
7	0.001	0.012	0.097	0.454	0.939	1.000
10	0.000	0.004	0.065	0.461	0.971	1.000
12	0.000	0.002	0.050	0.465	0.982	1.000
			α = 0.02			
			P			
r	0.940	0.950	0.960	0.970	0.980	0.990
1	0.048	0.081	0.135	0.225	0.372	0.611
3	0.006	0.019	0.060	0.173	0.426	0.812
5	0.001	0.005	0.023	0.130	0.442	0.894
7	0.000	0.001	0.013	0.098	0.451	0.936
10	0.000	0.000	0.005	0.068	0.459	0.969
12	0.000	0.000	0.002	0.053	0.463	0.981
			α = 0.01			
			P			
r	0.975	0.980	0.985	0.990	0.995	0.999
1	0.082	0.135	0.224	0.370	0.609	0.906
3	0.020	0.061	0.173	0.424	0.810	0.997
5	0.005	0.029	0.131	0.441	0.892	1.000
7	0.001	0.014	0.101	0.451	0.936	1.000
10	0.000	0.005	0.069	0.459	0.969	1.000
12	0.000	0.002	0.054	0.462	0.980	1.000

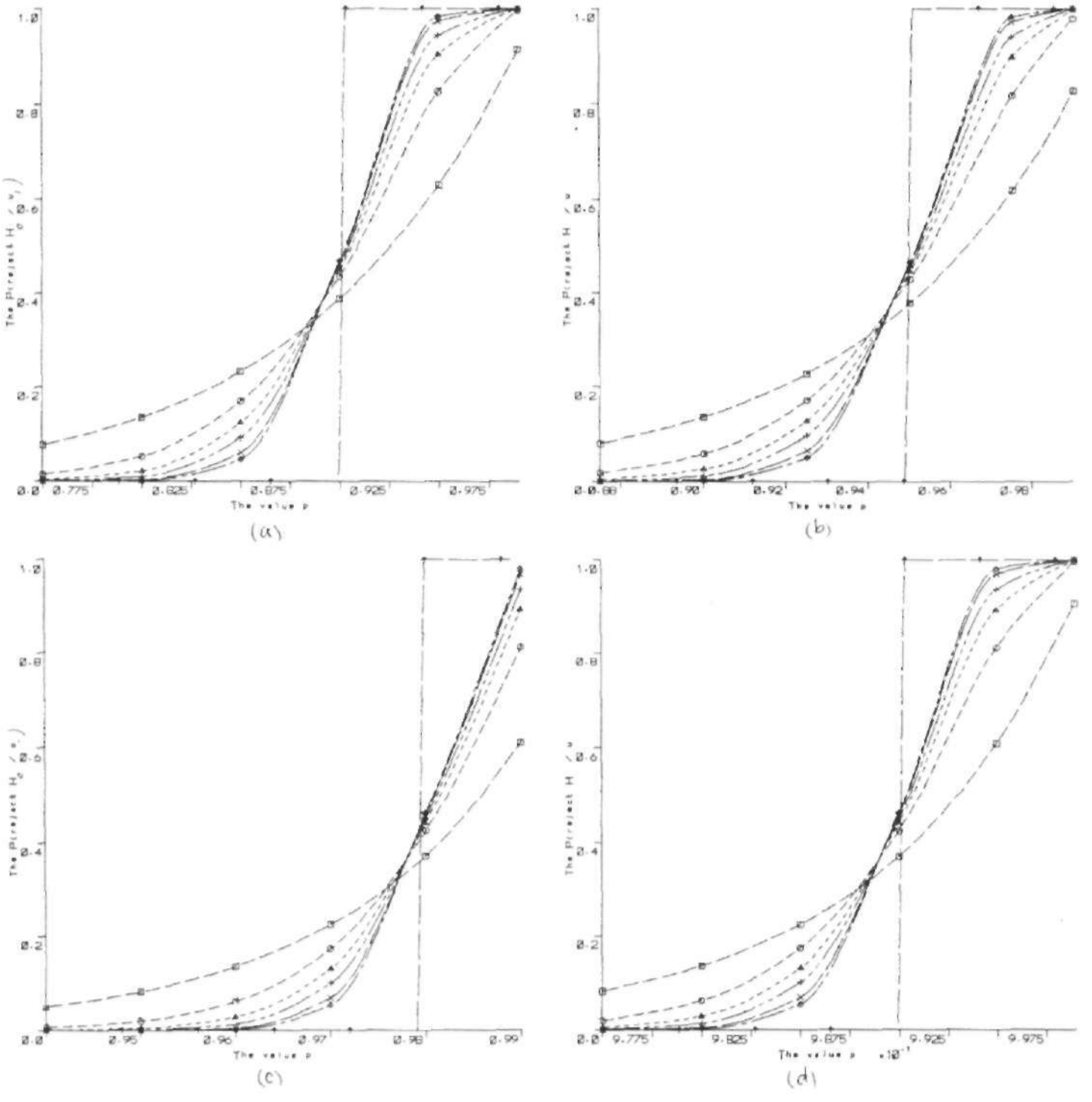


FIGURE 1.5 : Blurred critical regions for a one-sided α% Monte Carlo tests. r=1; r=3; r=5; r=7; r=10; r=12; $r\to\infty$, corresponding to $S\to\infty$.

Key: (a) α=10, (b) α=5, (c) α= 2, (d) α=1.

CHAPTER II

The average nearest neighbour methods in circular sampling windows

2.1 Introduction

In this chapter we consider methods for the analysis of data which consist either of distances measured from each object to its nearest neighbour or from sampling points to their nearest objects. We are concerned with testing whether a particular pattern is consistent with the null hypothesis of randomness. A description of the point pattern is usually obtained by applying this test and then using the value of the statistic to classify the pattern as regular, random or aggregated.

Nearest neighbour analysis was first used by ecologists and foresters, who however measured nearest neighbour distances only from a thin sample drawn from a large number of objects. In this situation, since the chosen objects are likely to be widely separated, their nearest neighbour distances can be assumed to be more or less independent. Edge effects are also negligible since the chosen objects are likely to be a long distance away from the edge of the region. In most cases however, nearest neighbour distances are measured from all the objects in a finite area (a map), in which case neither of these simplifications any longer holds.

The object of this chapter is to present revised expressions for the mean and variance of the average distance between a sampling point and the nearest object point of the point pattern, for use with circular regions, and to show that using these corrections the point-object analogue of the Clark-Evans statistic is approximately normally distributed with zero mean and unit variance.

2.2 Clark and Evans statistic: CE

Dice(1952) seems to have been the first to use distance between nearest neighbours in measuring departure from the Poisson process. Clark and Evans(1954) observed that the method of Dice is somewhat laborious, for it requires several measurements from each centre of origin and makes use of third moment statistics in testing for the degree of departure from the random distribution.

Further study of the nearest neighbour methods led Clark and Evans(1954) to suggest a much simpler statistic, which requires but a single measurement from each centre of origin, and looks superior in its simplicity of computation and ease of interpretation. The distance from an individual object to its nearest neighbour, irrespective of direction, provides the basis for this statistic. More formally, let $u_1, u_2, u_3, \ldots, u_n$ be n objects in the study region D. Also let,

$$w_i = \min_j d(u_i, u_j), \quad i = 1, 2, \ldots, n, \quad j \neq i$$

(where $d(u_i, u_j)$ is the distance between u_i and u_j), be the nearest neighbour distance of the i^{th} object in D. Then the mean observed distance $\bar{w} = \sum w_i/n$.

For a random distribution of objects of intensity ρ per unit area, the probability that a randomly chosen circle of area πw^2 will contain x objects can be approximated by,

$$P(X = x) = \{\pi \rho w^2\}^x \exp(-\rho\pi w^2) / x! \quad , x = 0, 1, \ldots \qquad (2.1)$$

Substituting x = 0 in equation (2.1), we obtain the probability that there are no other objects in the circle of radius w. Thus

$$P(X = 0) = P(\text{there are no other objects in a circle of radius } w)$$

$$= P(W > w)$$

$$= \exp(- \rho\pi w^2)$$

But $P(W \leq w)$ is the probability distribution function of the random variable W, the object-to-object nearest neighbour distance, whence

$$F(w) = 1 - P(W > w)$$

$$= 1 - \exp(- \rho\pi w^2)$$

Differentiating F(w) with respect to w gives us the probability density function f(w):

$$f(w) = 2 \pi\rho w \exp(- \rho\pi w^2), \quad w > 0 \qquad (2.2)$$

From (2.2), the mean distance $E(\bar{W})$ which would be expected for an infinite Poisson process is,

$$E(\bar{W}) = E(W) = \int_0^\infty 2\pi\rho \, w^2 \exp(- \pi\rho w^2) \, dw$$

$$= [1/(\pi\rho)^{\frac{1}{2}}] \int_0^\infty t^{\frac{1}{2}} \exp(- t) \, dt$$

$$= [1/(\pi\rho)^{\frac{1}{2}}] \Gamma (3/2)$$

$$= 0.5/\sqrt{\rho} \qquad (2.3)$$

The index of non-randomness R_ω ,

$$R_\omega = \bar{w} \,/\, E(\bar{W})$$

$$= 2\sqrt{\rho}\ \ \bar{w} \qquad (2.4)$$

can then be used as a measure of the degree to which the observed distribution approaches or departs from random expectation. In a random distribution R_ω is approximately unity. Under conditions of maximum aggregation $R_\omega = 0$, since all the objects occupy the same locus and the distance to the nearest neighbour is therefore 0. Under conditions of maximum spacing, the individual objects will be distributed in a hexagonal pattern (c.f. Diggle, 1983, p 67) and every individual will be equidistant from six other individuals. In such a distribution, the mean distance to nearest neighbour will be maximized.

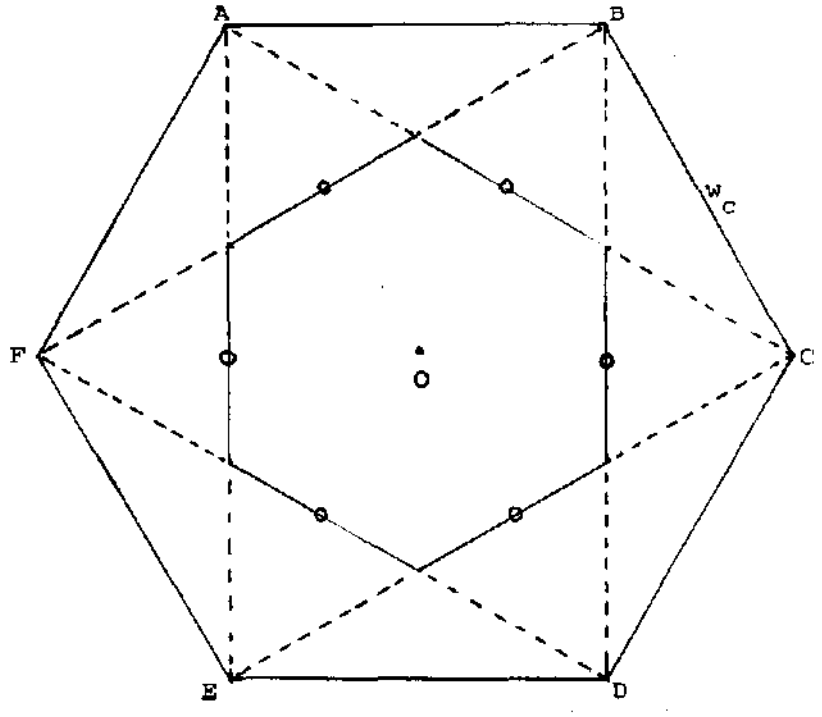


FIGURE 2.1 : the Dirichlet tessellation (——o——) of the object O, that is surrounded by six other objects (A to F) in the hexagonal pattern,

Let w_c denote the constant distance between nearest neighbours in this distribution. Each object occupies a 'territory' consisting of that part of the study region which is closer to it, than to any other object in the region. Figure 2.1 is an illustration of this territory and is referred to as a Dirichlet tesselation of the object 0 in the hexagonal pattern.

The area of the territory of the object 0 is therefore given as,

$$A_c = 6\ (w_c^2\ \sqrt{3}\ /\ 12)$$
$$= w_c^2 \sqrt{3}\ /\ 2$$

and so the density ρ of the hexagonal pattern in an infinite plane is of course,

$$\rho = 1\ /\ A_c = 2\ /\ w_c^2\ \sqrt{3}.$$

In general however, ρ may not be known, in which case we estimate it by n/A. Solving for w_c, we obtain,

$$w_c = \sqrt{2}\ /\ \rho^{\frac{1}{2}}\ \ 3^{1/4}$$

Since w_c is the greatest possible value of $\bar{w}$, the maximum possible value of the ratio R_ω is 2.14914. Thus R_ω has a limited range. If the value of R_ω indicates that a given distribution of objects may not be randomly distributed, the significance of the departure can be tested by calculating the value of the statistic,

$$CE = \{\ \bar{w}\ -\ E(\bar{W})\}\ /\ \{\ Var(\bar{W})\}^{\frac{1}{2}} \qquad (2.5)$$

which was first proposed by Clark and Evans(1954). They suggested that for all practical purposes this statistic should be considered to have as a

null distribution a normal distribution with mean zero and variance unity.

The variance of $\bar{W}$ can be evaluated from

$$\mathrm{Var}(\bar{W}) = \sum_{i=1}^{n} \mathrm{Var}(w_i)/\, n^2 + 2 \sum_{i>j}^{n} \sum^{n} \mathrm{Cov}(w_i , w_j) / n^2 \qquad (2.6)$$

If we assume that the w_i are uncorrelated, then $\mathrm{Cov}(w_i, w_j) = 0$ for all $i \neq j$, and (2.6) then reduces to,

$$\mathrm{Var}(\bar{W}) = \mathrm{Var}(W) / n$$

but

$$E(W^2) = \int_0^{\infty} 2 \pi \rho\, w^3 \exp(- \pi\rho w^2)\, dw$$

$$= [\, 1 /\pi\rho\,] \int_0^{\infty} t \exp(- t)\, dt$$

$$= [\, 1 / \pi\rho] \;\Gamma(2) = 1/ \pi\rho.$$

Thus $\mathrm{Var}(W) = 1/ \pi\rho - (1 /2\sqrt{\rho})^2$

$$= (4 - \pi) / 4\pi\rho$$

and $\mathrm{Var}(\bar{W}) = (4 - \pi) / 4 n \pi\rho \qquad (2.7)$

However, these formulae for the mean and variance of $\bar{W}$ ignore edge-effects and the non-independence of the different nearest neighbour distances. Therefore, the moments of $\bar{W}$ should be revised to take account of these problems, so that a statistically valid test can be performed using the statistic CE.

2.2.1 Edge corrections for CE

Donnelly(1978) observed that the edge effect corrections to the mean and variance of $n\bar{W}$ could be approximated well by an additional term proportional to the length of the edge of the study area and dependent on the density ρ of objects. Since the dimensions of $\bar{W}$ and $E(\bar{W})$ are length and $Var(\bar{W})$ are length squared, this imposes restrictions on the forms of correction factors and Donnelly found the following formulae to be appropriate:

$$E^{*}(n\bar{W}) = 0.5\sqrt{(n A)} + a P \qquad (2.8)$$

$$Var^{*}(n\bar{W}) = c A + b P\sqrt{(A / n)} \qquad (2.9)$$

where A is the area of the study region and P is its perimeter. The correction terms are aP and $bP\sqrt{(A / n)}$. a, b and c are unknown constants.

Some 6000 to 100000 simulations of $(n\bar{W})$ for between 5 and 64 random objects in various shapes of region, including circles, ellipses, squares and rectangles, were performed by Donnelly in order to determine these constants. After examining some scattergrams, he arrived at the formulae:

$$E^{*}(n\bar{W}) = 0.5\sqrt{(n A)} + (0.051 + 0.041/\sqrt{n}) P \qquad (2.10)$$

$$Var^{*}(n\bar{W}) = 0.07 A + 0.037 P\sqrt{(A / n)} \qquad (2.11)$$

Furthermore, by using a combination of some analytical methods and numerical integration he obtained an estimate of the constant c more accurately as 0.0703 and the value of 0.051 in (2.10) as 0.051368. The statistic R_{ω} defined in (2.4) can be revised to take account of these edge corrections, by replacing the expected mean by $E(\bar{W})$ defined in (2.10).

2.3 Analogue of the CE statistic: M

The non-independence of the different nearest neighbour distances leads De Vos(1973) to suggest an analogous statistic to the CE statistic. This statistic is defined by

$$M = \{ \bar{x} - E(\bar{X}) \} / \{Var(\bar{X})\}^{\frac{1}{2}} \qquad (2.12)$$

where the definitions of $\bar{x}$ and $\bar{X}$ parallel those for $\bar{w}$ and $\bar{W}$ and the difference is simply that x_i is the distance between the i^{th} sampling point and its nearest object. If we use m sampling points then,

$$x_i = \min_j d(o_i , u_j), \quad i = 1, 2, \ldots, m$$

where $d(o_i,u_j)$ is the distance between the i sampling point o_i to the j^{th} object u_j of the process. For an infinite Poisson process, the random variables W and X have identical distributions, whence, for randomly placed sample points,

$$E(\bar{X}) = 0.5 / \sqrt{\rho} \qquad (2.13)$$

$$Var(\bar{X}) = (4 - \pi) / 4 m\pi\rho \qquad (2.14)$$

De Vos suggests that for a Poisson process, the statistic M will be approximately Normally distributed with zero mean and unit variance.

An index of non-randomness for use with the M statistic is

$$R_m = 2 \sqrt{\rho} \quad \bar{x} \qquad (2.15)$$

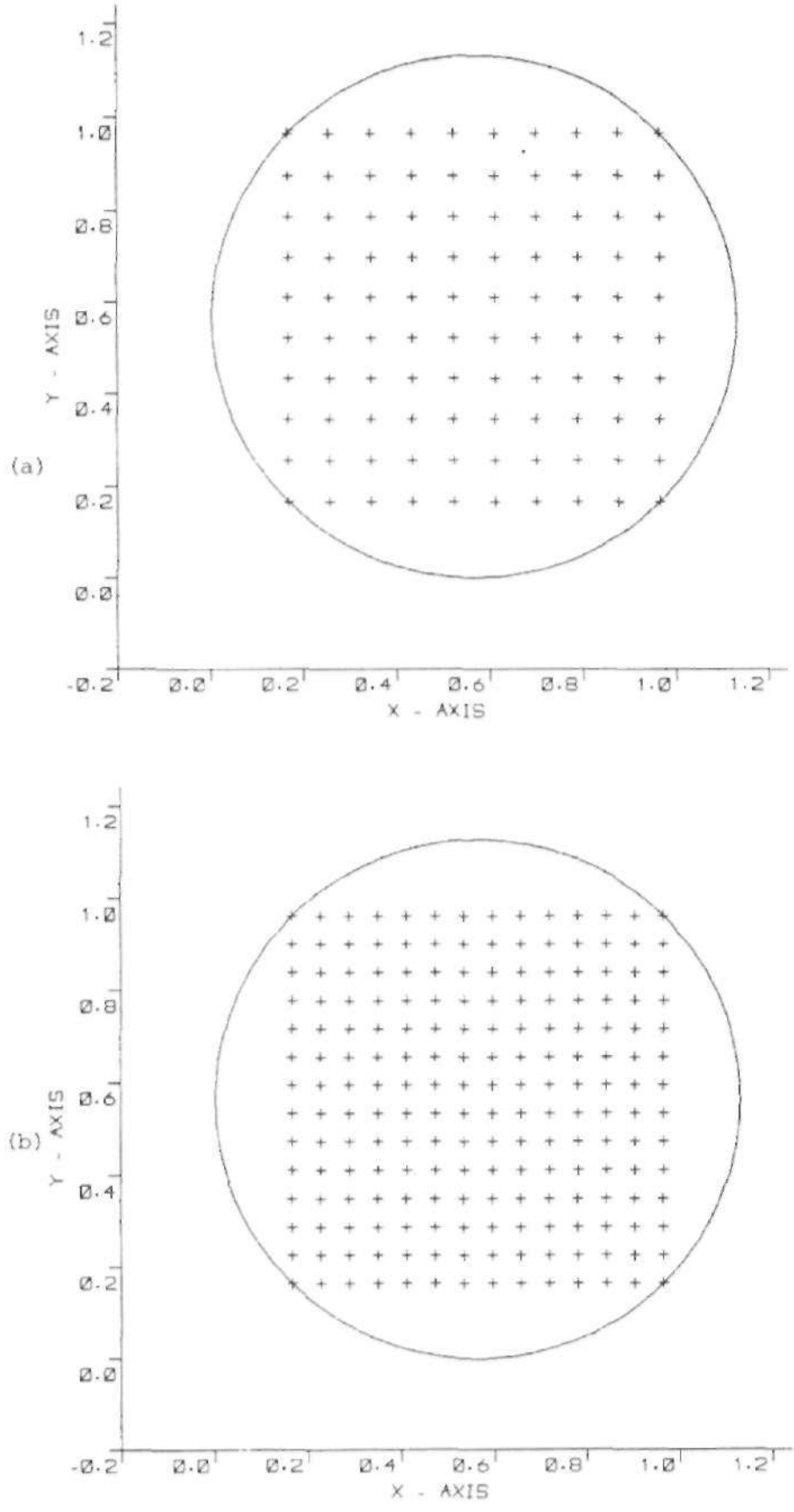


FIGURE 2.2 : Regular lattice of sampling points in the circular window of unit area, consisting of: (a) m=100, and (b) m=196 sampling points.

which should be used as a measure of the degree to which the observed pattern approaches or departs from the Poisson forest. For a Poisson forest R_m is approximately equal to unity. Under conditions of maximum aggregation all the objects occupy the same locus which means that x_i distances would be on the average, much larger than expected and so the ratio R_m would be greater than unity. However under conditions of maximum spacing these distances would be very small. This implies that the ratio R_m would be less than unity.

In any given distribution the mean observed value $\bar{X}$ is R_m times as great as would be expected in a random distribution with similar intensity. Thus an R_m value of 0.5 would indicate that the nearest neighbours of the points are on average, half as far apart as would be expected under the null hypothesis of randomness.

A major difficulty in the application of the statistic M has been that the theory applies only to an unbounded study area. However in practice, study is limited to a finite number of objects in a restricted region. The moments of $\bar{X}$ are therefore affected by this bounded region and so render the null distribution of M inappropriate.

2.4 Edge corrections for M

In this section, we assume a circular window D, centred at (R, R) and radius R, and our edge corrections relate only to a regular lattice of sampling points as favoured by Diggle(1979b). Our results are based on a lattice obtained by partitioning a square of side $\sqrt{2}$ R. The position of the $(i,j)^{th}$ sampling point P_h say, is $[\sigma + (i-1)\Delta , \sigma + (j-1)\Delta]$, where $i = 1, 2, \ldots, k$; $j = 1, 2, \ldots, k$; $h = k(i-1)+ j$; $\sigma = (1- \sqrt{2}/2)R$ and $\Delta = \sqrt{2}\, R/(k-1)$. When collecting information for the 'refined' distance analysis, opinions have varied over a suitable choice of m, (see Upton and

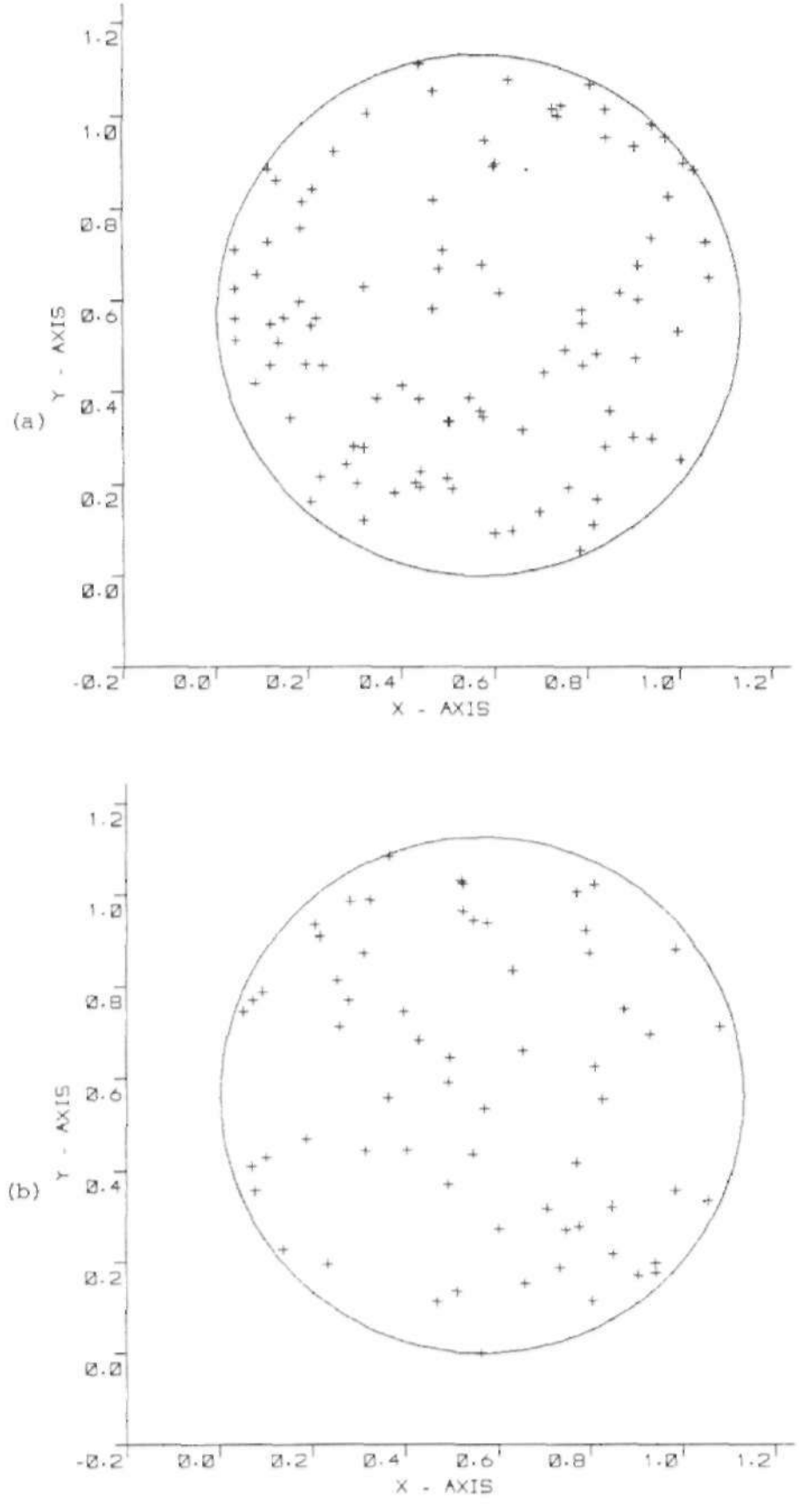


FIGURE 2.3: Partial realizations of a Poisson process of (a) n=97 and (b) n=63, random objects in a circular region of unit area.

Fingleton,1985, p 81). Given that the sampling window contains n objects we have chosen the integer k so that

$$k = \begin{cases} \sqrt{n} & \text{if } \sqrt{n} \text{ is an integer} \\ \\ \text{Int}[\sqrt{n}\,] + 1, & \text{otherwise} \end{cases} \qquad (2.16)$$

where Int[G] means the integer part of G. Figures 2.2a and b illustrate such a partition for a circular window of unit area, consisting of m = 100 sampling points and m = 196 sampling points respectively.

We consider cases where the number of random objects, n, in any given circular window, varied between 7 and 100. Figures 2.3a and b present example realizations of a Poisson process consisting of n = 97 and n = 63 random objects in a circular window of unit area. We used upwards of a total of 140000 simulations of total point-object nearest neighbour distances for random objects in various circular regions in the plane.

The quantities: $\text{Var}^*(\overline{X})/\ A$, $E^*(\overline{X})/\ \sqrt{A}$ and $P\ /\ \sqrt{A}$, where A is the area and P is the perimeter of the circular region D, are independent of the value chosen for R. For fixed R therefore, the observed values of the mean and variance of $\overline{X}$ are obtained by

(i) simulating s = 1000 Poisson processes of n objects each, in D [using the NAG library routine with seed G05CBF(1000)].

(ii) generating the values: $T_1, T_2, \ldots, T_s$, where T_k is the total point-object nearest neighbour distances of the k^{th}Poisson process in (i).

(iii) using (ii) to compute the mean and variance of $\overline{X}$, defined as

$$E^*(\overline{X}) = \sum_{k=1}^{s} T_k\ /\ m\ s \qquad (2.17)$$

$$\mathrm{Var}^*(\bar{X}) = \sum_{k=1}^{s} T_k^2 / s\,m^2 - \{ E^*(\bar{X}) \}^2 \qquad (2.18)$$

Table 2.1. Values of $\mathrm{Var}^*(\bar{X})/A$ and C obtained for 30 different values of n by simulation, using regular lattice of sampling points.

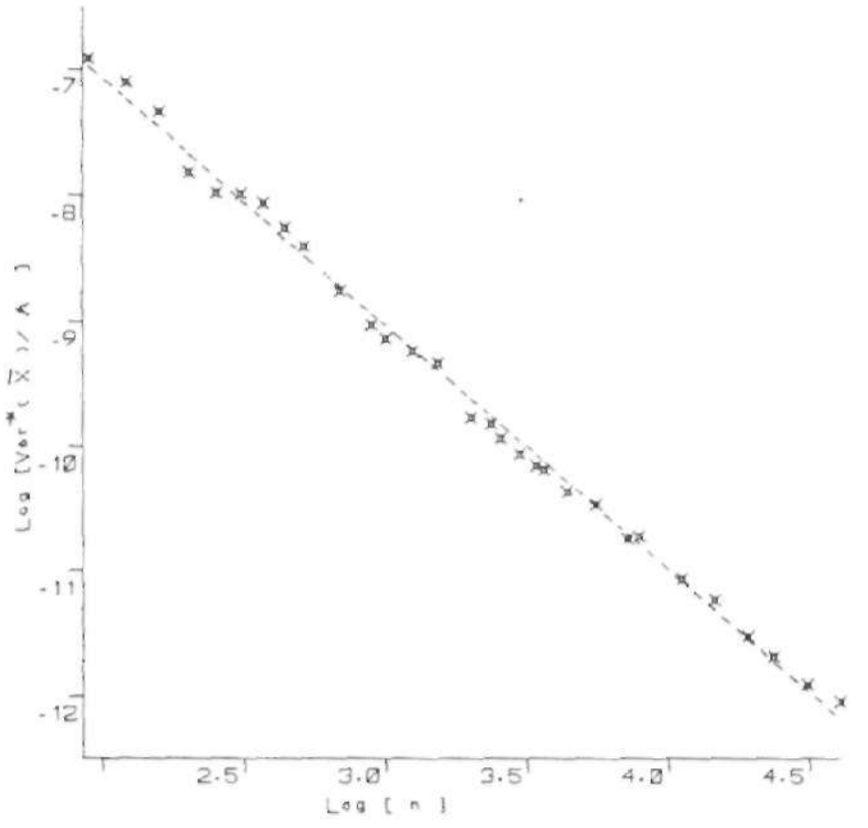
m	n	$\mathrm{Var}^*(\bar{X}) / A$	C
9.0	7.0	0.0009926423	0.0387006178
9.0	8.0	0.0008196411	0.0368962549
9.0	9.0	0.0006445861	0.0338812806
16.0	10.0	0.0004031404	0.0194936434
16.0	11.0	0.0003438739	0.0180489749
16.0	12.0	0.0003416230	0.0173553005
16.0	13.0	0.0003163780	0.0157911729
16.0	14.0	0.0002623712	0.0154624948
16.0	15.0	0.0002267350	0.0142857159
25.0	17.0	0.0001584257	0.0091232066
25.0	19.0	0.0001205167	0.0081183231
25.0	20.0	0.0001078524	0.0079437006
25.0	22.0	0.0000976126	0.0071293594
25.0	24.0	0.0000884169	0.0071211782
36.0	27.0	0.0000574858	0.0047122745
36.0	29.0	0.0000544147	0.0046550307
36.0	30.0	0.0000485874	0.0045086560
36.0	32.0	0.0000426980	0.0042945708
36.0	34.0	0.0000387773	0.0039985239
36.0	35.0	0.0000375681	0.0038948509
49.0	38.0	0.0000314685	0.0030582592
49.0	42.0	0.0000284544	0.0029450222
49.0	47.0	0.0000215728	0.0026000986
49.0	49.0	0.0000219733	0.0024646637
64.0	57.0	0.0000156667	0.0018648185
64.0	64.0	0.0000132280	0.0016672748
81.0	72.0	0.0000099547	0.0012415675
81.0	79.0	0.0000084847	0.0010990702
100.0	89.0	0.0000067462	0.0008744650
100.0	100.0	0.0000058932	0.0008331595

From dimensional considerations we obtain these formulae

$$E^*(\bar{X}) = 0.5/\sqrt{\rho} + a\,R\,/\,n^{b} \qquad (2.19)$$

$$\mathrm{Var}^*(\bar{X}) = c\,R^2\,/\,n^{d} \qquad (2.20)$$

(a)



(b)

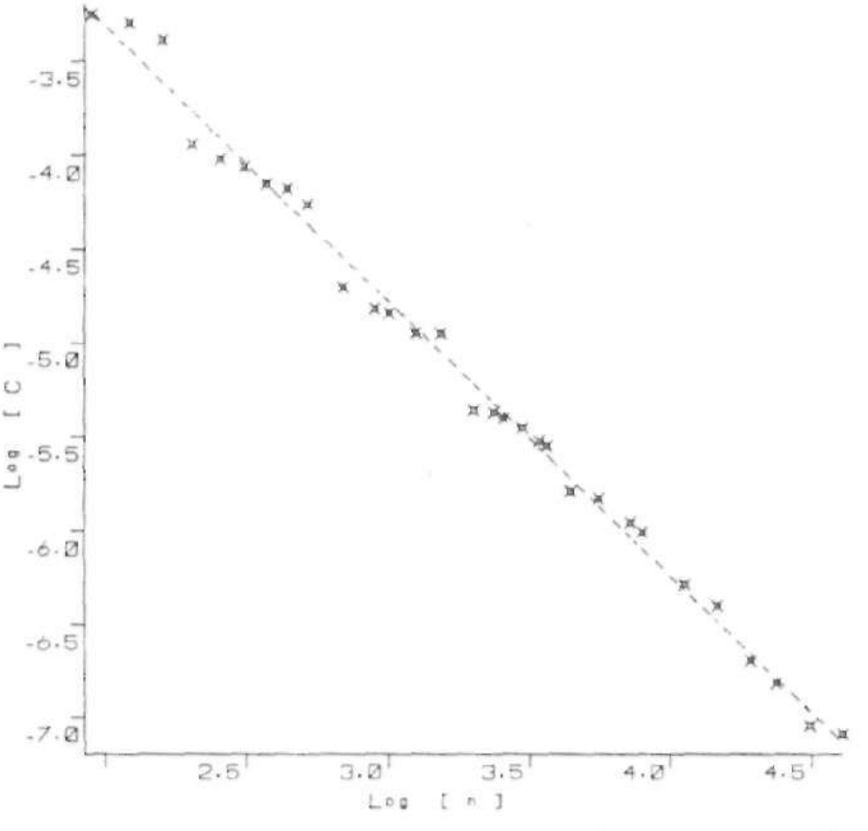


Figure 2.4 : Edge effects on: (a) $Var^{*}(\bar{X})$ and (b) $E^{*}(\bar{X})$. Simulations of the average point-object nearest neighbour distance for random objects in various circular regions in the plane.

where a , b , c and d are unknown constants, and the index * is used to distinguish these quantities from the formulae defined in equations (2.13) and (2.14) relating to an unbounded infinite plane. The values of $Var^*(\bar{X})/A$ for various values of n is presented in Table 2.1. $Log\{Var^*(\bar{X})/A\}$ is plotted against log{n} in Figure 2.4a. The correlation coefficient r between $log\{Var^*(\bar{X})/A\}$ and log{n} is -0.998, which together with the resulting scattergram suggest that the equation defined in (2.20) should adequately fit the data. Using ordinary least squares on the log values, we obtain estimates of c and d , and equation (2.20) becomes,

$$Var^*(\bar{X}) = 0.1317\, R^2 / n^{1.9566} \qquad (2.21)$$

Similarly the values of C, where

$$C = \{E^*(\bar{X}) - 0.5/\sqrt{\rho}\} / \sqrt{A} \qquad (2.22)$$

for various values of n is presented in Table 2.1. The correlation coefficient r between log{C} and log{n} is -0.997. This value of r together with the corresponding scatter plot given in Figure 2.4b suggests a strong linear association between the log values. Using ordinary least squares, we obtain the values of a and b, whence

$$E^*(\bar{X}) = 0.5/\sqrt{\rho} + 1.1995\, R / n^{1.4645} \qquad (2.23)$$

Using these edge corrections we obtain corrected statistics analogous to the uncorrected statistics R_m and M , defined in equations (2.15) and (2.12) namely

$$R_m^* = \bar{x} / E^*(\bar{X}) \qquad (2.24)$$

and

$$M^* = [\bar{x} - E^*(\bar{X})] / \{Var^*(\bar{X})\}^{\frac{1}{2}} \qquad (2.25)$$

Table 2.2. Sample moments and value of $D_s(Y)$ for the statistics $Y=M$ and $Y=M^*$ for a Poisson process, in a circular region of unit radius.

m	n	Statistic	M_1	M_2	M_3	M_4	$D_s(Y)$
36	35	M	0.53	0.69	0.28	1.71	7.66
		M^*	0.03	0.94	0.44	3.15	1.21
49	49	M	0.46	0.77	0.24	1.96	6.43
		M^*	0.04	1.06	0.39	3.72	0.71
64	57	M	0.43	0.84	0.40	2.59	5.51
		M^*	0.01	1.02	0.54	3.84	1.08
81	76	M	0.35	0.81	0.26	2.30	4.65
		M^*	0.00	1.02	0.37	3.70	0.99
81	79	M	0.34	0.79	0.19	1.93	4.41
		M^*	-0.01	1.05	0.29	3.35	1.00
100	95	M	0.30	0.80	0.16	2.03	4.09
		M^*	-0.02	1.02	0.23	3.29	1.08
Theoretical values		N(0,1)	0.00	1.00	0.00	3.00	0.00

In order to test these edge corrections we generated random patterns within a circular window of radius 1. We then obtain the values of Y: y_1, $y_2,\ldots,y_s$, for s = 1000 simulations at each of a variety of combinations of m and n and calculated the first four sample moments,

$$M_1 = \sum_{i=1}^{s} y_i / s, \qquad (2.26)$$

$$M_r = \sum_{i=1}^{s} (y_i - M_1)^r / s, \quad r = 2, 3, 4 \qquad (2.27)$$

of both the uncorrected, Y = M and the edge corrected, Y = M^* statistics, as shown in Table 2.2. We also calculated the value of the Kolmogorov-Smirnov statistic $D_s(Y)$ defined as

$$D_s(Y) = \sqrt{s} \sup \{ | \hat{F}_s(Y) - F(Y) | \} \qquad (2.28)$$

where $\hat{F}_s(Y)$ is the empirical distribution function:

$$\hat{F}_s(Y) = \begin{cases} 0 & \text{if } y < y_{(1)} \\ k/s & \text{if } y_{(k)} \leq y < y_{(k+1)} \\ 1 & \text{if } y \geq y_{(s)} \end{cases}$$

and F(Y) is the distribution function of a Standard normal distribution with mean zero and variance unity. Here $y_{(1)}, y_{(2)}, \ldots, y_{(s)}$ are the corresponding order statistics of the sample $y_1, y_2, \ldots, y_s$. The test statistic (2.28) is a value of the random variable $D_s(Y)$, which depends on $y_1, y_2, \ldots, y_s$ through $\hat{F}_s(Y)$, and it provides a measure of how far $\hat{F}_s(Y)$ is from F(Y). Clearly large values of $D_s(Y)$ will make us doubt the asymptotic normality of the statistic Y.

For the test of a null hypothesis of a unit normal distribution the test statistic $D_s(Y)$ has critical values 1.36 (5%) and 1.63 (1%). Table 2.2 shows clearly the sensitivity of the mean and variance of the M statistic to the circular region. However the results for the M^* statistic are all entirely acceptable. Note that m_3 for the corrected statistic is worse than that for the uncorrected statistic.

2.5 Examples

In this section, we shall apply both the M and M^* statistics and the CE and CE^* statistics to simulated clustered and regular alternatives as well as to an artificial random pattern.

The objects that constitute the simulated random pattern in a given circular window D, are generated using the rejection technique. This technique involves generating a pair of values at random from a uniform distribution on (0,2R). The pair is then rejected if it falls outside the circular region. This procedure is repeated until the required number, n, of objects is generated in D. Figures 2.3a and b present example realizations of this pattern.

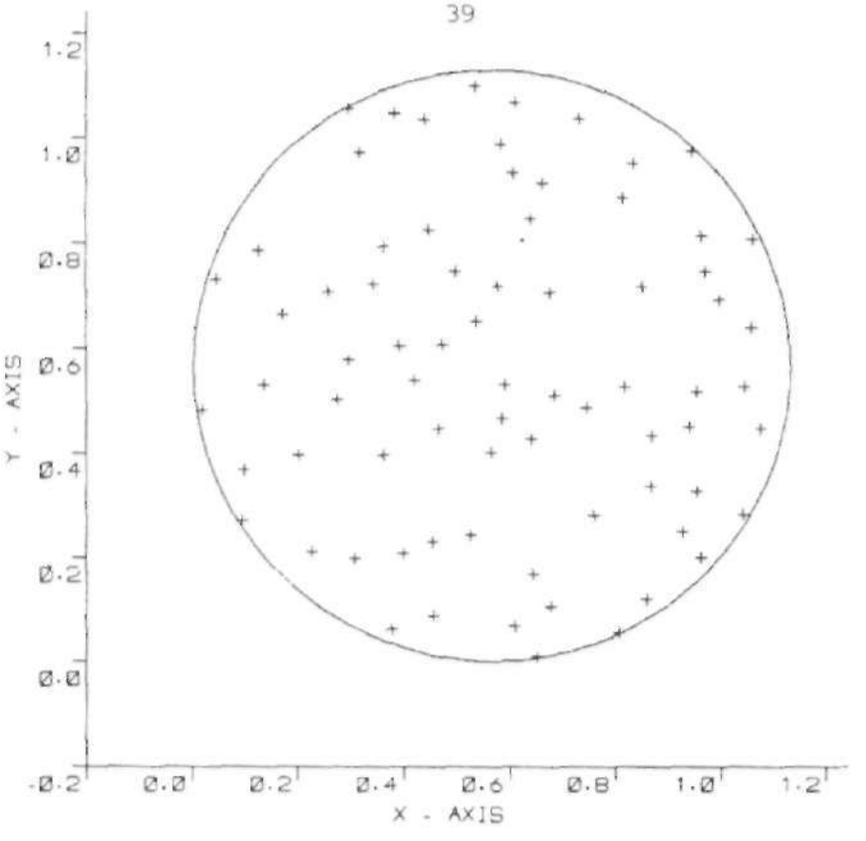
For the regular alternative we use a Diggle et al (1976) simple sequential inhibition process. This process is characterised most naturally by its packing intensity

$$\tau = N (\sigma / 2 R)^2, \qquad (2.29)$$

where σ is the minimum permissible distance between any two objects of the process, and N is the number of objects of the process. For our simulation, we generated a pair of values at random from a uniform distribution on a square of side 2R, regarded as a torus. The pair is then rejected if it falls within a distance σ away from any previously accepted objects in the torus. Finally, only those objects that fall within the window D are considered. A partial realization of this pattern with $N = 100$, $\tau = 0.25$ and consisting of 74 objects in a circular region of unit area is presented in Figure 2.5a.

For our clustered alternative, we use a Neyman and Scott (1958) Poisson cluster process. For our simulation we used the case of 20 randomly distributed "mother" objects surrounded by a total of 60

(a)



(b)

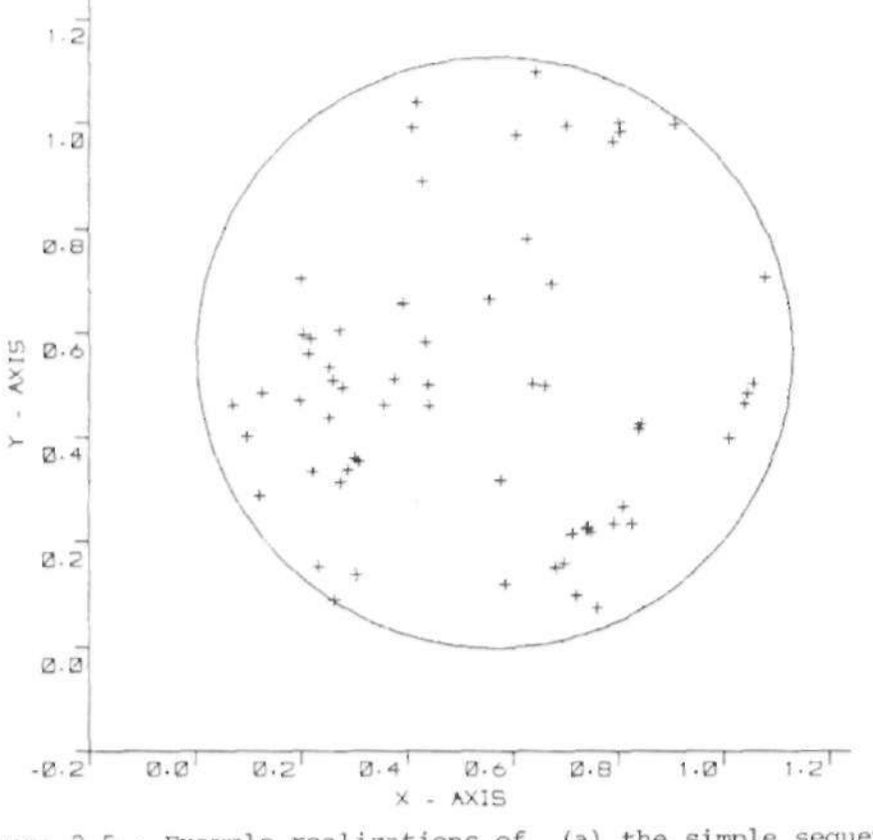


Figure 2.5 : Example realizations of (a) the simple sequential inhibition process (τ=0.25, n=74) and (b) the Poisson cluster process (r=0.1975, n=63) in a circular region of unit area.

"daughter" objects within a "square" of side 2R. The assignment of daughters to mothers is at random, with each daughter being placed at a distance of $r = 0.1975$ units from its mother and at an angle generated at random from a uniform distribution on $(0, 2\pi)$. In certain cases this resulted in the daughter being initially placed outside the square area. In these cases the square is regarded as a toroid and the daughter is appropriately relocated. The mothers and daughters are assumed indistinguishable and are therefore retained in the final pattern. Finally, only those objects that fall within the circular window D are considered. An example realization of this pattern consisting of 63 objects in a circular window D, of unit area is illustrated in Figure 2.5b.

Table 2.3 Summary of the analysis of the three patterns using the statistics M and M^*.

Distribution	Poisson process	Simple sequential inhibition process	Poisson cluster process
n m	97 100	74 81	63 64
$\bar{x}$	0.05606	0.05325	0.08047
ρ	97	74	63
Uncorrected statistic			
$E(\bar{X})$	0.05077	0.05812	0.06299
$\sqrt{\{Var(\bar{X})\}}$	0.00265	0.00338	0.00412
R_m	1.10423	0.91610	1.27738
M	1.99396	-1.44463	4.24513
Edge-corrected statistic			
$E^*(\bar{X})$	0.05160	0.05936	0.06456
$\sqrt{\{Var^*(\bar{X})\}}$	0.00233	0.00304	0.00356
R^*_m	1.08640	0.89698	1.24636
M^*	1.91289	-2.01353	4.47414

Tables 2.3 and 2.4 present a summary of the analysis of the three patterns, for the statistics M and M^* and CE^* and CE respectively. The values of M^* and CE^* obtained for the Poisson process of Figure 2.2a, are neither greater than 1.96 nor less than -1.96 (5%), so the hypothesis that the objects are randomly distributed is not rejected. By contrast, if we do not correct for boundary effects and use the uncorrected statistic M , we obtain 1.994 which is clearly significant.

For the Poisson cluster process of Figure 2.5b, both values of R_m and R_m^* suggest a significant deviation towards a clustered alternative. However, for the Simple sequential inhibition process of Figure 2.5a, the value of M^* obtained is significant. The corresponding value of R_m^* for this realization suggests a deviation towards a regular alternative. By contrast, when the uncorrected statistic M is applied to the same distribution, it failed to detect the apparent regularity in the data.

The values of R_ω and R_ω^* obtained using the statistics CE and CE^* for the Poisson cluster process are all less than unity, suggesting a significant deviation towards a clustered alternative. Similarly when the same statistics are applied to the Simple sequential inhibition process, the values 6.608 and 5.225 are obtained. These values are highly significant. The corresponding values of R_ω and R_ω^* are 1.412 and 1.340, suggesting a deviation towards a regular alternative.

A part of the material of this chapter will appear as Doguwa and Upton (1988b).

Table 2.4 Summary of the analysis of the three patterns using the statistics CE and CE^* .

Distribution	Poisson process	Simple sequential inhibition process	Poisson cluster process
n	97	74	63
$\bar{w}$	0.05060	0.08147	0.05338
ρ	97	74	63
Uncorrected statistic			
$E(\bar{W})$	0.05077	0.05812	0.06299
$\sqrt{\{Var(\bar{W})\}}$	0.00269	0.00353	0.00415
R_ω	0.99664	1.40156	0.84738
CE	-0.06323	6.60831	-2.31740
Edge-corrected statistic			
$E^*(\bar{W})$	0.05280	0.06081	0.06618
$\sqrt{\{Var^*(\bar{W})\}}$	0.00298	0.00395	0.00468
R^*_ω	0.95834	1.33958	0.80665
CE^*	-0.73791	5.22478	-2.73564

CHAPTER III

The nearest neighbour methods in squares and rectangular windows

3.1 Introduction

We have seen in Chapter II, that the statistic M defined in equation (2.12) is flawed in that edge-effects are ignored when deriving the mean and variance of $\bar{X}$ and its asymptotic normality. Moreover, the edge-corrections proposed for M are only valid for circular sampling windows and not for square and rectangular regions. The object of this chapter is to present revised expressions for the mean and variance of the average distance between a regular grid point and the nearest object point of the point process for use with square and rectangular sampling windows and to show that using these corrections, the edge corrected version of M is a powerful detector of departures from randomness in the clustered direction.

3.2 Edge corrections for M

In this section, we assume a rectangular sampling window, and our edge corrections relate to a regular lattice of sampling points. This lattice is obtained by partitioning each square or rectangular window into $(k+1)^2$ similar subwindows and then using the $m = k^2$ inner corners of these subwindows. That is, for a given window of dimension L_x by B_y, the position of the $(i,j)^{th}$ sampling point, P_h say, where $i = 1, 2, \ldots, k$; $j = 1, 2, \ldots, k$ and $h = k(j-1) + i$ is $[\, i\Delta_x , j\Delta_y \,]$. Here, $\Delta_x = L_x/(k+1)$ and $\Delta_y = B_y/(k+1)$. Figures 3.1a and b illustrate such a partition for a square window of unit area, consisting of $m = 100$ sampling points and $m = 196$ sampling points respectively. Given that the sampling window contains n objects we have chosen the integer k as in equation (2.16).

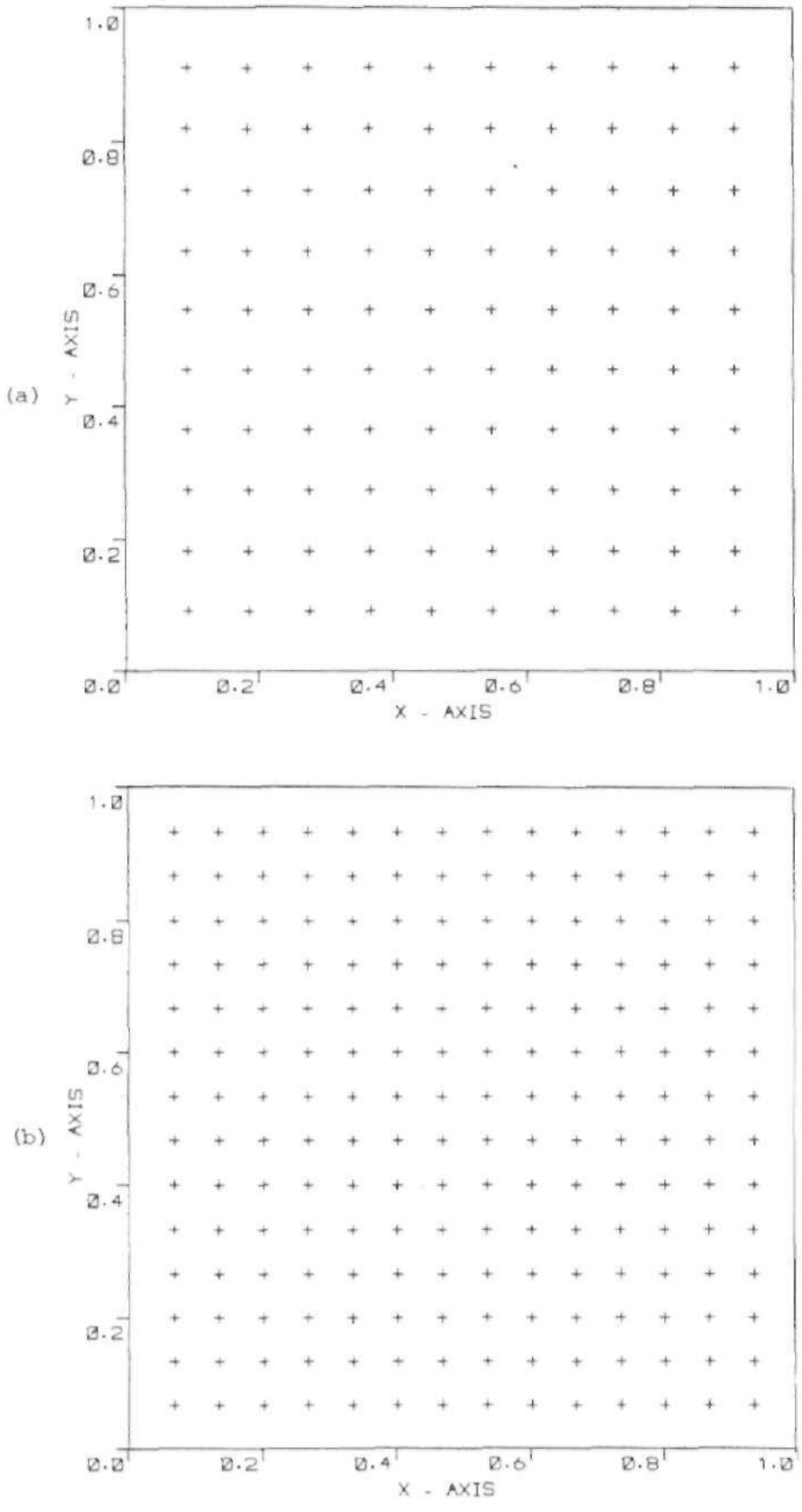


Figure 3.1 : Regular lattice of sampling points in a unit square window consisting of : (a) m=100 and (b) m=196 sampling points.

In order to obtain our edge corrections we considered a range of rectangular sampling windows having length/breadth ratios ranging from 1.0 to 3.0. We proceeded by keeping constant the number n of objects and varying the length/breadth ratio R, of the study area. The observed values of the mean and variance of $\bar{X}$ are then obtained for each R by:

(i) simulating s = 1000 Poisson processes of n objects each, in a region of ratio R [using the NAG Library Routine with seed G05CBF(1000)].

(ii) generating the values: $T_1, T_2, \ldots\ldots, T_s$, where $T_k = \sum_{i=1}^{m} x_i$ from the Poisson processes in (i).

(iii) using (ii) to compute:

$$E^{+}(\bar{X}) = \sum_{k=1}^{s} T_k / m\, s \qquad (3.1)$$

$$Var^{+}(\bar{X}) = \sum_{k=1}^{s} T_k^2 / s\, m^2 - \{ E^{+}(\bar{X}) \}^2 \qquad (3.2)$$

The procedures (i) to (iii) are then repeated for other values of n. From dimensional considerations we obtained these formulae,

$$E^{+}(\bar{X}) = 0.5 / \sqrt{\rho} + b_0 \sqrt{A} + k_0 P \qquad (3.3)$$

$$Var^{+}(\bar{X}) = b_1 A + k_1 P \sqrt{A} \qquad (3.4)$$

where b_0, k_0, b_1 and k_1 are expected to be functions of n.

We used values of n between 4 and 100 and upwards of 100000 simulations for each combination of window and number n of objects. For the case n = 16, the values of R, $Var^{+}(\bar{X})/A$, $P/\sqrt{A}$ and C, where

$$C = \{ E^{+}(\bar{X}) - 0.5/\sqrt{\rho} \} / \sqrt{A} \qquad (3.5)$$

Table 3.1. Values of $Var^{+}(\bar{X})/A$, C, R and $P/\sqrt{A}$ for n = 16, obtained by simulations.

R	$P/\sqrt{A}$	$Var^{+}(\bar{X})/A$	C
1/1	4.0000	0.00021071	-0.00231188
3.5/3	4.0119	0.00021320	-0.00227020
4/3	4.0415	0.00021959	-0.00214113
5/3	4.1312	0.00023814	-0.00170551
2/1	4.2426	0.00026067	-0.00121124
2.5/1	4.4272	0.00030145	-0.00038649
19/7	4.5090	0.00032031	-0.00001358
3/1	4.6188	0.00034681	0.00050115

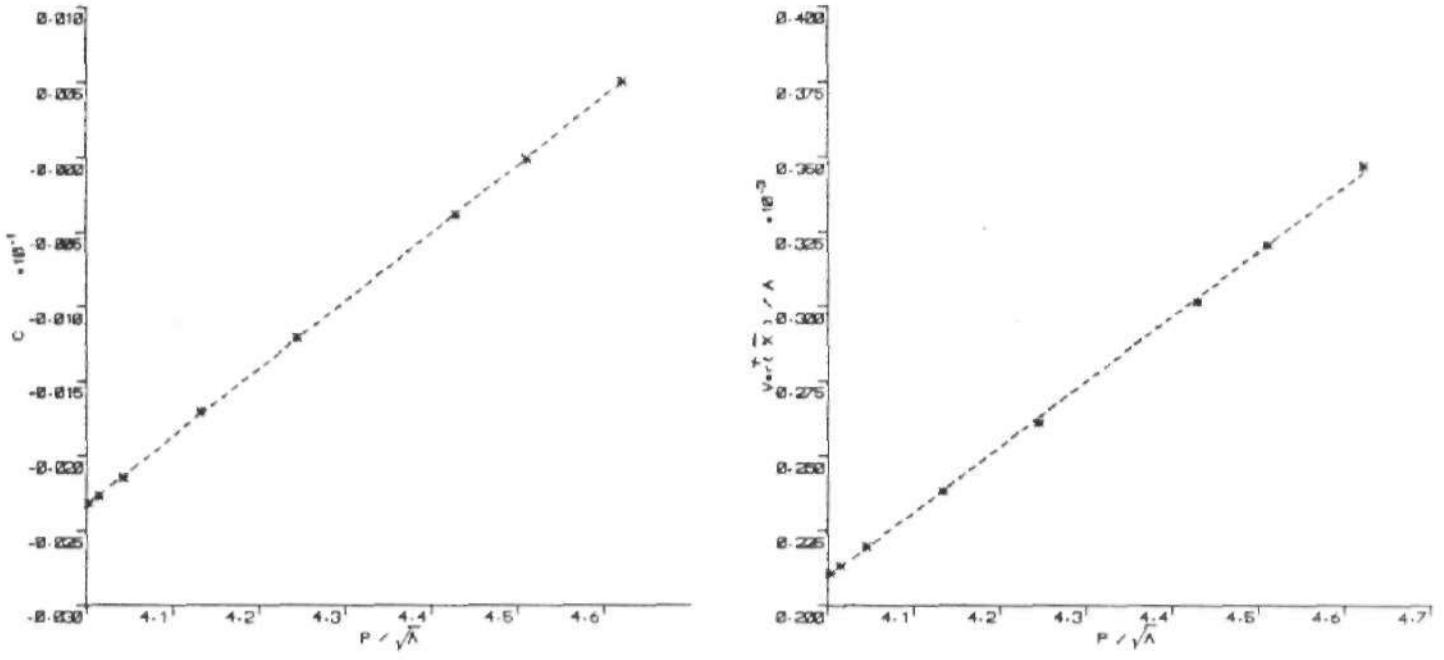
are tabulated in Table 3.1. The corresponding scattergrams, given in Figure 3.2, for C against $P/\sqrt{A}$, and $Var^{+}(\bar{X})/A$ against $P/\sqrt{A}$, suggest a strong linear relationship of the form,

$$Var^{+}(\bar{X})/A = b_1 + k_1 P/\sqrt{A} \qquad (3.6)$$

$$C = b_0 + k_0 P/\sqrt{A} \qquad (3.7)$$

Relationships corresponding to (3.6) and (3.7) hold for other values of n, though with different values for the constants.

For the variance, 18 different values of n were used, and the values of b_1 and k_1, were estimated in each case. These values are tabulated in Table 3.2, together with the correlation coefficient



(a) (b)

Figure 3.2 : The scattergrams (* * *) and the fitted lines (--------) of (a) C against $P/\sqrt{A}$ and (b) $Var^{+}(\bar{X})/A$ against $P/\sqrt{A}$ for the case n=16.

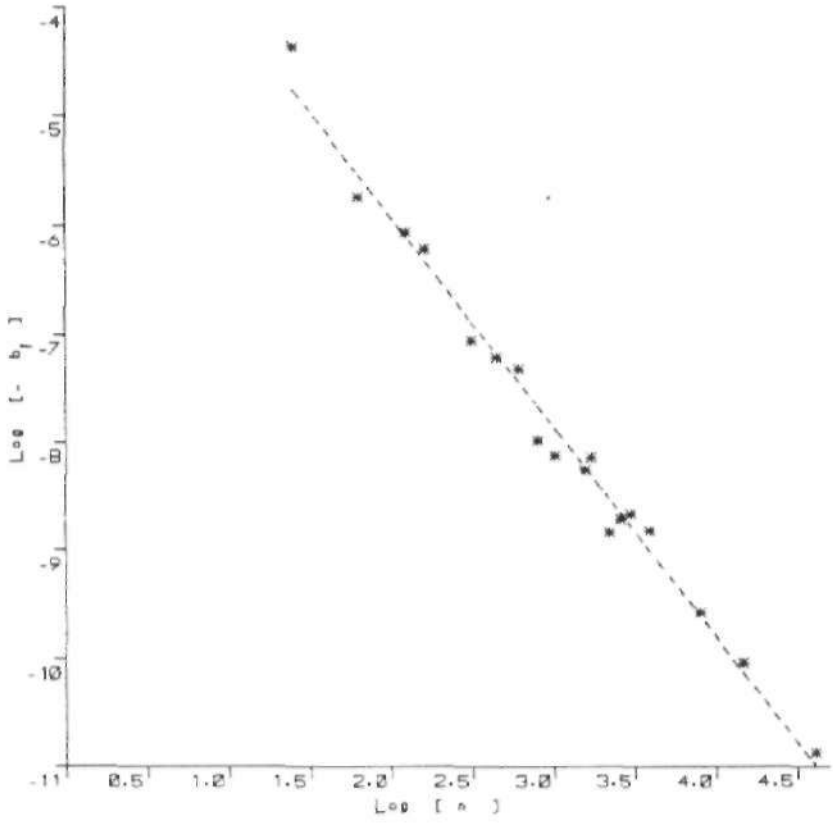
$r = \text{corr}(\text{Var}^{+}[\bar{X}]/A,\ P/\sqrt{A})$, which exceeds 0.99 in every case. Log $\{-b_1\}$ and log$\{k_1\}$ are plotted against log$\{n\}$ in Figure 3.3. The correlation coefficient r between log$\{-b_1\}$ and log$\{n\}$ and between log$\{k_1\}$ and log$\{n\}$ is -0.993 and -0.996 respectively. These values, together with the scatterplots suggest a relationship which is of the form

$$f(n) = e\ n^{d} \qquad (3.8)$$

Table 3.2. Estimates of b_1 and k_1 for different values of n.

n	b_1	k_1	r
4	-0.01267680	0.003947179	0.9948
6	-0.00321071	0.001130756	0.9935
8	-0.00234290	0.000795762	0.9954
9	-0.00199445	0.000663717	0.9952
12	-0.00086062	0.000293694	0.9977
14	-0.00073484	0.000244257	0.9942
16	-0.00066082	0.000217686	0.9997
18	-0.00034040	0.000121117	0.9988
20	-0.00029558	0.000104264	0.9996
24	-0.00025866	0.000086729	0.9987
25	-0.00028989	0.000093961	0.9999
28	-0.00014469	0.000050857	0.9992
30	-0.00016298	0.000053139	0.9989
32	-0.00017206	0.000053784	0.9986
36	-0.00014708	0.000046079	0.9988
49	-0.00006914	0.000022107	0.9999
64	-0.00004363	0.000014048	0.9997
100	-0.00001899	0.000005938	0.9994

(a)



(b)

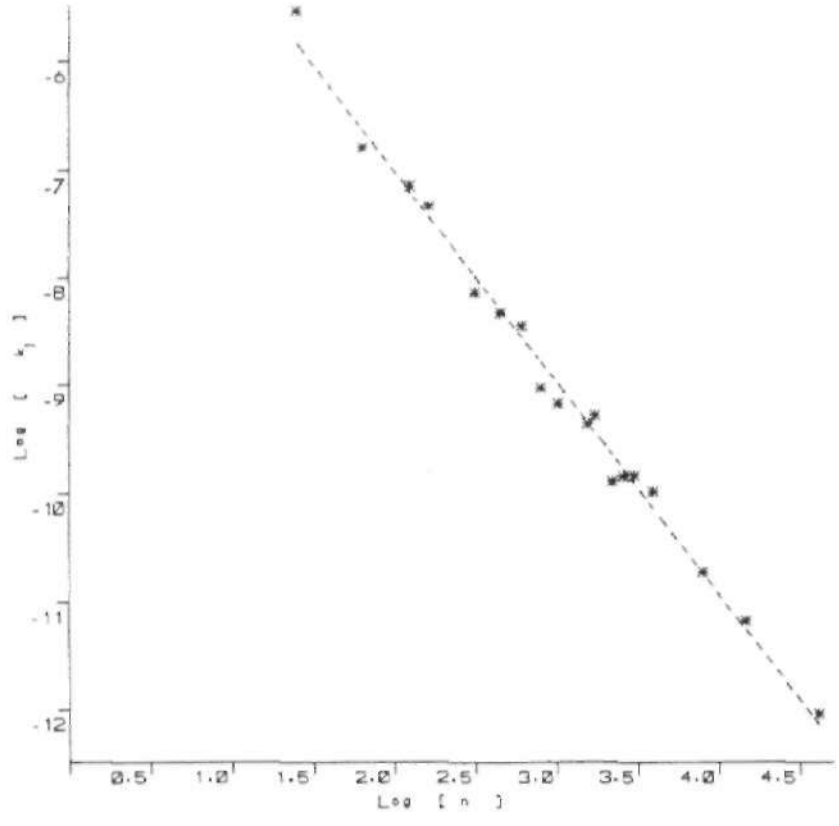


Figure 3.3 : The scattergrams (* * *) and the fitted lines of (a) log $[-b_1]$ against log[n] and (b) log $[k_1]$ against log[n] for the variance of $\bar{X}$.

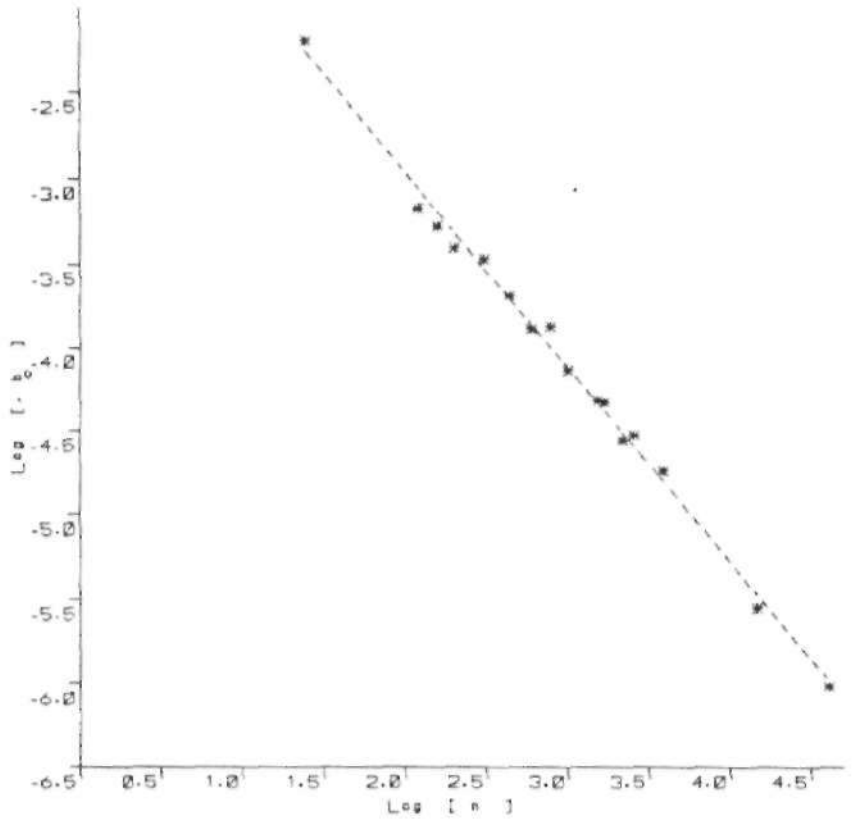
For the mean , 16 different values of n were used to estimate the values of the constants b_0 and k_0. These values are given in Table 3.3 together with the correlation coefficient r = Corr(C, P/ $\sqrt{A}$), which exceeds 0.995 in every case.

Table 3.3. Estimates of b_0 and k_0 for different values of n.

n	b_0	k_0	r
4	-0.11156860	0.02370474	0.9989
8	-0.04198899	0.00906248	0.9985
9	-0.03793382	0.00813189	0.9998
10	-0.03317367	0.00745401	0.9972
12	-0.03107437	0.00713886	0.9999
14	-0.02495672	0.00562903	0.9991
16	-0.02048584	0.00454203	0.9999
18	-0.02080001	0.00485157	0.9990
20	-0.01588578	0.00359153	0.9996
24	-0.01337687	0.00306951	0.9983
25	-0.01324221	0.00295389	0.9998
28	-0.01047494	0.00250205	0.9991
30	-0.01080990	0.00254557	0.9987
36	-0.00872799	0.00197492	0.9999
64	-0.00389466	0.00094457	0.9998
100	-0.00243802	0.00059134	0.9963

The scattergrams of the log values are presented in Figure 3.4. The values of the correlation coefficient r between the log values of $-b_0$ and n and between the log values of k_0 and n are both approximately -0.997. These values together with the scatterplots also suggest a relationship of the form given in equation (3.8). The constants e and d for the fitted curves are given in Table 3.4

(a)



(b)

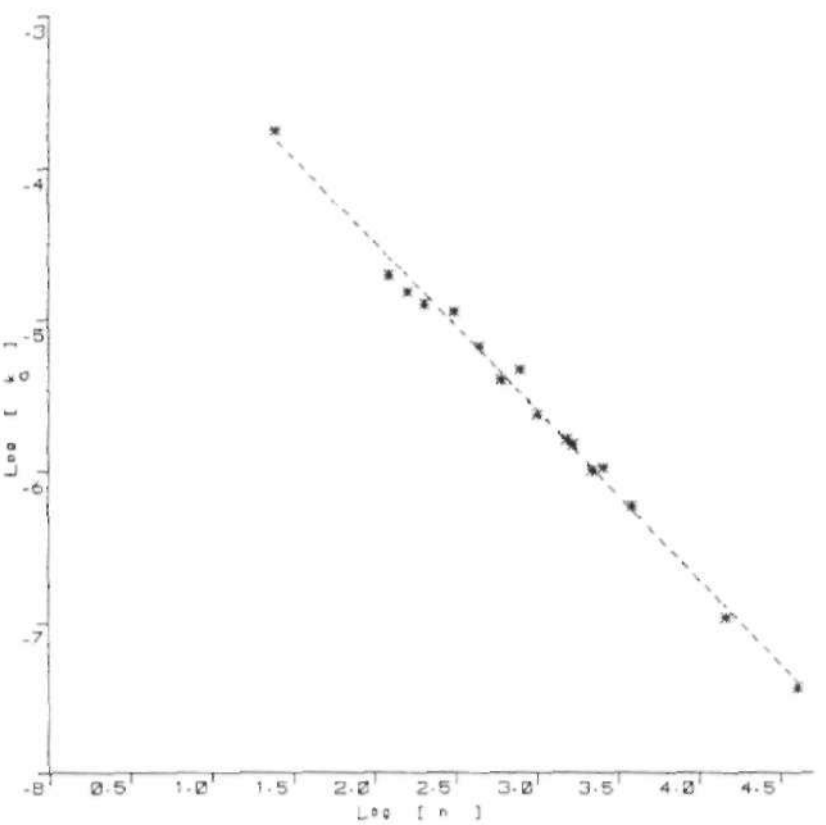


Figure 3.4 : The scattergrams (* * *) and the fitted lines of (a) log $(-b_0)$ against log(n) and (b) log $[k_0]$ against log [n] for the mean of $\overline{X}$.

From equations (3.6) to (3.8), we arrived at the following corrected moments

$$E^{+}(\bar{X}) = 0.5/\sqrt{\rho} - 0.5219\sqrt{A} \,/\, n^{1.1590} + 0.1044\, P \,/\, n^{1.1156} \qquad (3.9)$$

$$Var^{+}(\bar{X}) = 0.04445\, P\sqrt{A} \,/\, n^{1.9585} - 0.1265\, A \,/\, n^{1.9387} \qquad (3.10)$$

Table 3.4. Estimates of e and d

f(n)	e	d	r
b_0	-0.5219282	-1.158967	-0.9970
b_1	-0.1265228	-1.938685	-0.9930
k_0	0.1044379	-1.115572	-0.9965
k_1	0.0444535	-1.958486	-0.9957

Using these edge-corrections we obtain corrected statistics analogous to the uncorrected statistics R_m and M defined in equations (2.15) and (2.12) namely

$$R_m^{+} = \bar{x} \,/\, E^{+}(\bar{X}) \qquad (3.11)$$

and

$$M^{+} = \{ \bar{x} - E^{+}(\bar{X}) \} \,/\, \{ Var^{+}(\bar{X}) \}^{\frac{1}{2}} \qquad (3.12)$$

To test these edge corrections we generated random patterns within a rectangle having a length/breadth ratio of 10.0 - a much larger ratio than any considered during the derivation of these corrections. We obtained values of Y: $y_1, y_2, .., y_s$, for s = 1000 simulations at each of a variety

of combinations of m and n and calculated the first four moments, of both the uncorrected $Y = M$ and the edge corrected $Y = M^+$ statistics, as shown in Table 3.5, which also display corresponding results for a square window.

Table 3.5. Sample moments and Value of $D_s(Y)$ for the statistic $Y = M$ and $Y = M^+$.

m	n	Statistic	M_1	M_2	M_3	M_4	$D_s(Y)$
Length/breadth ratio 1							
49	47	M	-0.05	0.70	0.31	2.07	2.25
		M^+	0.02	0.95	0.49	3.79	0.90
49	49	M	-0.06	0.68	0.15	1.49	2.76
		M^+	-0.01	0.96	0.25	2.97	0.97
100	89	M	-0.03	0.73	0.21	1.69	1.76
		M^+	0.00	0.93	0.31	2.75	1.04
100	100	M	-0.02	0.69	0.20	1.60	1.99
		M^+	0.00	0.99	0.34	3.31	0.77
Length/breadth ratio 10.0							
49	47	M	0.79	3.26	1.86	35.31	8.80
		M^+	0.04	1.05	0.34	3.69	0.78
49	49	M	0.78	3.28	1.99	37.96	8.96
		M^+	0.05	1.11	0.39	4.30	0.95
100	89	M	0.73	3.37	1.90	34.65	8.75
		M^+	0.01	1.00	0.31	3.02	0.71
100	100	M	0.65	3.26	2.10	34.86	7.80
		M^+	-0.02	1.08	0.40	3.81	1.29
Theoretical values N(0,1)			0.00	1.00	0.00	3.00	-

We also calculated the value of the Kolmogorov - Smirnov statistic $D_s(Y)$ defined in equation (2.28)

For the test of a null hypothesis of a unit Normal distribution the test statistic $D_s(Y)$ has critical values 1.36 (5%) and 1.63 (1%). Table 3.5 shows clearly the sensitivity of the mean and variance of the

uncorrected statistic M, to the shape of the study region. The results for the edge-corrected statistic M_i^+ are all entirely acceptable.

Table 3.6. Edge effects on the statistics (M, R_m) and (M^+,R_m^+) as applied to the Japanese black pine, Biological cells and the Redwood seedlings.

Distribution	Japanese Black pine	Biological cells	Redwood seedlings
Area	32.4900	1.0000	625.0000
Perimeter	22.8000	4.0000	100.0000
n m	65 81	42 49	62 64
$\bar{x}$	0.3638	0.0560	2.0540
Uncorrected statistics			
$E(\bar{X})$	0.3535	0.0772	1.5875
$\sqrt{Var(\bar{X})}$	0.0205	0.0058	0.1037
R_m	1.0291	0.7253	1.2939
M	0.5007	- 3.6785	4.4976
Edge-corrected statistics			
$E^+(\bar{X})$	0.3525	0.0767	1.5828
$\sqrt{Var^+(\bar{X})}$	0.0192	0.0052	0.0884
R_m^+	1.0319	0.7291	1.2977
M^+	0.5851	- 3.9622	5.3283

3.3 Analysis of Japanese black pine saplings, biological cells and redwood seedlings

Both the uncorrected and the edge corrected statistics are applied to:

(i) Japanese black pine saplings (Figure 3.5a) consisting of 65 trees in a 5.7 metre square plot(Numata 1961). Previous analyses of these data by Bartlett(1964) and Besag and Diggle(1977) concluded that the observed distribution of the 2080 inter-tree distances is compatible with the

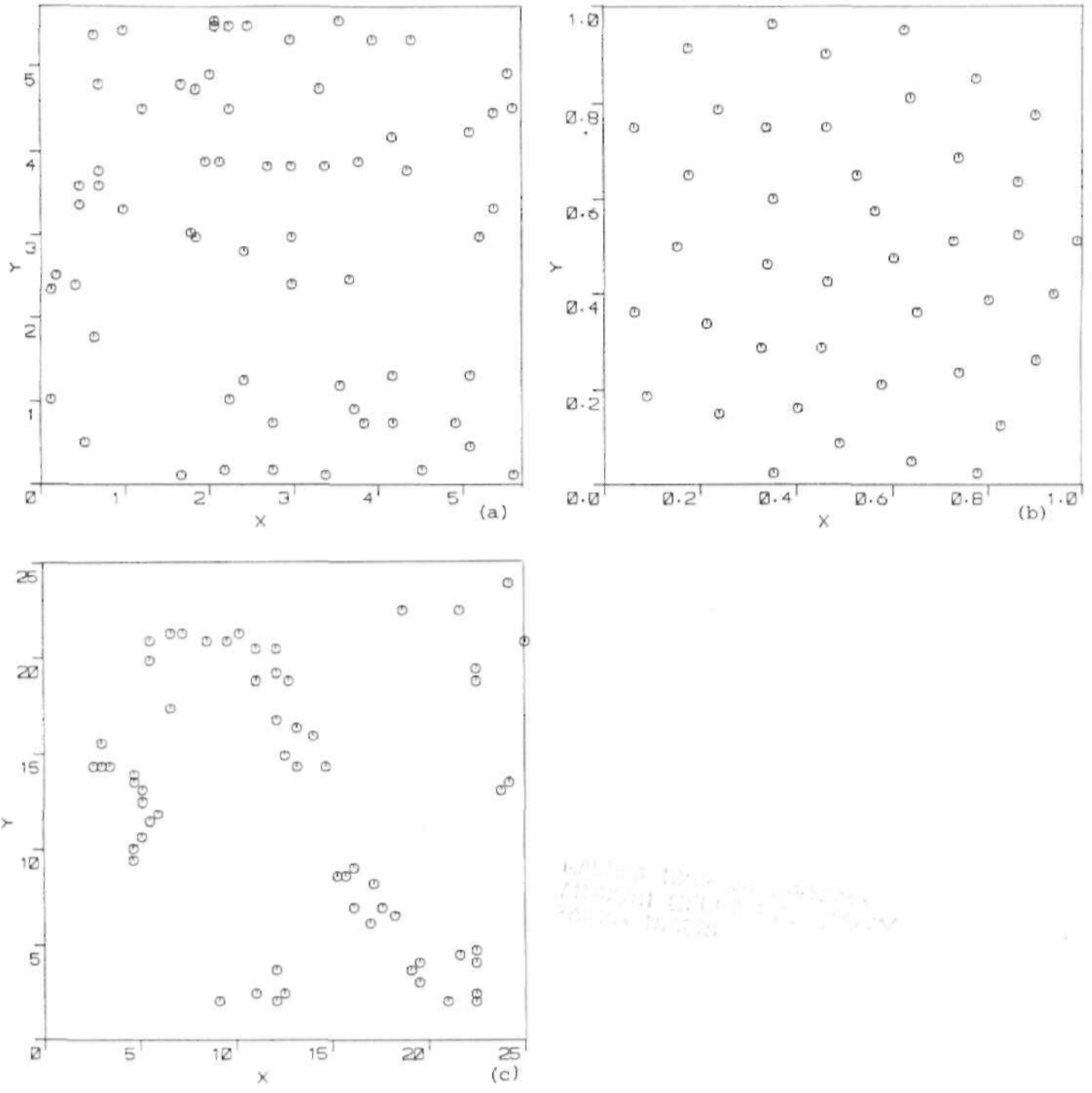


Figure 3.5 : (a) locations of 65 Japanese black pine saplings in a square of side 5.7m. (b) Locations of the 42 cell centres in a unit square and (c) locations of 62 redwood seedlings in a square of side 25m.

hypothesis of randomness.

(ii) The Biological cells data (Figure 3.5b) consisting of 42 cell centres in a unit square (Ripley, 1977). The cell centres are distributed more or less regularly over the unit square.

(iii) The redwood seedlings (Figure 3.5c) consisting of 62 trees in a 25 metre square plot (Ripley, 1977). Previous analysis of these data suggests a deviation towards an aggregated alternative.

Table 3.6 presents a summary of the analyses of the three patterns, for the statistics M and M^+ . For the Japanese black pine saplings, a test of significance based on the uncorrected M test gave a value of 0.5007, indicating that a departure from the hypothesis of randomness might occur 61.7% of the time purely by chance. However when the edge-corrected M^+ test is applied, a value of 0.5851 is obtained; indicating that such a departure can occur 56% of the time purely by chance. The index of non-randonness, R_m^+ for this data is equal to 1.03, which is not significantly different from one. This value suggests that there is no significant interaction between the trees, and that they all occur randomly in the study area.

For the Biological cells data, the value of R_m^+ is much smaller than one. This value comfirms the degree of regularity in the data shown by previous studies. The corresponding value of M^+ using the edge-corrected moments is -3.9622, which is highly significant.

The value of R_m^+ for the Redwood data is much greater than expected, suggesting aggregation in the data. The corresponding value of M^+ is highly significant.

Note that these edge-corrections for M make little difference in extreme cases, as was the case in the examples above.

3.4 Alternative statistics to CE and M

3.4.1 Quadrat count index of dispersion

If the study region D is partitioned into $m = k^2$ smaller subregions or 'quadrats', each of area A_k, and a count $\{z_i\}$, $i = 1, 2, .., m$, made of the number of objects in each of the m quadrats, then under the null hypothesis of a random distribution of objects, the random variable Z follows a Poisson distribution with mean $\lambda = \rho A_k$. The parameter ρ is the intensity of the process, defined as the mean number of objects per unit area. Explicitly, the probability distribution of Z is,

$$P[\ Z = z\ ] \quad = \quad \lambda^{z} \quad \exp\{\ -\ \lambda\ \}\ /\ z\ !, \qquad (3.13)$$

where $z = 0, 1, 2, \ldots\ldots$ and $Var(Z) = E(Z) = \lambda$. For alternatives involving patches of objects (aggregation) we would expect Var(Z) to be greater than E(Z), while for a more regularly spaced objects, $Var(Z) < E(Z)$. These properties led ecologists to consider the statistic,

$$Q \quad = \quad Var(Z)\ /\ E(Z) \qquad (3.14)$$

as a population index to measure pattern. A natural sample statistic to Q is the sample variance to mean ratio q due to Clapham(1936). This statistic is given by the equation,

$$q \quad = \quad \sum_{i=1}^{m} (z_i\ -\ \bar{z}\ )^2 /\ (m\ -\ 1)\ \bar{z} \qquad (3.15)$$

whose intuitive appeal rests on the equality of the mean and variance of the Poisson distribution. The numerator,

$$S^2 = \sum_{i=1}^{m} (z_i - \bar{z})^2 / (m-1) \qquad (3.16)$$

estimates the variance of Z when no distributional assumptions are made, whilst the denominator , $\bar{z}$ estimates the variance under the Poisson forest. Thus, in the case of a Poisson forest, q equals unity, and the individual objects are then regarded as being located at random. The objects are said to be clustered when $q > 1$ and regular when $q < 1$.

In order to assess the significance of the departure from randomness, we use a closely related statistic I, first used by Fisher et al (1922):

$$I = (m-1)q \qquad (3.17)$$

who pointed out that under the Poisson forest the sampling distribution of I is approximately Chi-squared with (m-1) degrees of freedom.

The distribution of the index of dispersion I, and the validity of assuming that it is distributed as Chi-squared with (m-1) degrees of freedom, has been discussed at some length by Hoel(1943). He concluded that the assumption of the Chi-squared distribution was valid for m as small as 5, as long as the Poisson parameter λ is greater than or equal to 5; and that for λ less than 5, the approximation remains fairly accurate. However Hoel's method was not altogether satisfactory in that it was based on a comparism of moment ratios, these moments themselves being infinite series.

Kathirgamatamby (1953) considered an alternative approach by considering the 'overall' distribution of the index of dispersion for any given total T, of the observed values of the counts. Now the probability statement connected with the test of significance based on (3.17) takes the form:

$$P\left[\ I\ >\ \chi^2_{m-1,\ \alpha}\ \right]\ =\ \alpha$$

or

$$P\left[\left(\sum_{i=1}^{m}(z_i-\bar{z})^2-\chi^2_{m-1,\alpha}\quad \bar{z}\right)\ >\ 0\ \right]\ =\ \alpha \qquad (3.18)$$

If k_1 and k_2 denote the first two of Fisher's k-statistics, then equation (3.18) becomes,

$$P\left[\{(m-1)\ k_2\ -\ k_1\ \chi^2_{m-1,\alpha}\ \}\ >\ 0\right]\ =\ \alpha$$

Let,

$$S\ =\ (m-1)k_2\ -\ k_1\ \chi^2_{m-1,\alpha}$$

Kathirgamatamby calculated the exact moments of S and used a curve fitting technique to obtain the probability integrals, which were compared with those of χ^2. His results suggests that for either m large, λ large, or both m and λ large, the χ^2 distribution is a reasonably good approximation. In fact, there appears to be little risk of error for m as small as 6 provided that λ is greater than or equal to unity.

The index of dispersion test is extensively used to detect spatial pattern by, for example, plant ecologists. Perry and Mead (1979) examine its power using a semi-analytical technique over a wide class of aggregated alternatives to the null hypothesis of the Poisson process. Their results suggest that the index of dispersion provides a powerful test of randomness against these alternatives. Furthermore, Payandeh (1970) arrived at the same conclusion but argued that results using the index of dispersion may be greatly affected by the quadrat size.

Other test statistics based on quadrat counts, which have been proposed, are fairly closely related to the index of dispersion. As an example, the test procedure usually recommended for Morisita's index, I_σ (Morisita, 1959) is to calculate,

$$F = [I_\sigma (\sum_{i=1}^{m} z_i - 1) + m - \sum_{i=1}^{m} z_i] /(m -1)$$

However, $F = I/(m-1)$ and hence the test for Morisita's index is equivalent to that for the index of dispersion.

The other main developments in tests based on quadrat counts is the use of contiguous quadrat methods initiated by Greig-Smith (1952). Further developments in this area are provided by among others, Mead(1974), Upton(1984) and Upton and Fingleton (1985).

3.4.2 Quick test using small distances.

Sometimes a quick test of the Poisson forest of a spatial point pattern is required, for example to decide whether a more detailed analysis would be justified. One such test can be constructed by concentrating on small distances and using as test statistics the first few ordered inter-object distances $d_1 \leq d_2 \leq \ldots\ldots$, which can usually be picked out easily by eye.

Ripley and Silverman(1978) suggest that the upper tail of d_1 should give a uniformly most powerful test of randomness against a model of randomly nonoverlapping discs as formalized by Kelly and Ripley(1976). They have also noted some advantages in using other distances, in particular, d_3 and d_5, in that they are less likely to be affected by either measurement errors or inhomogeneity. Silverman and Brown(1978) have shown that the statistic

$$S_k = n(n-1)\pi d_k^2/A \qquad (3.19)$$

Table 3.7. Number of occasions (max 50) in which a test of randomness at the 5% level resulted in rejection of the null hypothesis when the data actually arose from a Strauss process with interaction range r and strength c = h(r)

Entries within the table refer to results for statistics d_1 to d_8 arranged in the following way:

$$d_3 \quad \begin{matrix} d_1 & d_2 \\ d_5 & d_4 \\ d_7 & d_8 \end{matrix} \quad d_6$$

					n = 32							
c =	0.3				0.15				0.0			
r = 0.03	2	7 4 3	5 4 3	3	6	7 4 5	7 5 6	4	7	16 2 4	8 5 3	3
r = 0.06	20	16 13 9	25 17 8	9	43	35 27 19	44 32 16	20	46	50 32 23	50 39 20	29
r = 0.09	22	14 31 38	17 29 42	37	39	24 47 49	31 44 49	48	50	50 50 50	50 50 50	50
					n = 64							
c =	0.3				0.15				0.0			
r = 0.015	5	11 7 6	3 7 4	6	5	9 6 5	7 6 3	5	10	9 5 6	9 5 5	3
r = 0.035	34	17 28 24	29 36 19	27	47	28 43 31	40 50 28	37	50	50 50 44	50 50 42	46
r = 0.045	31	18 39 44	21 33 44	41	43	30 50 50	37 47 50	50	50	50 50 50	50 50 50	50

converges in distribution to a Chi-squared variable with 2k degrees of freedom. Ripley and Silverman (1978) have shown that the Chi-squared approximation is adequate provided that $k \leq 10$ when $n \geq 30$ or $n \geq 15$ for $k = 1$. Thus S_k can be used to test for any significant departure of d_k

from the Poisson hypothesis without resorting to Monte Carlo simulations.

Table 3.7 shows the results of an investigation into the robustness of d_k, for values of $k \leq 8$. The statistic d_k is computed by regarding the sampling window as a torus. The alternative considered is the Strauss process with parameters r and c, and is simulated using the algorithm of Ripley(1979b). Note that c = 0 corresponds to a hard core model of radius r, and that c > 0 represents a non-strict inhibition (or soft-core).

The results of Ripley and Silverman(1978) suggest that the test based on d_1 is more powerful than those based on either d_3, or d_5 against a hard-core model, whereas tests based on d_3 against the Strauss process and the pairwise interaction process (as formalized by Ripley(1977)) are more powerful than those based on d_1 and d_5.

For small (n=32) and moderate (n= 64) sample sizes, it is obvious from Table 3.7 that both d_1 and d_2 are more robust than the other statistics against the hard-core model, with d_1 being marginally preferable. However, for the soft-core model, d_2 is marginally more robust than d_1. There is little to choose between d_3 and d_4, however both statistics are slightly more robust than d_5. For r large, both d_7 and d_8 are clearly preferable to all the other statistics against the soft core model. Repeated simulations using different seeds produced very similar results.

3.4.3 Squared nearest-neighbour distances.

If we define $V = W^2$, then from equation (2.2), we have

$$g(v) = f(w) \left| dw/ dv \right|$$

$$= \pi \rho \exp(- \pi \rho v) \quad , v > 0 \qquad (3.20)$$

Thus the random variable V has an exponential distribution with parameter

$\pi\rho$. It follows therefore that $E[V] = 1/\pi\rho$ and $Var[V] = 1/(\pi\rho)^2$.

Suppose $v_1, v_2, \ldots, v_n$ are the squared nearest neighbour distances of the n objects in D. Brown(1975) and Brown and Rothery(1978) consider the average ($\bar{V}$), the square of the coefficient of variation (S) and the ratio of the geometric mean to the arithmetic mean (G) of the squared distances. These are defined as

$$\bar{V} = \sum_{i=1}^{n} v_i / n \qquad (3.21)$$

$$S = \sum_{i=1}^{n} (v_i - \bar{V})^2 / (n-1)\,\bar{V}^2 \qquad (3.22)$$

$$G = \exp\{\frac{1}{n} \sum_{i=1}^{n} \log v_i\} / \bar{V} \qquad (3.23)$$

Eberhardt(1967) proposed an essentially equivalent form of S, but his statistic was based on distances as opposed to squared distances. Ripley(1979a) noted that no adequate approximation to the sampling distribution of any of the statistics (3.21) to (3.23) is known.

A natural interpretation of πv_i is the area searched in finding the nearest neighbour of the i^{th} object. This suggests some edge corrections for (3.21) to (3.23) by replacing v_i by the actual area searched, a_i say within the sampling window D to obtain,

$$\bar{V}_a = \sum_{i=1}^{n} a_i / n \qquad (3.24)$$

$$S_a = \sum_{i=1}^{n} (a_i - \bar{V}_a)^2 / (n-1)\,\bar{V}_a^2 \qquad (3.25)$$

$$G_a = \exp\{\frac{1}{n} \sum_{i=1}^{n} \log a_i\} / \bar{V}_a \qquad (3.26)$$

Alternatively (for a square or rectangular window D of dimensions a x b), we can use toroidal edge-corrections to obtain,

$$\bar{V}_t = \sum_{i=1}^{n} v_i^t / n \qquad (3.27)$$

$$S_t = \sum_{i=1}^{n} (v_i^t - \bar{V}_t)^2 / (n-1)\, \bar{V}_t^2 \qquad (3.28)$$

$$G_t = \exp\{\frac{1}{n} \sum_{i=1}^{n} \log v_i^t\} / \bar{V}_t \qquad (3.29)$$

where $v_i^t = \underset{j}{\text{Min}} \{ v_{ij} \}$, $i \neq j$

and $v_{ij} = \{p(x_i, x_j, a)\}^2 + \{p(y_i, y_j, b)\}^2$

$$p(z_i, z_j, c) = \text{Min}(|z_i - z_j|, c - |z_i - z_j|)$$

The values of $\bar{V}_a$, $\bar{V}_t$ and S that would be expected if the pattern were random would be close to $1/\rho$, $1/\pi\rho$ and 1 respectively. This suggests using

$$\bar{V}'_a = |\bar{V}_a - 1/\rho| \qquad (3.30)$$

$$\bar{V}'_t = |\bar{V}_t - 1/\pi\rho| \qquad (3.31)$$

and $$S' = |S - 1| \qquad (3.32)$$

as test statistics.

Table 3.8. Number of occasions (max 50) in which a test of randomness at the 4% level resulted in rejection of the null hypothesis when the data actually arose from (a) a Strauss process with interaction range r and strength c = h(r) and (b) a Poisson cluster process with parameter μ and σ.

(a)

Entries within the table refer to results for six statisitcs arranged as follows:

N	c	r	$\bar{V}_a'$	$\bar{V}_t'$	G_a	G_t	S_a'	S_t'
25	0	0.04	0	1	9	7	0	0
25	0	0.06	0	2	29	37	0	0
25	0	0.08	4	12	40	50	0	0
25	0.2	0.08	1	8	23	30	0	0
25	0.3	0.15	5	25	4	5	0	0
100	0	0.015	0	2	21	21	1	0
100	0	0.03	5	16	50	50	11	20
100	0.2	0.03	4	11	44	47	6	13
100	0.3	0.05	27	42	43	43	27	32
100	0.5	0.05	6	17	25	25	10	19

(b)

N	μ	σ	$\bar{V}_a'$	$\bar{V}_t'$	G_a	G_t	S_a'	S_t'
25	1	0.10	16	11	0	0	5	3
25	1	0.05	46	34	1	0	27	31
25	2	0.08	37	35	0	0	14	6
25	3	0.08	46	46	0	0	9	8
100	1	0.05	33	36	0	0	23	27
100	4	0.05	50	50	0	0	31	28
100	2	0.08	16	14	0	0	12	12
100	3	0.12	3	2	1	0	12	14

The statistic G_a is the ratio of the geometric mean of the a_i to the arithmetic mean of the a_i and therefore lies in the interval (0,1). This follows from the fact that for any given series of positive values, not all the same, the geometric mean is always less than the arithmetic mean. The value of G_a would largely depend on the amount of variability (or dispersion) of the a_i. The amount of dispersion of the a_i's for a Poisson forest would be larger on average compared to either a regular or a clustered pattern. In such a distribution G_a would tend to zero. However for a regular or clustered pattern, the variability amongst the a_i's will be small, and so the geometric mean and the arithmetic mean would converge on each other, and so G_a will then tend to one.

Table 3.8 (a and b) shows the results of an investigation into the effectiveness of the two edge-correction methods for the three statistics V, S and G. The alternatives considered were the Strauss processes and the Poisson cluster processes.

It can be seen from the tables that toroidal edge-correction is generally effective, and is clearly preferable in the case of the regular alternatives. However, for clustered alternatives there is little to choose between the two edge-correction methods. Furthermore, these results suggest that V is powerful against clustering while G is effective against regularity.

3.5 Power study

In this section we compare the power of the M^+ and the CE^* tests with the alternatives considered in Section 3.4 of this chapter. The simulations involve patterns of $n = 64$ objects generated in D, a square of unit side.

For the quadrat index of dispersion, we use the statistic I defined in (3.17). Although m here is arbitrary, the formal equivalence of I to Pearson's Chi-squared goodness-of-fit criterion for a uniform distribution on D suggests the choice m = 16 which with a total of 64 objects gives $\bar{z} = 4$ and the null distribution of I is then Chi- squared with 15 degrees of freedom.

Table 3.9 Number of occasions (max 50) in which a test of randomness at the 4% level resulted in rejection of the null hypothesis when the data actually arose from a Poisson cluster process with parameters μ and σ .

Entries within the table refer to results for the six statistics arranged as follows:

$$\begin{pmatrix} I & CE^* & M^+ \\ G_t & S_t' & \bar{V}_t' \end{pmatrix}$$

σ =	0.04	0.08	0.12	0.16
μ = 1	$\begin{pmatrix} 27 & 45 & 42 \\ 0 & 33 & 46 \end{pmatrix}$	$\begin{pmatrix} 22 & 8 & 21 \\ 0 & 4 & 9 \end{pmatrix}$	$\begin{pmatrix} 12 & 2 & 10 \\ 0 & 1 & 0 \end{pmatrix}$	$\begin{pmatrix} 6 & 0 & 6 \\ 2 & 1 & 1 \end{pmatrix}$
μ = 2	$\begin{pmatrix} 45 & 50 & 50 \\ 0 & 29 & 50 \end{pmatrix}$	$\begin{pmatrix} 37 & 26 & 36 \\ 0 & 17 & 10 \end{pmatrix}$	$\begin{pmatrix} 27 & 2 & 21 \\ 0 & 8 & 0 \end{pmatrix}$	$\begin{pmatrix} 21 & 1 & 13 \\ 0 & 6 & 1 \end{pmatrix}$
μ = 3	$\begin{pmatrix} 49 & 50 & 50 \\ 0 & 26 & 50 \end{pmatrix}$	$\begin{pmatrix} 44 & 30 & 43 \\ 0 & 15 & 19 \end{pmatrix}$	$\begin{pmatrix} 31 & 11 & 30 \\ 0 & 16 & 0 \end{pmatrix}$	$\begin{pmatrix} 20 & 4 & 14 \\ 0 & 7 & 4 \end{pmatrix}$

From the squared nearest neighbour distances, we have the statistics $\bar{V}_t'$, S_t' and G_t defined in equations (3.31), (3.32) and (3.29) respectively. They are then implemented using a straightforward Monte Carlo approach, and the Monte Carlo 4% significant points were derived using 500 simulations of the Poisson process.

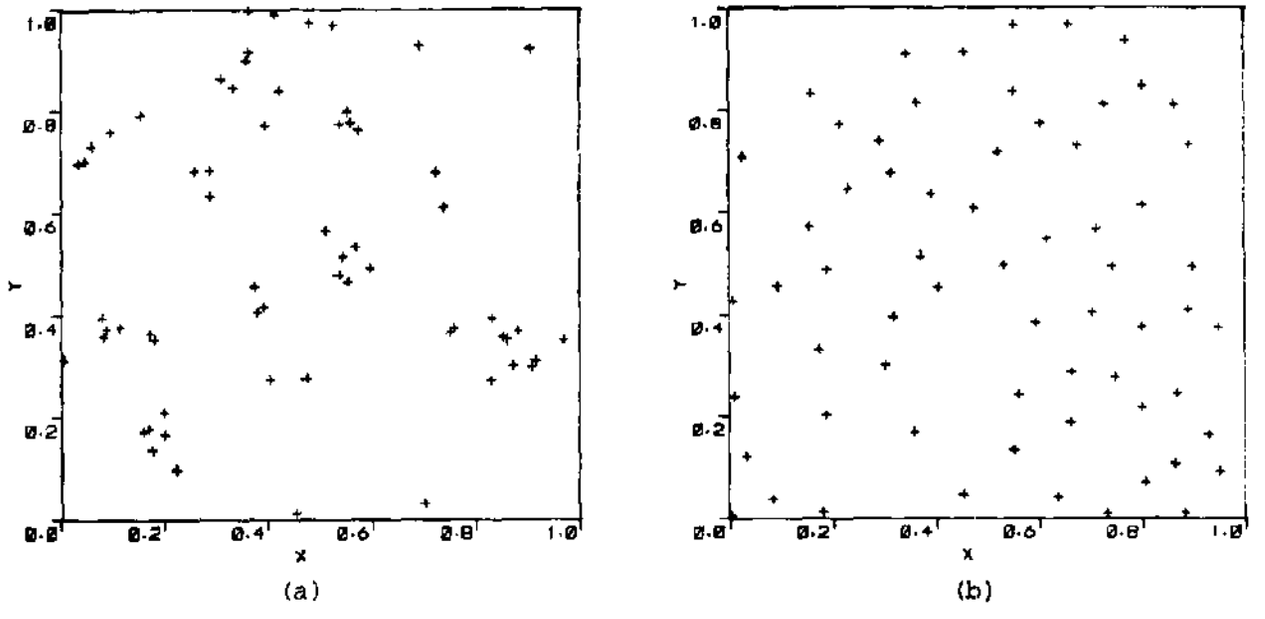


Fig. 3.6: Partial realizations of (a) a Poisson cluster process with parameters σ = 0.04 and μ = 2 and (b) a Strauss process with parameters C = 0.0 and R = 0.065; 64 plants in a unit square.

The alternative processes considered were the Poisson cluster processes and the Strauss processes described in Chapter I. The latter processes were simulated by the algorithm of Ripley(1979b). Figures 3.6a and b show partial realizations of the two processes consisting of 64 objects in the unit square D.

Fifty realisations were generated for each process and a range of parameter values. Table 3.9 and 3.10 record the numbers of occasions on which the hypothesis of spatial randomness was rejected by a 4% test.

Ripley(1979a) compared the edge-corrected CE^* statistic with six others and concluded that it showed up well, though it was less effective than Brown's statistic G_t for regular patterns and inferior to the quadrat based statistic I for clustered patterns (see Upton and Fingleton,1985 p 75 and pp 90 - 94). We can see from Table 3.9 and 3.10 that this is clearly the case.

Diggle(1979a) considered the CE^* statistic with six other statistics which included I. He found the CE^* statistic quite powerful. The result in Table 3.9 suggests that CE^* is still powerful, though it is less effective than I and the edge-corrected M^+ statistic. Also from this Table, it is clear that the Brown statistics are not so powerful against these alternatives.

As the results of Table 3.10 indicate, the M^+ statistic is very weak against the regular alternatives. Note however that the statistic G_t is quite powerful against these alternatives.

The rejection of the null hypothesis of spatial randomness is seldom an end in itself, but should be seen as an aid to a more ambitious analysis involving tests based on some functional statistics, such as the Ripley's K(t) function and the nearest neighbour distributions, discussed in subsequent chapters, together with graphical analysis.

CHAPTER IV

The Second Order Methods

4.1 Introduction

Suppose that an observed point pattern can be considered as a realization of a spatial point process model which is stationary and isotropic. The property of the underlying spatial point process elicited, directly or indirectly, by the second order methods is the second moment cumulative function K(t) introduced by Ripley(1976,1977). This function K(t) has attracted considerable attention and is defined through the relation,

$$\lambda^2 A\, K(t) = E\{ \text{number of ordered pairs of distinct objects, the first in D, the second within distance t of the first but not neccessarily in D} \} \qquad (4.1)$$

Here D is the window, typically a rectangle with sides a and b ($a \leq b$), diagonal of length d and area A. The parameter λ is the intensity of the object process defined as the mean number of objects per unit area. An equivalent definition is provided by the relation,

$$\lambda K(t) = E\{ \text{number of other objects within a distance t of an arbitrary object of the process} \}$$

$$= \int_0^{2\pi} \int_0^{t} \{\lambda_2 (r) / \lambda \} \, r \, dr \, d\theta \qquad (4.2)$$

where $\lambda_2(r)$ is the second order intensity function of the stationary isotropic process, and r is the distance between any two objects of the process.

The usual reference point for object patterns is the random object pattern or Poisson forest, for which $K(t) = \pi t^2$. This result suggests the use of the statistic L(t) defined by

$$L(t) = \left[K(t) / \pi \right]^{\frac{1}{2}} \qquad (4.3)$$

Besag, in the discussion of Ripley(1977) suggested the use of a square-root scale to linearize the plot of K(t) against t for a Poisson process. This also acts as a variance stabilizer.

In the case of a Poisson forest L(t) = t for all values of t. For a real object pattern , a plot of L(t) against t can be used to detect the nature of any departures from randomness. For clustered or aggregated patterns, there are an abundance of objects at short distances from one another and hence $L(t) > t$, whereas with repulsion between the objects (regularity), there will be a deficit of objects at short distances and hence $L(t) < t$. The relations $L(t)>t$, $L(t)<t$ are for small t, asymptotically $L(t) \rightarrow t$.

Although this chapter is ostensibly concerned with the estimators of K(t), it will be noted that these estimators are not obtained directly but are derived from the estimators of either $\lambda^2 AK(t)$ or $\lambda K(t)$, the left hand sides of equations (4.1) and (4.2). Furthermore, equation (4.3) involves $\{K(t)\}^{\frac{1}{2}}$ rather than K(t) itself. An optimal estimator of K(t) need not be optimal for $\{K(t)\}^{\frac{1}{2}}$, and we therefore examine the properties of the existing estimators of K(t) in the context of L(t). We also introduce a new estimator of K(t) motivated by definition (4.2), which is unbiased for a Poisson process and which we find from simulations to be approximately unbiased for non-random process models and to have a somewhat smaller mean

squared error than the alternatives suggested previously.

4.2 The estimators of K(t)

4.2.1 The naive estimator

A naive approach consists of counting the number of observable pairs of objects, lying within the window D, that are less than a distance t apart. The resulting estimator, $\hat{K}_1(t)$ is given by the equation

$$\lambda^2 \hat{K}_1(t) = \sum_{i \neq j}^{n} \sum^{n} 1_{ij} / A \qquad (4.4)$$

where $1_{ij} = 0$ if the distance between the i^{th}object and the j^{th}object is more than t, and $1_{ij} = 1$, otherwise. Usually the value of λ^2 would be unknown, in which case it can be replaced by the estimate, $n(n-1)/A^2$, which is unbiased for a Poisson process.

The resulting estimator $\hat{K}_1(t)$, is evidently negatively biased, since it fails to take proper account of neighbouring objects lying undetected outside D but in its vicinity. Now

$$E\{ A \lambda^2 \hat{K}_1(t)\} = E\{ \sum_{i \neq j}^{n} \sum^{n} 1_{ij} \} \qquad (4.5)$$

Ohser et al (1985) show that for a Poisson process, the right-hand side of (4.5) is

$$E\{ \sum_{i \neq j}^{n} \sum^{n} 1_{ij} \} = \lambda^2 \int_0^t \gamma_D(r)\, dK(r) \qquad (4.6)$$

where $\gamma_D(r) = E\{\text{area of } (D \cap D+ y)\}$ and y is uniformly distributed on the boundary of the circle center the origin and radius r. The

function $\gamma_D(r)$ can be interpreted in the following way:

Consider the object X_j situated at a distance r from the arbitrary object X_i. Suppose that it is known that the line $X_i X_j$ makes an angle θ to some reference direction. A moment's consideration reveals that the position of X_j is restricted, because it is known that X_i lies within the window. If θ is known then it is an easy matter to calculate the area of the restricted region within which X_j must lie. However, a different value of θ would lead to a different position for the restricted region and this need not have the same area. If the process is isotropic, then all the values of θ are equally likely and we then require $\gamma_D(r)$, the average area of the corresponding equally likely restricted regions.

For our rectangular window Ohser et al (1985) deduce that for small enough r, $\gamma_D(r)$ is approximately equal to $A - r(2a+2b)/\pi$. Therefore,

$$E\{\sum_{i\neq j}^{n}\sum^{n} 1_{ij}\} = \lambda^2 \int_0^t \gamma_D(r)\, dK(r)$$

$$\simeq \lambda^2\{A\int_0^t dK(r) - [(2a+2b)/\pi]\int_0^t r\, dK(r)\}$$

However for a Poisson process, $K(r) = \pi r^2$, and $dK(r) = 2\pi\, rdr$. Whence

$$E\{\sum_{i\neq j}^{n}\sum^{n} 1_{ij}\} \simeq \lambda^2 A\, \pi\, t^2 - 4\,\lambda^2 t^3(a+b)/3$$

Thus

$$E\{\hat{K}_1(t)\} \simeq \pi t^2 - 4t^3(a+b)/3ab, \text{ for small enough } t.$$

4.2.2 Border edge correction.

A simple procedure that avoids the problem inherent in (4.4) is to consider only those objects within a variable inner window D_σ which shrinks as t increases. Thus, for the case $t = t'$, the inner window is a centrally located rectangle of dimensions $(a - 2t')$ by $(b - 2t')$. The effect is that the positions of any objects up to a distance t' outside the inner window are known. The resulting estimator $\hat{K_2}(t)$ is given by the equation,

$$\lambda^2 \hat{K_2}(t) = \sum_{i}^{n_o} \sum_{j}^{n} 1_{ij} \; / \; A_o \qquad (4.7)$$

Here A_o is the area of D_o and n_o is the number of objects in D_o. If λ^2 is unknown, it can be estimated by the estimate $n_o(n-1)/AA_o$. Evidently, $\hat{K_2}(t)$ is unbiased for all values of t that are less than a/2 and providing that the inner window is not empty of objects. To see this, we obtain the expected value of (4.7) conditional on the number n_o of objects in D_o as,

$$E\{\lambda^2 A_o \hat{K_2}(t) \; / \; N(D_o) = n_o \} = E\left[\sum_{i}^{n_o} \sum_{j}^{n} 1_{ij}\right]$$

$$= \sum_{i}^{n_o} \sum_{j}^{n} E[\, 1_{ij}] \text{ , for a Poisson process}$$

$$= \sum_{i}^{n_o} \sum_{j}^{n} \int_0^t \left\{ \int_{D \cap \partial b(x_i, r)} dV \right\} dr \; / \; A, \text{ where } r = d(X_i, X_j)$$

$$= n_o(n-1) \int_0^t 2\pi \, r \, dr \; / \; A$$

$$= n_o(n-1) \; \pi \, t^2 / \; A$$

where V is a one dimensional Lebesgue measure on $\partial b(X,r)$, the boundary of the circle centered at X and radius r. Now

$$E\{ \hat{K}_2(t) / N(D_o) = n_o \} = n_o(n-1) \pi t^2 / A A_o \lambda^2 = K(t)$$

However, the rapidly decreasing size of D_o inevitably leads to a rapid increase in the variance of this estimator.

4.2.3 Ripley's estimator

Ripley(1976,1977) suggested considering every ordered pair of objects (X_i,X_j) within the sampling window and assigning a scaling factor S_{ij} to each pairing. The scaling factor is defined by,

$(S_{ij})^{-1}$ = The proportion of the perimeter of the circle, centred on object X_i and passing through object X_j, which lies within the sampling window D

$$= V[D \cap \partial b(X_i,r)] / 2 \pi r \qquad (4.8)$$

Note that S_{ij} is not necessarily equal to S_{ji}. We shall refer to object X_i as the central object and object X_j as the distant object.

Ripley's estimator $\hat{K}_3(t)$ is given by the equation,

$$\lambda^2 \hat{K}_3(t) = \sum_{i \neq j}^{n} \sum^{n} 1_{ij} S_{ij} / A \qquad (4.9)$$

Usually the value of λ^2 will be unknown, in which case we suggest replacing it by the estimate, $n(n-1)/A^2$ which is unbiased for a Poisson process. For a Poisson process, $\hat{K}_3(t)$ is unbiased for values of t for which $2t < d$. This follows, since

$$E\{\lambda^2 A \hat{K}_3(t)/N(D) = n\} = E\{\sum_{i\neq j}^{n}\sum^{n} S_{ij}1_{ij}\}$$

$$= \sum_{i\neq j}^{n}\sum^{n} E\{S_{ij}1_{ij}\}$$

$$= \sum_{i\neq j}^{n}\sum^{n} \int_0^t \{\int_{D\cap \partial b(x_i,r)} S_{ij}\, dV\}\, dr / A$$

$$= \sum_{i\neq j}^{n}\sum^{n} \int_0^t S_{ij} V[D\cap \partial b(X_i,r)]\, dr / A$$

But $S_{ij}\, V[D\cap \partial b(X_i,r)] = 2\pi r$, for all i and j, provided that,

$$V[D\cap \partial b(X_i,r)] \neq 0 \qquad (4.10)$$

However (4.10) is satisfied if and only if $2t < d$. Whence

$$E\{\lambda^2 A \hat{K}_3(t)/N(D) = n\} = [n(n-1)/A]\int_0^t 2\pi r\, dr, \quad \text{for } 2t < d$$

$$E\{\hat{K}_3(t)/N(D) = n\} = K(t)$$

Ripley's estimator is limited to values of t for which $2t < d$. The restriction occurs because the formulation of $\hat{K}_3(t)$, assumes that each of the objects in D can assume the role of a central object. However if $2t > d$, then there will be a 'null region' in the interior of D containing objects for which this central role has been removed, because the entire perimeter of the circle of radius t centered on one of these objects lies outside the sampling window.

4.2.4 Ohser's estimator

Ohser(1983) modified Ripley's estimator (4.9) to take account of the null region and to extend its range to all values of $t < d$. Let $A(t)$ be the area of the null region, let $n(t)$ be the number of objects lying within this region and define $B(t) = A - A(t)$ and $m(t) = n - n(t)$. Ohser's modified estimator $\hat{K}_4(t)$ is then given by the equation,

$$\lambda^2 \hat{K}_4(t) = \sum_{i}^{m(t)} \sum_{j}^{n} S_{ij} 1_{ij} / B(t) \qquad (4.11)$$

If the value of λ^2 is unknown then it can be replaced by the estimate, $(n-1)\, m(t)/ A\, B(t)$. Note however that $\hat{K}_3(t)$ and $\hat{K}_4(t)$ are equal for $2t < d$, since then $m(t) = n$ and $B(t) = A$. If t is sufficiently large ($2t > d$) for there to be a null region then although the objects in that region cannot be central objects, they will be distant objects for all the central objects.

For a Poisson process and conditional on the number of objects $N[D(t)] = m(t)$, the expectation

$$E\{ \lambda^2 B(t) \hat{K}_4(t)/ N[D(t)] = m(t)\} = E[\sum_{i}^{m(t)} \sum_{j}^{n} S_{ij} 1_{ij}]$$

$$= \sum_{i}^{m(t)} \sum_{j}^{n} E[S_{ij} 1_{ij}]$$

$$= \sum_{i}^{m(t)} \sum_{j}^{n} \int_0^t \{ \int_{D \cap \partial b(x_i, r)} S_{ij} dV \} dr/ A$$

$$= \sum_{i}^{m(t)} \sum_{j}^{n} \int_0^t S_{ij} V[D \cap \partial b(X_i, r)] dr/ A$$

but $S_{ij}\, V[D \cap \partial b(X_i, r)] = 2\pi r$ for $t < d$.

So $E\{\lambda^2 B(t) \hat{K}_4(t)/N[D(t)] = m(t)\} = [m(t)(n-1)/A] \int_0^t 2\pi r\, dr$

and $E\{\hat{K}_4(t) / N[D(t)] = m(t)\} = K(t)$

4.2.5 Ohser and Stoyan's estimator

Ohser and Stoyan(1981) introduced an estimator $\hat{K}_5(t)$ of $K(t)$ which did not assume isotropy, but is here applied to isotropic processes. They suggest scaling up each ordered pair (X_i, X_j) by the scaling factor S_{ij} defined through the relation

$$(S_{ij})^{-1} = \gamma_D(r) / A \qquad (4.12)$$

For a rectangular sampling window, $\gamma_D(r)$ defined in (4.6) simplifies to

$$\gamma_D(r) = [2/\pi] \int_{\theta_1}^{\theta_2} f(r,\theta)\, d\theta \quad , \; 0 \leq \theta_1 < \theta_2 \leq \pi/2. \qquad (4.13)$$

where

$$f(r,\theta) = A - a\, r \cos\theta - b\, r \sin\theta + r^2 \sin\theta \cos\theta$$

$$\theta_1 = \begin{cases} 0 & \text{if } r < b \\ \cos^{-1}(b/r) & \text{if } r \geq b \end{cases}$$

$$\theta_2 = \begin{cases} \pi/2 & \text{if } r < a \\ \pi/2 - \cos^{-1}(a/r) & \text{if } a \leq r \leq d \end{cases}$$

It can be shown that (4.13) further simplifies to,

$$\gamma_D(r) = \begin{cases} A - r(2a + 2b - r)/\pi & \text{if } r < a \\ [2A \sin^{-1}(a/r) - 2rb\{1-(1-a^2/r^2)^{\frac{1}{2}}\} - a^2]/\pi & \text{if } a \le r < b \\ [2A\{\sin^{-1}(a/r) - \cos^{-1}(b/r)\} - a^2 - b^2 - r^2 + 2r\{a(1-b^2/r^2)^{\frac{1}{2}} + b(1-a^2/r^2)^{\frac{1}{2}}\}]/\pi & \text{if } b \le r < d \end{cases} \quad (4.14)$$

For a circular sampling window of diameter d, $\gamma_D(r)$ is independent of θ, and is given as,

$$\gamma_D(r) = \text{area of } (D \cap D + y)$$

$$= \text{area of the intersection of two circles of diametres d, with their midpoints separated by a distance r} \quad (4.15)$$

$$= \begin{cases} 0.5\, d^2 \cos^{-1}(r/d) - 0.5\,(d^2 - r^2)^{\frac{1}{2}} & \text{for } r \le d \\ 0, & \text{otherwise.} \end{cases}$$

Thus the estimator $\hat{K}_5(t)$ takes account of the effective reduction in the area of D and is given by the equation,

$$\lambda^2 \hat{K}_5(t) = \sum_{i \neq j}^{n} \sum^{n} 1_{ij} S_{ij} / A \quad (4.16)$$

For a Poisson forest, $\hat{K}_5(t)$ is of course unbiased, since from (4.6)

$$E\{\lambda^2 A \hat{K}_5(t)\} = \sum_{i \neq j}^{n} \sum^{n} \int_0^t \gamma_D(r)\, S_{ij}\, dK(r)/A^2$$

$$= \lambda^2 A \int_0^t 2\pi r \, dr = A\lambda^2 K(t)$$

Ripley(1982) noted that this estimator is unbiased for small distances but suggested that it had an appreciably greater variance than his own $\hat{K_3}(t)$. This is borne out by the results that are presented later.

4.2.6 Vere-Jones estimator

For objects uniformly distributed in D, Vere-Jones (1978) considered estimating $\lambda^2 K(t_2) - \lambda^2 K(t_1)$ for $t_1 < t_2$ by

$$n \{ \sum_{i \neq j}^{n} \sum^{n} \hat{1}_{ij} \} / A \sum_{i=1}^{n} \{ r_i(t_1, t_2) \}^{-1} \qquad (4.17)$$

where $\hat{1}_{ij} = 1$ if $t_1 < d(X_i, X_j) \leq t_2$ and $\hat{1}_{ij} = 0$, otherwise. The function $r_i(t_1, t_2)$ is defined through the relation,

$$\{ r_i(t_1, t_2) \}^{-1} = \text{the proportion of the area of an annulus with center } X_i \text{ and radii } t_1 \text{ and } t_2 \text{ that lies within the sampling window D.} \qquad (4.18)$$

However, if $t_1 = 0$ and $t_2 = t$, then (4.17) reduces to

$$\hat{\lambda^2 K_6}(t) = n \{ \sum_{i \neq j}^{n} \sum^{n} 1_{ij} \} / A \sum_{i=1}^{n} \{ r_i(t) \}^{-1} \qquad (4.19)$$

where $\{r_i(t)\}^{-1}$ = the proportion of the area of the disc with centre X_i and radius t that lies within D.

$$= \int_0^t V[\, D \cap \partial b(X_i, r)]\, dr \;/\; \pi t^2 \qquad (4.20)$$

For a Poisson process and conditionally on N(D) = n, the objects are independently uniformly distributed in D, so

$$E[\lambda^2 \hat{K_6}(t) \;/\; N(D) = n\,] = E\,[\, n \{\sum_{i\neq j}^{n}\sum^{n} 1_{ij}\} \;/\; A \sum_{i=1}^{n} \{\, r_i(t)\,\}^{-1}]$$

$$= \lambda E\,\{\sum_{i\neq j}^{n}\sum^{n} 1_{ij}\} \;/\; \sum_{i=1}^{n} \{\, r_i(t)\,\}^{-1}$$

$$= \lambda^2 \sum_{i=1}^{n} \int_0^t \{ \int_{D\cap\partial b(X_i,r)} dV \;\}\, dr \;/\; \sum_{i=1}^{n} \{r_i(t)\}^{-1}$$

$$= \lambda^2 \sum_{i=1}^{n} \int_0^t V[D \cap \partial b(X_i, r)]\, dr \;/\; \sum_{i=1}^{n} \{r_i(t)\,\}^{-1}$$

$$= \lambda^2 K(t), \quad \text{for } t < d/2.$$

Thus the estimator $\hat{K_6}(t)$ is limited to values of t for which $2t < d$. Ripley(1982) notes that the bias in this estimator is negligible for moderate sample sizes.

4.2.7 The new estimator

The second of the definitions of K(t) suggests calculating the average number of distant objects within the circle of radius t that surrounds a central object. In many cases the circle does not lie entirely within the sampling window, so that some edge correction will be needed.

We define the new estimator of K(t) as being given by

$$\lambda \hat{K_7}(t) = \sum_{i}^{m(t)} \sum_{j}^{n} r_i(t)\, 1_{ij} / m(t) \qquad (4.21)$$

where $r_i(t)$ is defined in equation (4.20), and the first summation is over the m(t) objects lying in the non-null region. However, in this chapter we restrict attention to the case where $2t < d$ so that there is no null region and the definition of $\hat{K_7}(t)$ can be more simply stated as

$$\lambda \hat{K_7}(t) = \sum_{i \neq j}^{n} \sum_{i \neq j}^{n} r_i(t)\, 1_{ij} / n.$$

If λ is unknown we replace it by the estimate $(n-1)/A$, where the reduction in the numerator comes about because we are concerned with estimating the density of neighbours. For a Poisson process and conditionally on there being m(t) objects in the non-null region D(t): $N[D(t)] = m(t)$, the objects are independently uniformly distributed in D, so

$$E\{ \lambda \hat{K_7}(t) \mid N[D(t)] = m(t)\} = E[\sum_{i}^{m(t)} \sum_{j}^{n} r_i(t)\, 1_{ij}]/ m(t)$$

$$= \sum_{i}^{m(t)} \sum_{j}^{n} \int_0^t \{ \int_{D \cap \partial b(X_i, r)} r_i(t)\, dV \}\, dr / A$$

$$= \sum_{i}^{m(t)} \sum_{j}^{n} r_i(t) \int_0^t V[D \cap \partial b(X_i, r)]\, dr / A$$

$$= \quad \lambda K(t) \qquad \text{for all} \quad t < d.$$

Thus the new estimator $\hat{K_7}(t)$ is for a Poisson process an unbiased estimator of K(t). Furthermore, our simulation results in the sequel suggest that $\hat{K_7}(t)$ is almost unbiased for non-random process models, and leads to an estimate of L(t) which in general has a smaller mean squared error than that obtained using the other estimators of K(t).

4.3 Theoretical values for K(t)

In order to study the properties of the various estimators of K(t) we considered random, clustered and regular processes. The shape of the window will have an effect on the performance of the estimators, and therefore, for each process type we used a unit square window and/or a rectangular window with a length/breadth ratio of 10.

The Poisson process or Poisson forest incorporates two basic properties, those of uniformity whereby the objects exhibit no tendency to occupy particular regions of the plane, and independence, whereby the locations of a given object is determined without reference to that of any other. These two basic properties imply that, the second order intensity function $\lambda_2(t) = \lambda^2$, for $t > 0$, and from equation (4.2),

$$\lambda K(t) = \int_0^{2\pi} \int_0^t \lambda r \, dr \, d\theta$$

$$\text{so} \quad K(t) = \pi t^2 \qquad (4.22)$$

To obtain F(t), consider an arbitrary cluster, with point objects (x_1, y_1) and (x_2, y_2), which are r distance apart. Since X and Y are from $N(0, \sigma^2)$, then

$$F(t) = P(r \leq t)$$

$$= P[(x_1 - x_2)^2 + (y_1 - y_2)^2 \leq t^2]$$

$$= P[\{(x_1 - x_2)/\sqrt{2}\ \sigma\}^2 + \{(y_1 - y_2)/\sqrt{2}\ \sigma\}^2 \leq t^2/2\sigma^2]$$

but $\{(x_1 - x_2)/\sqrt{2}\ \sigma\}^2$ is Chi-squared distributed with one degree of freedom. Similarly $\{(y_1 - y_2)/\sqrt{2}\ \sigma\}^2$ has the same distribution. Therefore

$$F(t) = P\{\chi_2^2 \leq t^2 / 2\sigma^2\}$$

$$= 1 - \exp(-t^2 / 4\sigma^2).$$

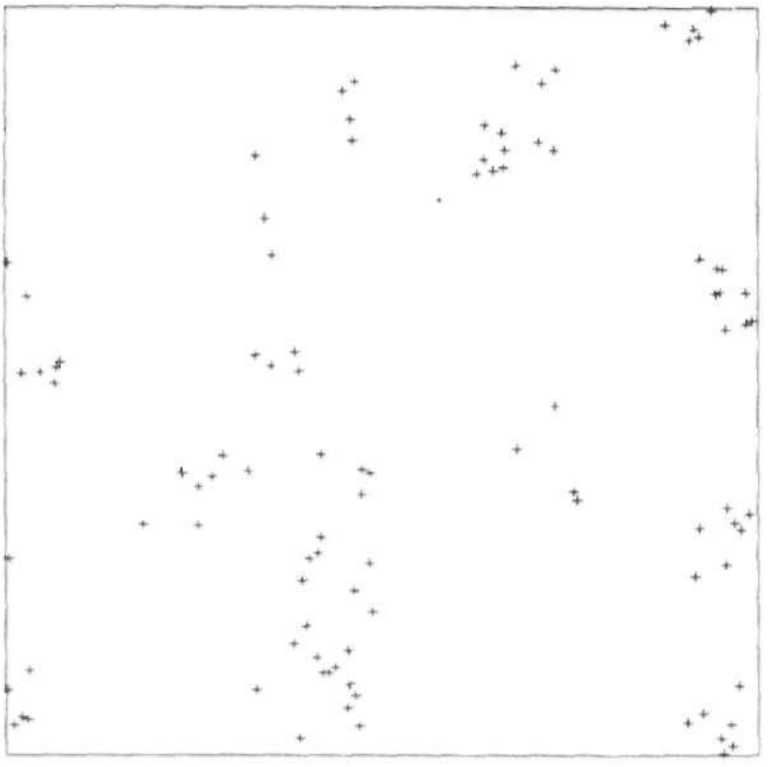
Thus

$$K(t) = \pi t^2 + \{1 - \exp(-t^2 / 4\sigma^2)\}/\rho \qquad (4.23)$$

In our simulations we used a cluster process with $\mu = 5$ and $\rho = 20$, in a unit square window, regarded as a torus. The distance of the daughter object from its parent was taken to be an observation from a Normal distribution with $\sigma = 0.035$. A partial realisation of this process is shown in Figure 4.1a.

As an example of an inhibition process we used Matern static inhibition process introduced by Matern (1960). Our realisations were obtained by thinning a Poisson forest of intensity $\rho = 145$ so as to remove

(a)



(b)

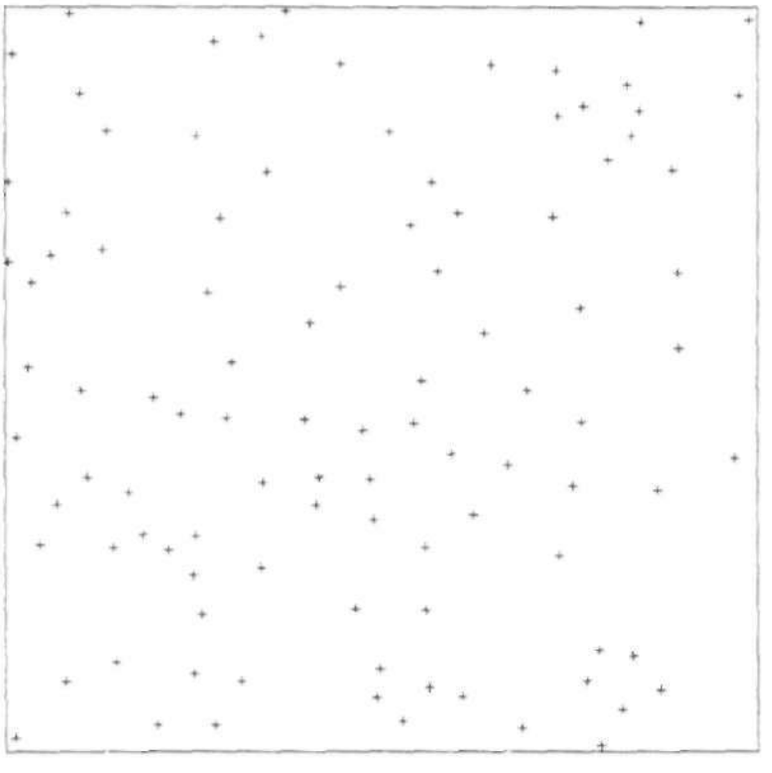


Figure 4.1 : Example realizations of (a) Poisson cluster process with $\mu=5$, $\sigma=0.035$ and $\rho=20$ and (b) Matern static inhibition process with $\sigma=0.035$ and $\rho=145$, in a unit square.

all pairs of objects that are within a distance $\sigma = 0.035$ units of each other. A partial realisation of this process is illustrated in Figure 4.1b.

The probability that an arbitrary object survives is $\exp(-\rho\pi\sigma^2)$ and so the intensity of the Matern static inhibition process is therefore $\lambda = \rho \exp(-\rho\pi\sigma^2)$. Also the conditional probability that two objects a distance $t > \sigma$ apart, both survive is $\exp\{-\rho D_\sigma(t)\}$, where

$$D_\sigma(t) = \begin{cases} 2\pi\sigma^2 + g(t,\sigma) & \text{if } \sigma \leq t < 2\sigma \\ 2\pi\sigma^2 & \text{if } t \geq 2\sigma \end{cases}$$

and $$g(t, \sigma) = t(\sigma^2 - t^2/4)^{\frac{1}{2}} - 2\sigma^2 \cos^{-1}(t / 2\sigma)$$

Now the second order intensity function can conveniently be expressed as,

$$\lambda_2(t) = \begin{cases} 0 & \text{if } 0 \leq t < \sigma \\ \rho^2 \exp\{-\rho D_\sigma(t)\} & \text{if } t \geq \sigma \end{cases} \qquad (4.24)$$

Note that (4.24) is as given in Ripley(1977). From (4.2) and (4.24), it is easy to show that for the Matern static inhibition process,

$$K(t) = \begin{cases} 0 & \text{if } t < \sigma \\ 2\pi\, f(\sigma, t) & \text{if } \sigma \leq t < 2\sigma \\ \pi[t^2 - 4\sigma^2 + 2f(\sigma, 2\sigma)] & \text{if } t \geq 2\sigma \end{cases} \qquad (4.25)$$

where $f(c,d) = \int_c^d x \exp\{ - \rho\, g(x,\sigma)\}\, dx$

The integral f(c,d) can easily be evaluated numerically.

4.4 Error Analysis: bias and mse of the estimators

Little progress has been made on the theoretical behaviour of $\hat{L}(t)$, the function of interest in studying patterns and we therefore display the results of simulations for this function for the various point processes considered. We concentrate on the bias of the estimators and on their mean squared errors (mse).

Suppose $\hat{L}(t)$ can be estimated many times by simulation. Then the expected value of $\hat{L}(t)$, is something we can estimate. For example, if we simulate the underlying process of interest s times to yield the results $\hat{L}^{(i)}(t)$, i = 1, 2,..., s, then

$$E\{\hat{L}(t)\} = \sum_{i=1}^{s} \hat{L}^{(i)}(t) / s \qquad (4.26)$$

This expected value may or may not equal the true value L(t). If it does, the estimate $\hat{L}(t)$ is said to be unbiased. Otherwise, it is said to be biased. The bias of the estimate, denoted by $b[\hat{L}(t)]$, is

$$b\{\hat{L}(t)\} = E\{\hat{L}(t)\} - L(t) \qquad (4.27)$$

The variance of the estimate, denoted by $Var[\hat{L}(t)]$ is defined as

$$Var[\hat{L}(t)] = E[\{\hat{L}(t) - E[\hat{L}(t)]\}^2]$$

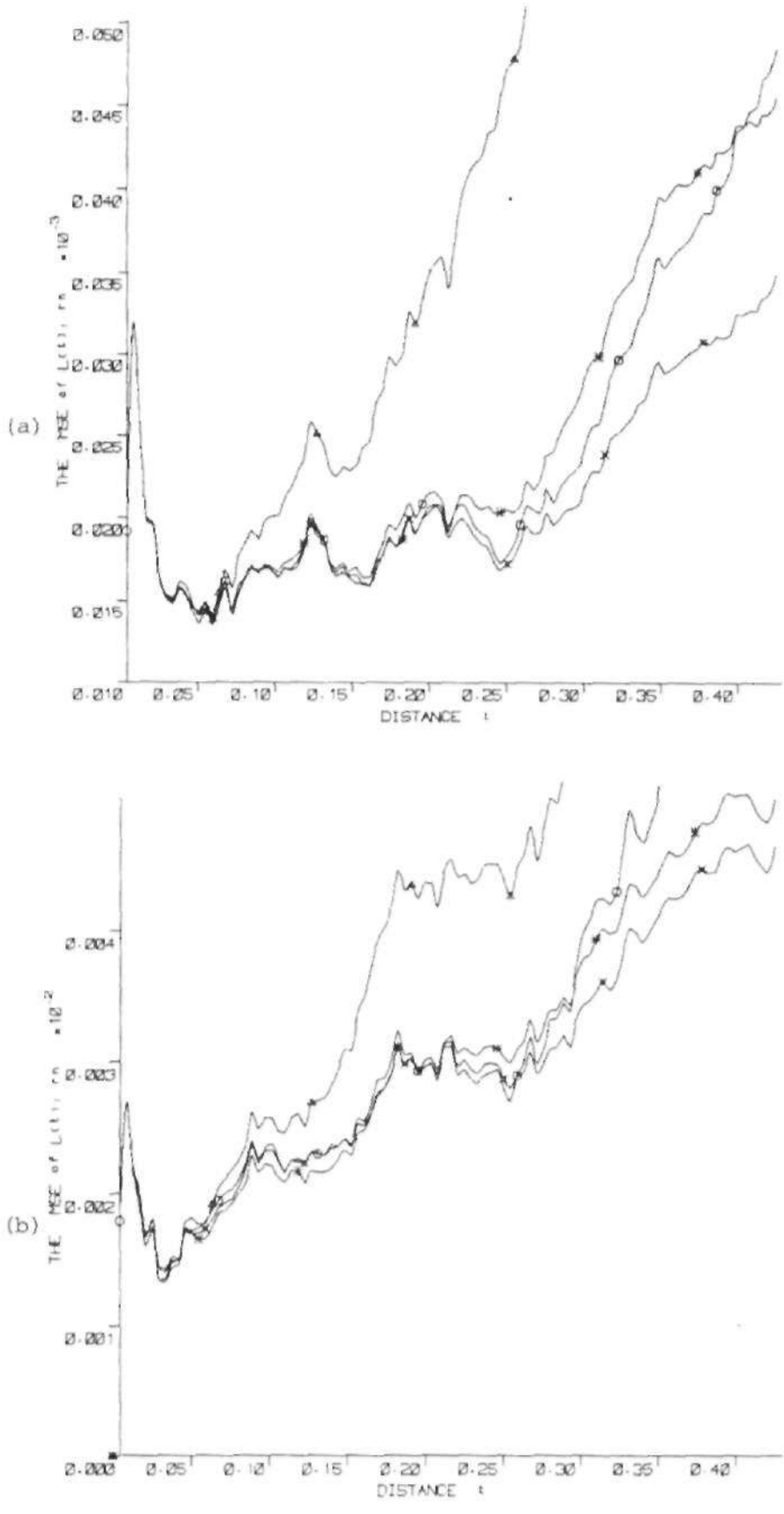


Figure 4.2 : The mean squared error of alternative estimators of L(t), for realizations of a Poisson process in (a) a unit square window and (b) a rectangular window of dimensions $10\sqrt{0.1} \times \sqrt{0.1}$

Key —o—o— $\hat{L}_3$; —Δ—Δ— $\hat{L}_5$; -*-*-* $\hat{L}_6$; —X—X—X— $\hat{L}_7$.

$$= \sum_{i=1}^{s} \{\hat{L}^{(i)}(t)\}^2 / s \; - [E\{\hat{L}(t)\}]^2 \qquad (4.28)$$

An assessment of the total estimation error is given by the mean square error which is defined as the expected value of the squared differences from the true value. The mean squared error of $\hat{L}(t)$ is given by,

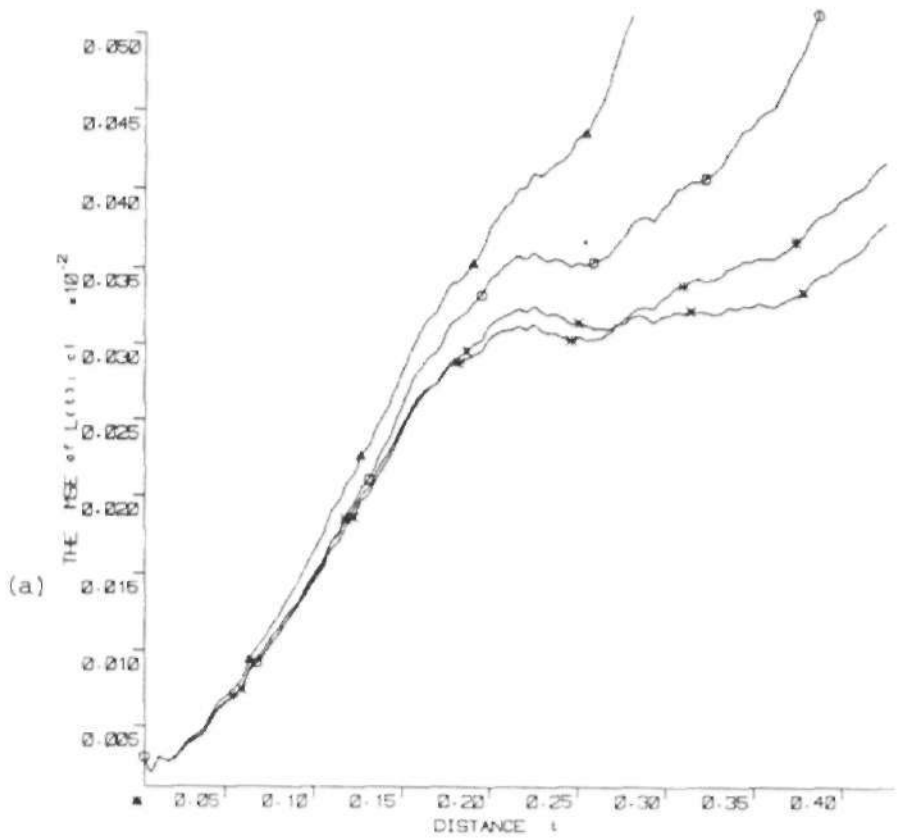
$$\text{mse}[\hat{L}(t)] = E[\{\hat{L}(t) - L(t)\}^2]$$

$$= \text{Var}[\hat{L}(t)] + \{b[\hat{L}(t)]\}^2 \qquad (4.29)$$

For every combination of window shape and object process we generated $s = 100$ partial realizations of the process and calculated the values of the estimators $\hat{L}_3(t)$, $\hat{L}_5(t)$, $\hat{L}_6(t)$ and $\hat{L}_7(t)$, their bias and mse at each of 100 equi-spaced values of t between 0 and 0.425 - since most of the useful information in $\hat{L}(t)$, however calculated is confined to relatively small values of t. Here we write $\hat{L}_i(t)$ to mean the estimated value of L(t) using the estimator $\hat{K}_i(t)$ in place of K(t).

Results are not shown for $\hat{L}_1(t)$ on the account of the considerable bias of the corresponding estimator of K(t), nor for $\hat{L}_2(t)$ whose variance is considerably greater, for moderate t than any of the other estimators. For the values of t considered here, $\hat{L}_4(t)$ is identical to $\hat{L}_3(t)$.

Figure 4.2 is concerned with the estimation of L(t) in the case of a Poisson process and shows results both for a unit square window and for a rectangular window of dimensions $10\sqrt{0.1}$ by $\sqrt{0.1}$. For each window, the values of the mse for each estimator are plotted against t. The most



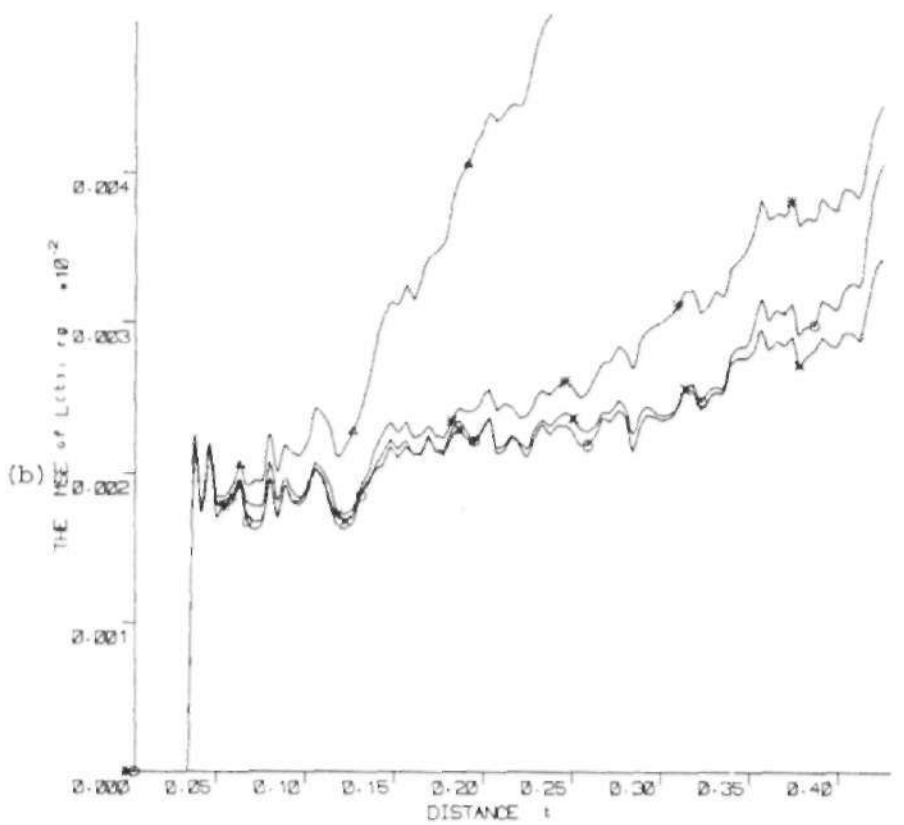


Figure 4.3 : The mean squared error of alternative estimators of L(t) for realizations of (a) Poisson cluster process and (b) Matern static inhibition process, in a unit square window.

Key: —o—o— $\hat{L}_3$; —Δ—Δ— $\hat{L}_5$; —×—×— $\hat{L}_6$; —⋈—⋈— $\hat{L}_7$.

obvious feature of Fig 4.2 is the apparently increased mse associated with the rectangular window. The mse plot suggests that $\hat{L_5}(t)$ is inferior to the other estimators for most values of t and that, for all values of t considered, the new estimator $\hat{L_7}(t)$ is preferable. As expected, all four estimators are almost unbiased and the major contribution to the mse comes from the variance of the estimators.

Figure 4.3 shows the results for the four estimators using a unit square window to estimate L(t) for a Poisson cluster Process (Fig 4.3a) and a Matern static inhibition process (Fig 4.3b). For both processes the mse plots show $\hat{L_5}(t)$ to be inferior to the alternatives, with $\hat{L_7}(t)$ being marginally preferable.

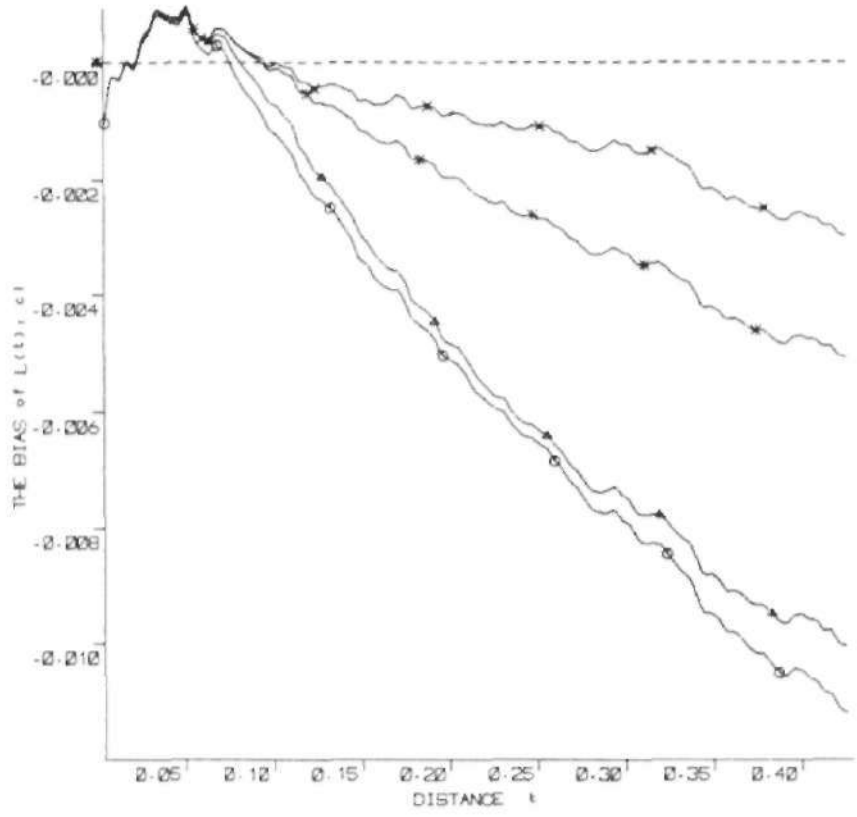
Figure 4.4 is concerned with estimating the bias of the various estimators, for the non-random processes. The values of the bias for each estimator are plotted against t for the Poisson cluster process (Fig 4.4a) and the Matern static inhibition process (Fig 4.4b).

In both cases the performance of the new estimator, $\hat{L_7}(t)$, is very similar to that of the Vere-Jones estimator, $\hat{L_6}(t)$, but is marginally preferable to it. Both these estimators clearly outperform the Ohser-Stoyan estimator $\hat{L_5}(t)$.

The Ripley estimator, $\hat{L_3}(t)$, displays an unexpected behaviour, performing well for the regular process, but poorly for the clustered process. Repeat simulations varying the parameters of these processes produced similar results.

Since in a real situation one does not know whether a process is regular, random or clustered, one needs a dependable estimator and this suggests that, at least for small values of t and with moderate numbers of objects, the new estimator is preferable to its predecessors.

(a)



(b)

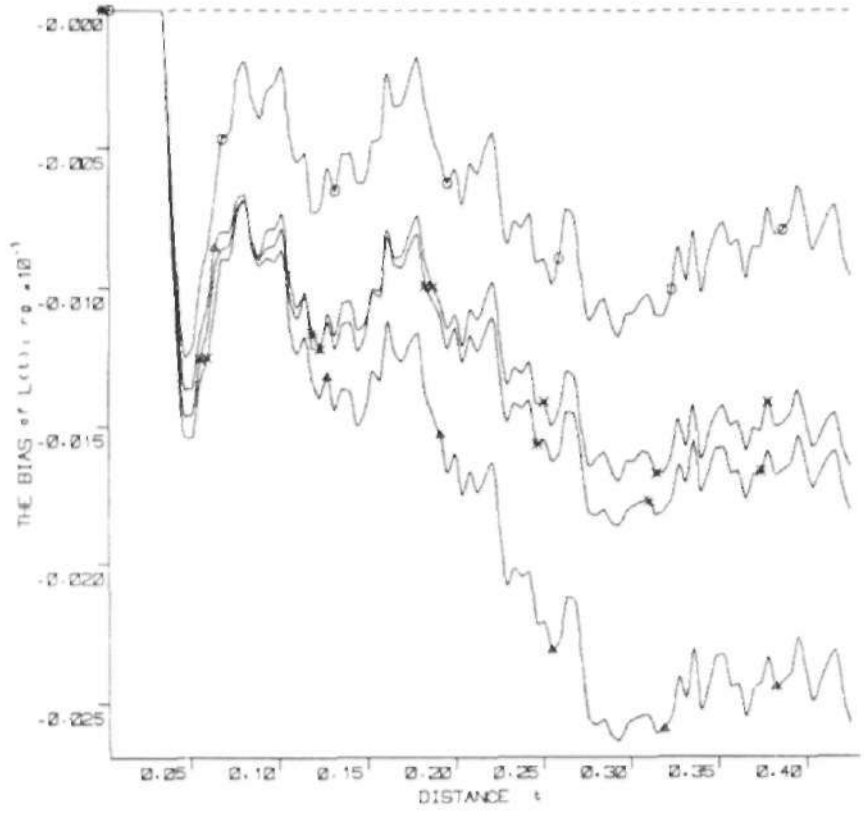


Figure 4.4 : The bias of alternative estimators of L(t), for realizations of (a) a Poisson cluster process and (b) a Matern static inhibition process, in a unit square window.

Key: —o—o— $\hat{L}_3$; —△—△— $\hat{L}_5$; —*—*— $\hat{L}_6$; —✳—✳— $\hat{L}_7$.

We should remark that the relatively poor performance of the Ohser-Stoyan estimator reflects the fact that it does not rely on the assumption of isotropy, and it is the only estimator available in the case of an anisotropic process.

In the next few sections we shall confine attention to $\hat{L}_7(t)$ since it is marginally preferable to the other estimators.

4.5 Graphical Analysis

To assess the significance or otherwise of departures from the null hypothesis of a Poisson forest, the conventional approach would be to find the sampling distribution of $\hat{L}(t)$ under the null hypothesis of randomness. We calculate the $\hat{L_7}(t)$, from each of s-1 independent simulations of n objects independently and uniformly distributed in D, the sampling window and define the upper and lower simulation envelopes,

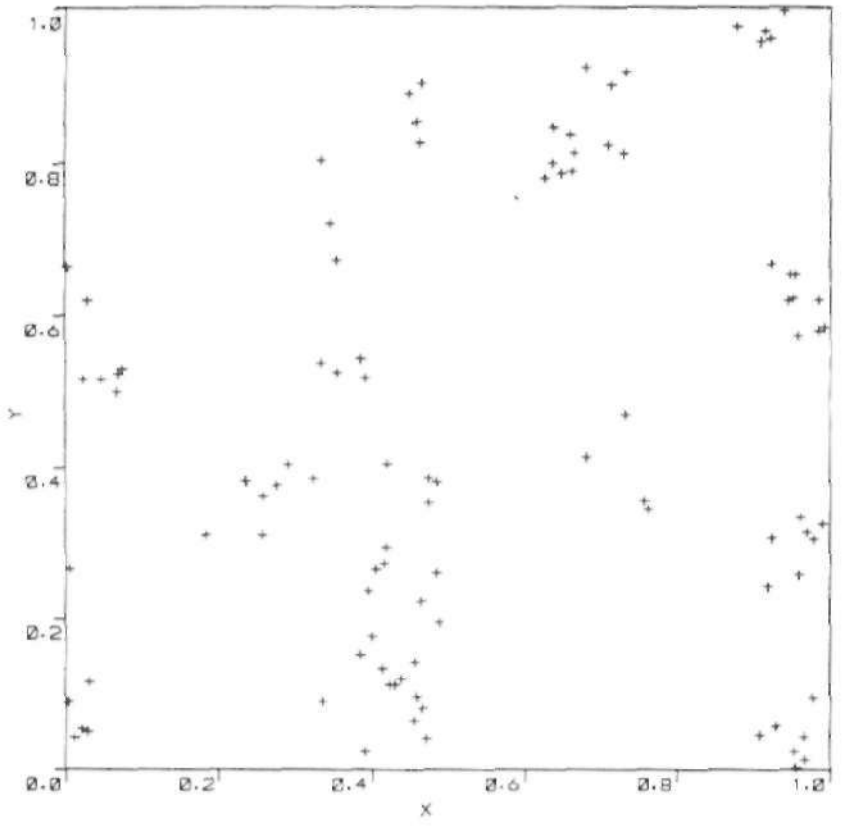
$$\begin{aligned} U(t) &= \max_i \{ \hat{L_7^i}(t) \} \\ L_0(t) &= \min_i \{ \hat{L_7^i}(t) \} \end{aligned} \qquad (4.30)$$

These simulation envelopes can also be plotted against t, and have the property that under the null hypothesis of randomness, and for each t

$$P[\hat{L_7}(t) > U(t)] = P[\hat{L_7}(t) < L_0(t)] = 1/s.$$

The simulation envelopes are intended to help in the interpretation of the plot of $\hat{L_7}(t)$ against t.

(a)



(b)

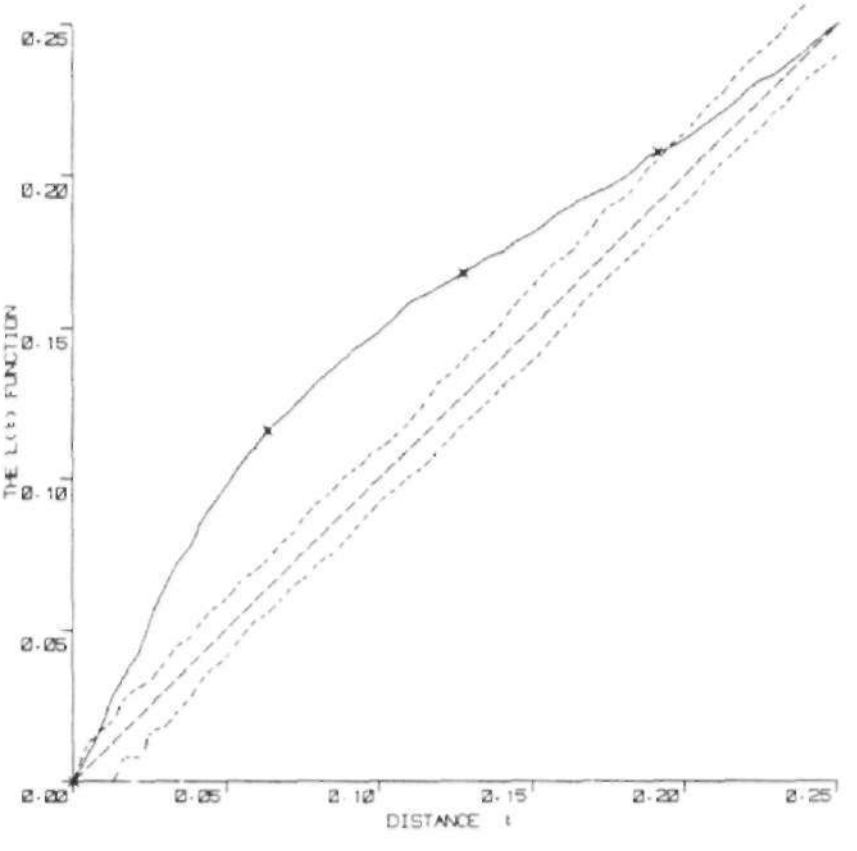
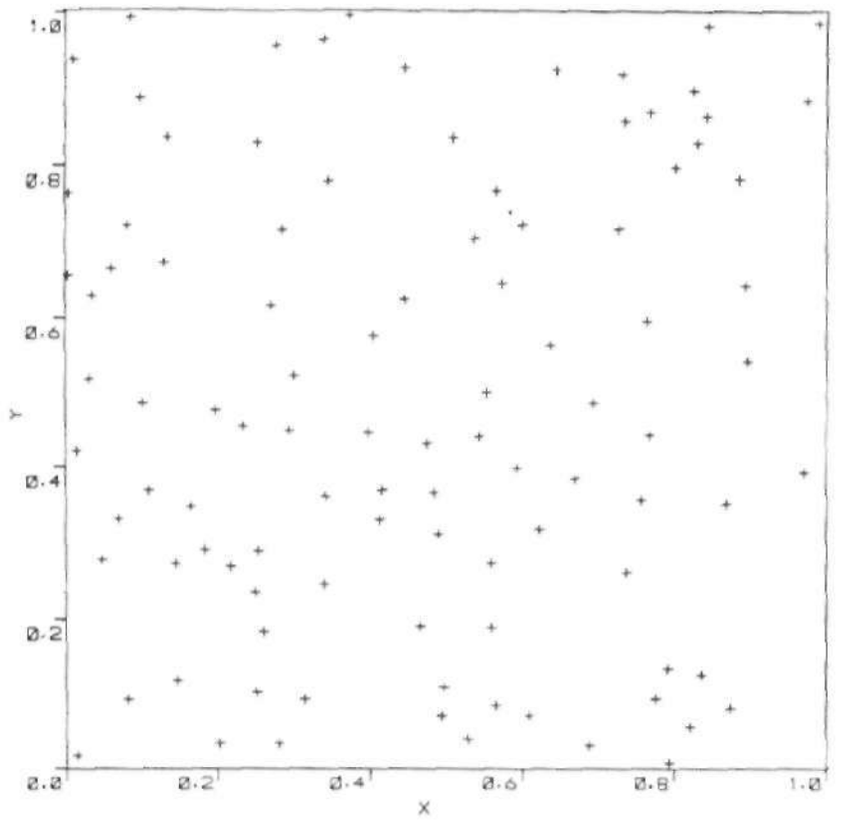


Figure 4.5 : (a) Poisson cluster process with parameters μ=5, ρ=20 and σ=0.035.

(b) A plot of $\hat{L}_7(t)$ (-x-x-x-) for the Poisson cluster process. The dashed lines (------) is the $\hat{L}_7(t)$ for a Poisson process. The dotted lines (.....) are the 99 simulation envelopes of the Poisson process.

(a)



(b)

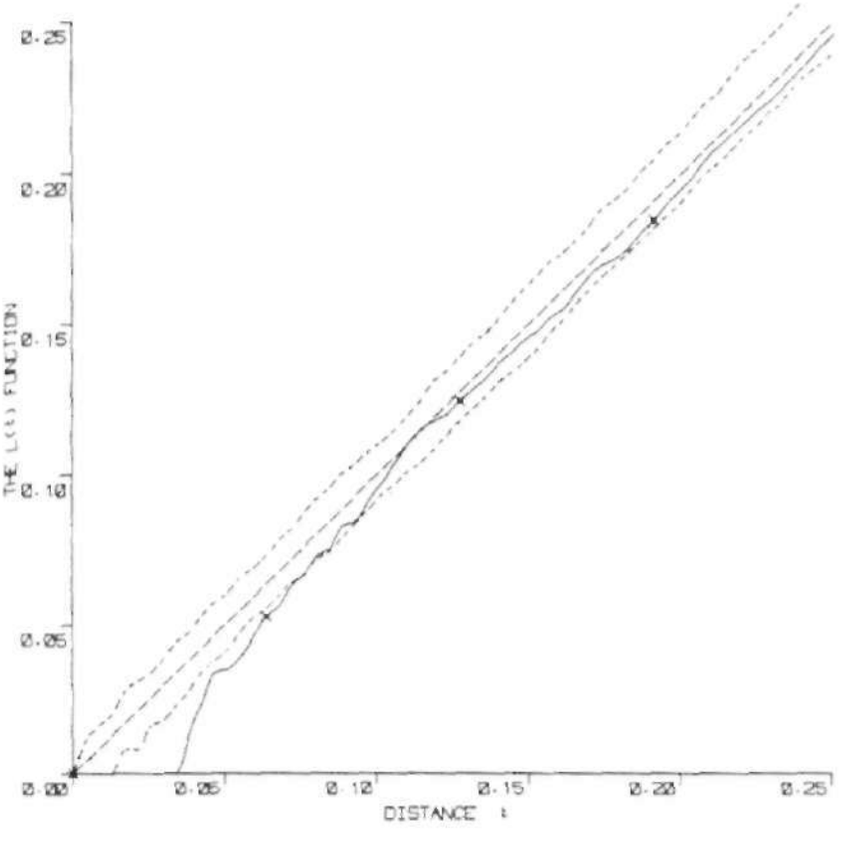


Figure 4.6 : (a) Matern static inhibition process with parameter ρ=145, σ=0.035
(b) A plot of $\hat{L}_7(t)$ (-x-x-x-) for the Matern static inhibition process. The dashed lines (-----) is the $\hat{L}_7(t)$ for a Poisson process. The dotted lines (.....) are the envelopes estimated from 99 simulations of a Poisson process.

4.5.1 Analysis of the two alternative patterns.

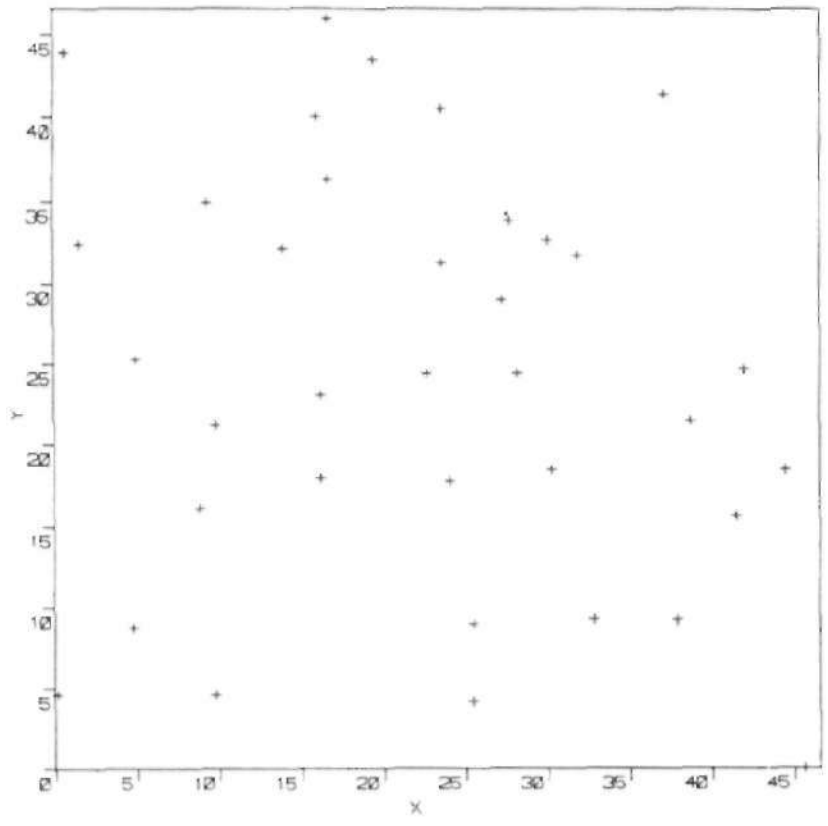
Figure 4.5b shows the behaviour of $\hat{L}_7(t)$ when used to test the hypothesis of a Poisson process (i.e that the objects are independently uniformly distributed in D). The dotted lines show the envelope for $\hat{L}_7(t)$ obtained from 99 partial realisations of a Poisson process, whilst the solid line indicates the values of $\hat{L}_7(t)$ obtained from an analysis of a single realisation of a Poisson cluster process given in Figure 4.5a. The $\hat{L}_7(t)$ values for the Poisson cluster process lie well above the Poisson envelope, suggesting a significant clustering with a peak at about t = 0.08 units. Similarly Figure 4.6b shows the behavior of the empirical $\hat{L}_7(t)$ function, when applied to the simulated Matern static inhibition process of Figure 4.6a The values of $\hat{L}_7(t)$ for this process lie well below the lower Poisson envelope for values of t near 0.035 units, suggesting a significant deviation towards a regular alternative.

4.5.2 Analysis of Waterstriders data

Here we consider some data that were analysed previously by Penttinen(1984) using the second-order method. These data, illustrated in Figure 4.7a, show the pattern of waterstriders, the fifth larval stage of limnoporus rufoscutellatus, in a square area of side 46.4cm. It is known that, in late larval and adult stages, these insects display territorialism and a regular pattern is anticipated.

Figure 4.7b shows the behaviour of the $\hat{L}_7(t)$ estimator. The dotted lines show the envelope for $\hat{L}_7(t)$ obtained from 99 partial realisations of the Poisson forest of similar intensity. The solid line indicates the values of $\hat{L}_7(t)$ obtained from the analysis of the waterstriders data. From this figure it is clear that there is a significant repulsion between the waterstriders (at the 1% level), at about t = 4.0 cm.

(a)



(b)

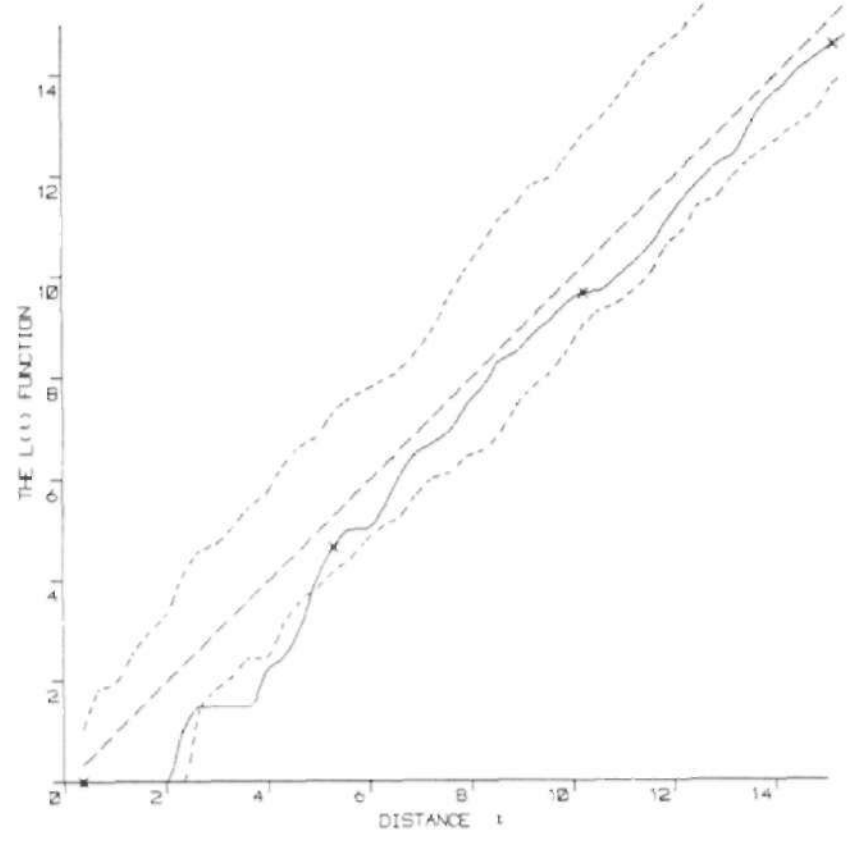


Figure 4.7 : (a) Positions of the waterstriders in a square of side 46.4 cm.
(b) A plot of $\hat{L}_7(t)$ (-x-x-x-) for the waterstriders data. The dashed lines (------) is the $\hat{L}_7(t)$ for a Poisson process, while the dotted lines (.....) are the envelopes from 99 simulations of a Poisson process.

4.5.3 Analysis of a cellular process

Baddeley and Silverman(1984) observed that the second-order methods investigate only the second-order characteristics of the underlying model and cannot detect differences between point patterns with identical K(t) functions. They exhibit a simple model of a point process, based on a cellular construction which has exactly the same second-order properties as a Poisson process, but whose realisations are manifestly different from those of the Poisson process.

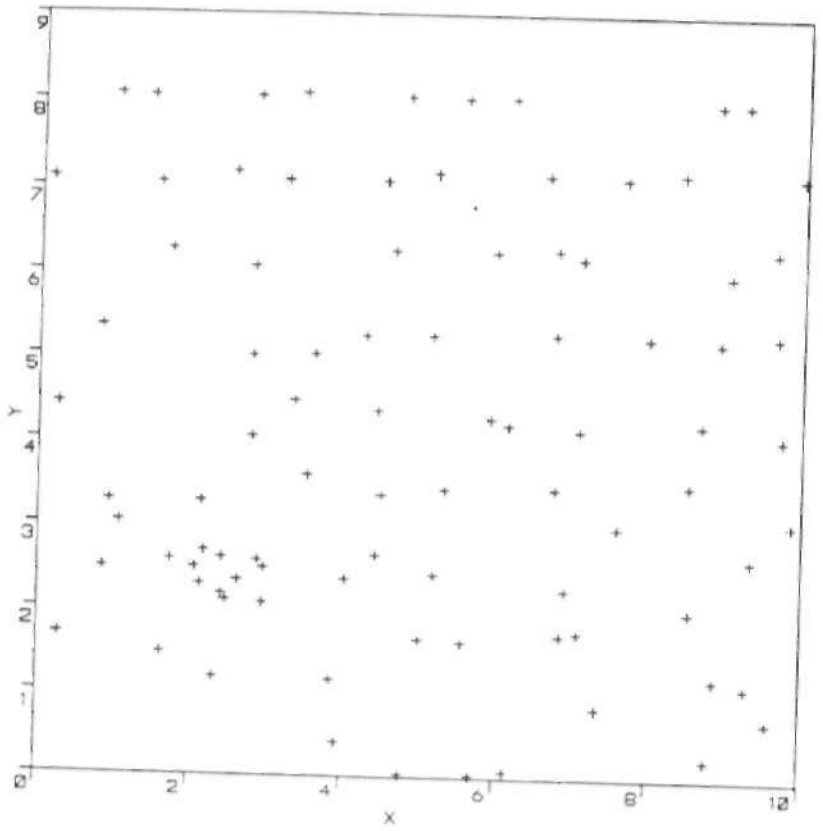
In order to simulate this process based on the cellular construction, we divide the region D into unit squares or cells, by randomly throwing down a square grid. In each cell we place a random number X of objects, where the random integers X, are to be independent for the different cells and have the probability density function f(x) defined as,

$$f(x) = \begin{cases} 1/10 & \text{if } x = 0 \\ 8/9 & \text{if } x = 1 \\ 1/90 & \text{if } x = 10 \end{cases} \qquad (4.31)$$

with mean and variance equal to unity. Thus most cells contain exactly one object, a few cells are empty, and very occasionally there is a tight cluster of 10 objects. The 'scale' of these clusters is the cell size.

Given the value of X, the objects inside these cells are independently and uniformly distributed. Figure 4.8a shows a typical realization of this pattern, consisting of 90 objects in a rectangular region of sides 10.0 x 9.0. The L(t) functions for the cell process, using $\hat{L}_7(t)$ together with the envelope for $\hat{L}_7(t)$ obtained from 99 partial realisations of the Poisson forest of intensity $\lambda = 1.0$ are presented in Figure 4.8b.

(a)



(b)

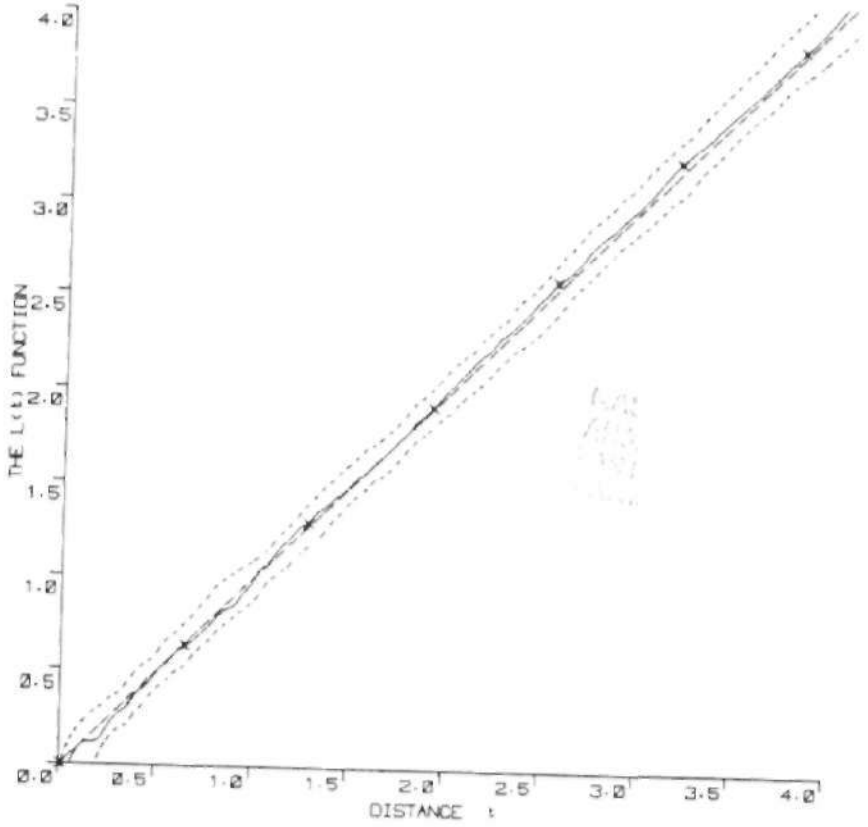


Figure 4.8 : (b) A plot of $\hat{L}_7(t)$ (-x-x-x-), for the cellular process data of Fig. 4.8(a). The straight line (-------) is the $\hat{L}_7(t)$ for a Poisson process. The dashed lines (.....) are the envelopes estimated from 99 simulations of a Poisson process.

We can see clearly that random fluctuations of the empirical $\hat{L}_7(t)$ functions do not lead to any distinguishable differences between the cell process and the Poisson process. The $\hat{L}_7(t)$ function for the cell process lies well within the 99% confidence bounds for the Poisson realizations. Thus the second-order analysis of the cell process would give no reason to reject the Poisson hypothesis.

4.6 The second-order neighbourhood function $S_i(t)$.

The K(t) function discussed in the previous sections cannot distinguish differences between patterns with identical second-order properties. In view of this, Getis and Franklin (1987) introduced the second order neighbourhood function $S_i(t)$, which while similar to the K(t) function differs in that consideration is given only to those pairs of objects having as one of its members a given object i. The $S_i(t)$ function is defined through the relation

$$\lambda S_i(t) = \text{number of further objects within distance t of an arbitrary object i.} \quad (4.32)$$

The estimate of the $S_i(t)$ function corresponding to the new estimator $\hat{K}_7(t)$ is given as,

$$\hat{S}_i(t) = A \sum_{j \neq i}^{n} 1_{ij} \, r_i(t) \; / \; (n-1). \quad (4.33)$$

From (4.33) we obtain,

$$\hat{M}_i(t) = \left[\hat{S}_i(t) / \pi \right]^{\frac{1}{2}} \quad (4.34)$$

The square-root is included in order to linearise the plot of $\hat{M}_i(t)$ against t, and to have $\hat{M}_i(t) = t$, when $\hat{M}_i(t)$ represents a pattern produced by a

Poisson process. If object i is a member of a cluster, then we should expect an abundance of neighbouring objects at short distances from object i, and hence $\hat{M}_i(t) > t$. If the object i is isolated, then there will be a deficit of neighbouring objects at short distances from object i and so $\hat{M}_i(t) < t$. Thus the function $\hat{M}_i(t)$ gives information as to the membership characteristics of a given object i. Furthermore, this function can be used to produce maps of pattern density at a given scale. However, suppose we are interested in knowing whether the given mapped pattern is random, clustered or regular. Obviously this function cannot give us the desired information.

Suppose the $\hat{M}_i(t)$ function can be calculated for all objects i, i = 1, 2, ...,n in D and for all distances of interest. We then define the functions $\hat{R}(t)$ and $\hat{O}(t)$ to be,

$$\hat{R}(t) = \max_i \{ \hat{M}_i(t) \} \qquad (4.35)$$

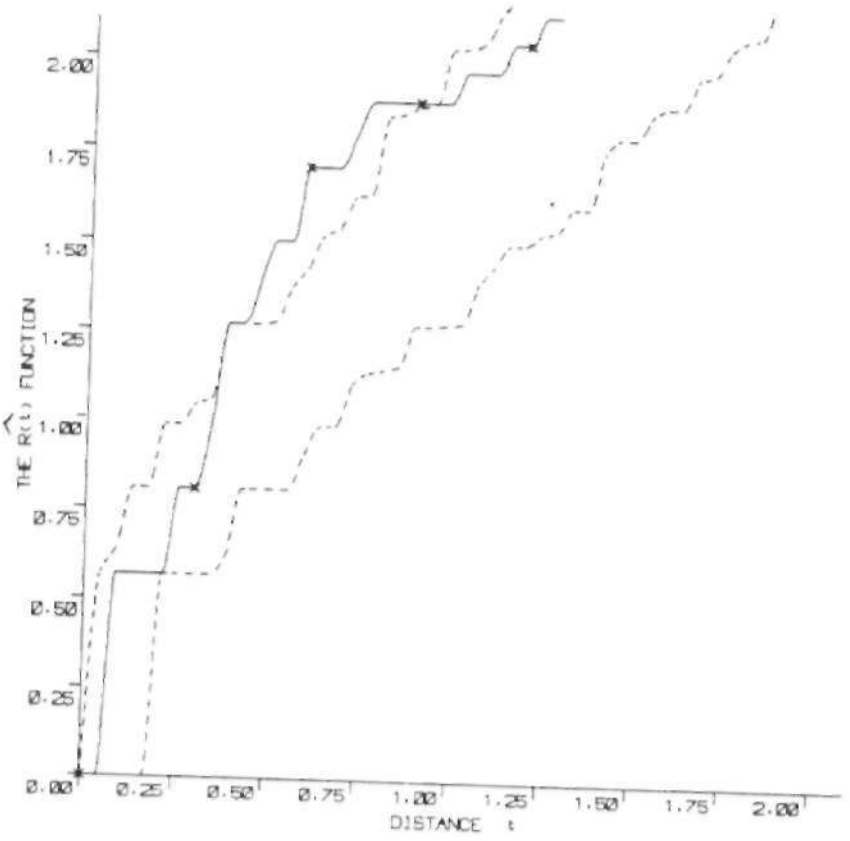
and

$$\hat{O}(t) = \sum_{i=1}^{n} \hat{M}_i(t) / n \qquad (4.36)$$

respectively. For a Poisson process, we should expect the functions $\hat{R}(t)$ and $\hat{O}(t)$ to be close to the value of t. For a clustered alternative, both values of $\hat{R}(t)$ and $\hat{O}(t)$ should be much greater than t, whereas the converse is expected to be true for regular alternatives.

We shall now analyse the cell data of Figure 4.8. Figure 4.9(a, b) shows the behaviour of the two estimators $\hat{R}(t)$, and $\hat{O}(t)$ when used to test the hypothesis of a Poisson process. For each estimator, the relevant diagram shows the corresponding envelope obtained from 99 partial realizations of the Poisson process, whilst the solid line indicates the values of the estimators obtained from an analysis of a single realization

(a)



(b)

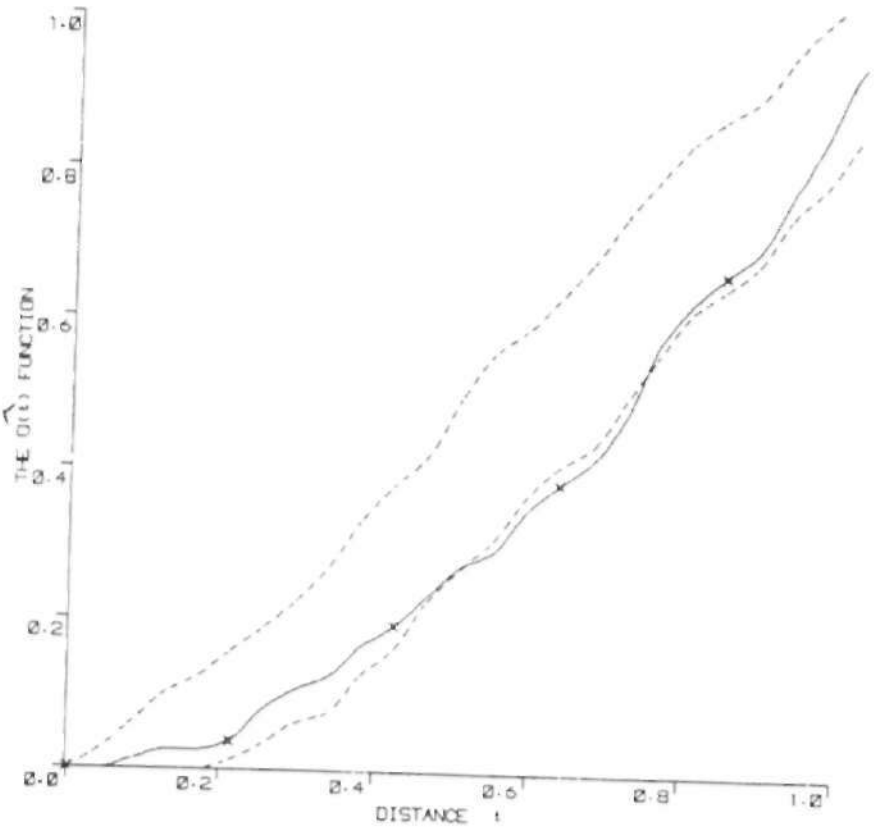


Figure 4.9 : Plots of (a) $\hat{R}(t)$ and (b) $\hat{O}(t)$ for the cellular process data of Figure 4.8(a). The dashed lines (-----) are the envelopes estimated from 99 simulations of a Poisson process.

of the cell data. The values of $\hat{R}(t)$ for this realization lie well above the Poisson envelope for some values of t, suggesting that the cell data is indeed significantly different from the Poisson process. Similarly the values of $\hat{O}(t)$ suggest a significant deviation from the randomness hypothesis towards a regular alternative.

Table 4.1: Estimated power of 4% tests against a Poisson cluster process (parents retained) with parameters μ and σ.

Entries within the table refer to results for the six statistics arranged as follows:

$$\begin{pmatrix} r & L_m \\ T_{n,2} & g \\ J & LI \end{pmatrix}$$

σ =	0.08	0.12	0.16
μ = 1	$\begin{pmatrix} 28 & 16 \\ 28 & 0 \\ 37 & 33 \end{pmatrix}$	$\begin{pmatrix} 11 & 3 \\ 19 & 1 \\ 24 & 12 \end{pmatrix}$	$\begin{pmatrix} 8 & 2 \\ 9 & 1 \\ 10 & 7 \end{pmatrix}$
μ = 2	$\begin{pmatrix} 36 & 30 \\ 39 & 8 \\ 48 & 46 \end{pmatrix}$	$\begin{pmatrix} 25 & 13 \\ 27 & 0 \\ 27 & 16 \end{pmatrix}$	$\begin{pmatrix} 12 & 8 \\ 13 & 7 \\ 13 & 9 \end{pmatrix}$
μ = 3	$\begin{pmatrix} 45 & 40 \\ 44 & 13 \\ 50 & 50 \end{pmatrix}$	$\begin{pmatrix} 34 & 22 \\ 33 & 1 \\ 38 & 33 \end{pmatrix}$	$\begin{pmatrix} 15 & 5 \\ 21 & 0 \\ 18 & 13 \end{pmatrix}$

4.7 Comparative study

The usual first step in the analysis of spatial point patterns is a test of the null hypothesis of a Poisson forest. Indeed, the analysis is often confined to quoting a test statistic or its significance level as a measure of the departure from the Poisson forest. Our aim is to investigate the power of such tests, particularly tests based on the inter-object distances since comparisons are much easier because all the tests involve about the same degrees of effort to perform.

4.7.1 Tests based on the $\hat{K}(t)$ function

The first two tests are based on the K(t) function and are given as,

$$r = \sup_{t \leq t_o} | \hat{K}(t) - \pi t^2 | \qquad (4.37)$$

$$L_m = \sup_{t \leq t_o} | \{\hat{K}(t)/\pi\}^{\frac{1}{2}} - t | \qquad (4.38)$$

The upper limit t_o was set at $1.25/\sqrt{\lambda}$, following Ripley(1979a).

4.7.2 Test based on the $\hat{S}_i(t)$ function

The $\hat{S}_i(t)$ function provides the following test statistic:

$$g = \sup_{t \leq t_o} | \sum_{i=1}^{n} \{\hat{S}_i(t) / \pi\}^{\frac{1}{2}} / n - t | \qquad (4.39)$$

4.7.3 Jolivet, Liebetrau and Rothman's statistics

Jolivet(1978), Liebetrau(1977) and Liebetrau and Rothman(1977) essentially used sample estimates of the average count in a quadrat of size r by c (in our case $r=c=t_o$) placed at random in the study region, regarded as a torus, to provide the following test statistics:

$$J = \sum_{i>j}^{n} \sum^{n} \phi(X_{ij}, Y_{ij}) \qquad (4.40)$$

$$LI = \sum_{i>j}^{n} \sum^{n} \phi(X_{ij}, Y_{ij})^2 \qquad (4.41)$$

where

$$\phi(X_{ij},Y_{ij}) = \{ t_o - \min(X_{ij}, a-X_{ij})\}_+ \{ t_o - \min(Y_{ij}, b-Y_{ij})\}_+$$

$$X_{ij} = | x_i - x_j | \text{ and } Y_{ij} = | y_i - y_j |,$$

for any arbitrary objects (x_i, y_i) and (x_j, y_j) in D; and the notation $\{R\}_+$ denotes the maximum of R and zero. Using these toroidal corrections, the maximum distances between the two objects in the x and y - directions are respectively a/2 and b/2. Consequently, using rectangular quadrats, the maximum interesting value of t will be the smaller of a/2 and b/2.

The tests (4.40) and (4.41) are one-sided and we should reject the null hypothesis of a Poisson forest for significantly large or small values of these statistics in favour of a clustered or regular alternatives respectively.

4.7.4 Hermans, Rasson and Weverbergh statistic

Hermans et al(1987) provide a new test of randomness which has an assymptotic Chi-squared distribution with 12 degrees of freedom. This test also uses the inter-object distances and is defined on a square of side 2π by:

$$T_{n,2} = \sum_{|p|+|q|\leq 2}^{*} \sum_{ij}^{n} \text{Cos}\{p(X_i - X_j) + q(Y_i - Y_j)\}/n \qquad (4.42)$$

where $\sum^*$ indicates the sum over all couples of integers, except for (p,q) = (0, 0). For a sampling window of dimensions a x b, $T_{n,2}$ is computed using:

$$T_{n,2} = 4 S_{n,2} / n + 12 \qquad (4.43)$$

where $S_{n,2} = \sum_{i>j}^{n} \sum^{n} [\text{Cos } a_{ij} + \text{Cos } b_{ij} + \text{cos } 2 a_{ij} + \text{Cos } 2 b_{ij} + 2 \text{ Cos } a_{ij} \text{ Cos } b_{ij}]$

$$a_{ij} = 2\pi(X_i - X_j)/a$$

$$b_{ij} = 2\pi(Y_i - Y_j)/b$$

We then reject the null hypothesis of a Poisson forest, for significantly large (clustering) or small (regularity) values of $T_{n,2}$.

Table 4.2: Estimated power of 4% tests against a Strauss Process with interaction range R and strength C.

Entries within the table refer to results for six statistics arranged as follows:

$$\begin{pmatrix} r & L_m \\ T_{n,2} & g \\ J & LI \end{pmatrix}$$

C =	0.30	0.15	0.00
R = 0.015	$\begin{pmatrix}1&2\\7&6\\9&7\end{pmatrix}$	$\begin{pmatrix}1&3\\1&4\\2&4\end{pmatrix}$	$\begin{pmatrix}2&3\\1&7\\5&2\end{pmatrix}$
R = 0.035	$\begin{pmatrix}1&13\\5&22\\14&17\end{pmatrix}$	$\begin{pmatrix}0&29\\3&29\\9&20\end{pmatrix}$	$\begin{pmatrix}0&50\\4&43\\19&26\end{pmatrix}$
R = 0.045	$\begin{pmatrix}1&24\\3&35\\16&24\end{pmatrix}$	$\begin{pmatrix}0&39\\2&49\\21&40\end{pmatrix}$	$\begin{pmatrix}0&50\\8&50\\33&49\end{pmatrix}$

The simulations involve patterns of n = 64 objects generated in D, a square of unit side. The alternative processes considered were the Poisson cluster processes and the Strauss processes. The Strauss processes were simulated by the algorithm of Ripley(1979b).

Fifty realisations were generated for each process and a range of parameter values. Tables 4.1 and 4.2 record the numbers of occasions on which the hypothesis of randomness was rejected by a 4% test based on each of the statistics (4.37) to (4.43). With the exception of the $T_{n,2}$

statistic, all tests were Monte Carlo tests using 499 simulations with m = 500 in the terminology of the Monte Carlo tests of Chapter I

Examining first the performance of the tests based on the $\hat{K}(t)$ function, it is clear that the statistic r is very powerful against clustered alternatives, but very weak against regularity. However the L statistic, whilst not as powerful as r against clustered alternatives, is more robust in that it is powerful against both alternatives.

For test based on the empirical $\hat{S}_i(t)$ function, it is clear that the g test is extremely powerful against regular alternatives. However, this test is very weak against clustered patterns.

The test of Jolivet (J) is slightly more powerful than the test of Leibetrau (LI) against clustered alternatives. For regular alternatives however, the LI test is clearly more powerful than the J test.

The Hermans et al statistic $T_{n,2}$ is not as powerful as r, L_m, LI and J for highly clustered patterns ($\sigma \leq 0.08$), but gets better as σ increases. Moreover this statistic is extremely weak against regular alternatives.

In conclusion, the statistics r, J, LI and $T_{n,2}$ are powerful detectors of aggregated alternatives, whereas the statistics g, L , LI and J are powerful against regular alternatives.

A part of the material of this chapter will appear as Doguwa(1988) and Doguwa and Upton(1988c).

CHAPTER V

'Refined' nearest neighbour methods

5.1 Introduction

The second-order methods described in Chapter IV, represent a natural and valuable starting point for the description of a spatial point process, but do not give a complete picture, since these methods cannot distinguish processes which have identical second order properties.

Roder(1975) and Diggle(1979) have suggested looking at the distribution function G(t) of the objects to their nearest neighbours, defined by

$$G(t) = P(\text{circle of radius } t, \text{ centred on an arbitrary object contains at least one other object}) \quad (5.1)$$

An equivalent definition of G(t) is given as,

$$G(t) = P(\text{the distance between an arbitrary object and its nearest neighbour is at most } t) \quad (5.2)$$

Analogously Ripley(1977) has suggested using the distribution function F(t) of the distance from an arbitrary point to its nearest object. This function is defined by,

$$F(t) = P(\text{the circle of radius } t, \text{ centred on an arbitrary point contains at least one object}) \quad (5.3)$$

or $F(t) = P($ the distance between an arbitrary point and its nearest neighbour is at most $t)$ (5.4)

The estimation of $G(t)$ (and $F(t)$), is complicated by the bounded nature of the pattern being studied. The problem manifests itself in two ways. First, the circle of radius t surrounding an object (or point in the case of $F(t)$) is certain to overlap one or more of the boundaries of the study region as t increases. Second, the position of the nearest neighbour to an object (or point) will only be known with certainty for those objects lying within the interior of the study region: objects lying near a boundary may well have a nearest neighbour lying outside the study region.

The estimators of $G(t)$ and $F(t)$ in current use are motivated by the two aspects of the boundary problem. Diggle(1979) suggested an estimator for $G(t)$that restricts attention to those objects for which the circle of radius t does not overlap the boundary. Ripley(1977) proposed a similar estimator for $F(t)$. As t increases so the number of informative objects or points reduces. Hanisch(1984) suggested an estimator for $G(t)$ that restricts attention to those objects whose nearest neighbour can be identified with certainty.

Both of the existing estimators therefore use information from a restricted subset of the available data. The new estimators proposed here use information from all the objects (or points) in the window. The estimators are unbiased for a random process, and the bias appears to be small for non-random processes. However, the principal gain resulting from the use of the new estimator is a dramatic reduction in the variability of the estimates produced. This is a natural consequence of the fuller use of the information inherent in the data.

The results are illustrated for the new estimators and for the existing competitors for cases of theoretical clustered and regular point processes. Finally three real point patterns are analysed using these methods.

Table 5.1: Categorization of the objects in D for the three edge-corrected methods of estimating G(t).

Set	Description	Estimators of G(t)			Any other object within t ?
		G_1	G_2	G_3	
1	$t \leq b < w$	+	-	+	no
2	$t < w \leq b$	+	+	+	no
3	$w \leq t \leq b$	+	+	+	yes
4	$w \leq b < t$	-	+	+	yes
5	$b < w \leq t$	-	-	+	yes
6	$b < t < w$	-	-	+	maybe

Key : + used ; - not used.

5.2 The existing estimators of G(t).

We are concerned with the n objects whose positions are known within a window D. The distances from object i to the nearest boundary of D and to the nearest object within D are b_i and w_i, respectively. For a given value of t there are six situations of interest, which are summarised in Table 5.1.

5.2.1 Diggle's estimator

Following Ripley (1977), Diggle(1979) suggested an estimate of G(t) which we denote as $\hat{G}_1(t)$, defined by

$$\hat{G}_1(t) = \frac{\sum_{i=1}^{n} \sigma(w_i, t)\ \sigma(t, b_i)}{\sum_{i=1}^{n} \sigma(t, b_i)} \qquad (5.5)$$

where $\sigma(y,z) = 1$ if $y \leq z$ and $\sigma(y,z) = 0$ otherwise.

This estimator restricts attention to objects belonging to sets 1, 2 and 3, which are those objects that can be surrounded within D by a complete circle of radius t. As t increases, the number of informative objects contained in these sets diminishes, and the estimator is undefined when

$$\sum_{i=1}^{n} \sigma(t,b_i) = 0.$$

In the case of a rectangular window of dimensions c x d, with c < d, the maximum value of t for which an estimate of G(t) is possible when using $\hat{G}_1(t)$ is c/2. Clearly, as t approaches c/2 the variance of the estimator will increase rapidly.

5.2.2 Hanisch's estimator

An alternative estimator has been suggested by Hanisch (1984). This estimator, which we denote by $\hat{G}_2(t)$, uses the information provided by objects belonging to sets 2, 3 and 4.

$$\hat{G}_2(t) = \frac{\sum_{i=1}^{n} \sigma(w_i, t)\ \sigma(w_i, b_i)\ s(w_i)}{\sum_{i=1}^{n} \sigma(w_i, b_i)\ s(w_i)} \qquad (5.6)$$

The weight function s(z) is related to the area within D within which a pair of objects separated by a distance z could lie. For a rectangular c x d window

$$s(z) = \{ (c - 2z)(d - 2z) \}^{-1} \qquad (5.7)$$

It will be seen that Hanisch's estimator confines attention to all objects whose nearest neighbour is known to lie within D.

Whilst both $\hat{G_1}(t)$ and $\hat{G_2}(t)$ are based on rational approaches to the problem of estimating G(t) it will be seen that they use information from different subsets of the objects: in addition to sets 2 and 3, $\hat{G_1}(t)$ uses set 1 whereas $\hat{G_2}(t)$ uses set 4. This suggests that there must be an alternative estimator that makes more complete use of the information available.

5.2.3 The new estimator of G(t).

Definition (5.1) refers to 'at least one other object', and not to the nearest neighbouring object. Thus, in a sense, the restriction by Hanisch to an estimator based on the position of the nearest neighbour is unnecessary. Consider set 5. Here the position of the nearest neighbour is unknown, but it is known that there is an object within a distance t. Likewise, for set 1, it is known that there is no object within a distance t, despite the location of the nearest neighbour being unknown. Thus sets 1 and 5 are informative concerning G(t).

We can now show that, for a Poisson process, set 6 can also be induced to provide some information. We propose that the resulting estimator that uses information from all n objects in the window will serve as a reasonably unbiased estimator of G(t) for non-random processes.

Consider an object X which is one of the objects forming a realization of a Poisson process of intensity λ per unit area. Suppose that $t > b$, so that C, the disc of radius t centred on X, overlaps the boundary of the window D. Denote the portion of C that lies inside D as I(t), with the outside portion being denoted as O(t). Let the area of O(t) be A(t), so that I(t) has area $\pi t^2 - A(t)$. For a rectangular window of sides c x d, with $c < d$ let e_1 and e_2 be the nearest and second nearest boundary distances of X respectively. Then for values of $t < c/2$, A(t) is defined by

$$A(t) = \begin{cases} t^2 \cos^{-1}(e_1/t) - e_1 (t^2 - e_1^2)^{\frac{1}{2}} & \text{if } e_1 < t \text{ and } e_2 \geq t \\ 0.5\, t^2\{ \pi/2 + \cos^{-1}(e_1/t) + \cos^{-1}(e_2/t)\} & \\ \quad - e_1 e_2 - 0.5\{e_1(t^2 - e_1^2)^{\frac{1}{2}} + e_2(t^2 - e_2^2)^{\frac{1}{2}}\} & \text{if } e_2 < t \end{cases} \qquad (5.8)$$

Suppose that there are $k \geq 0$ objects lying within a distance t of X. By the definition of a Poisson process all locations are equally likely. Hence p(t), the probability that an object, lying within a distance t of X, lies within O(t), is given by

$$p(t) = A(t)/ \pi t^2 \qquad (5.9)$$

Moreover, since for a Poisson process the object locations are all independent of one another, the probability that all k objects lie within O(t) is $\{p(t)\}^k$.

In order to obtain an idea of the value of G(t), we must consider the conditional probability, H(t), relating to the observable area I(t). Specifically, for an object in set 6 we define H(t) to be the probability that there is an object within a distance t of X, given that X is the only object lying within I(t).

$$\text{Now} \quad H(t) = 1 - P\,[\ \text{None in } O(t) \ \big|\ \text{None in } I(t)]$$

$$= 1 - P[\ \text{None in } O(t) \cap \text{None in } I(t)] \ / \ P[\text{None in } I(t)]$$

$$= 1 - P[\ \text{None in } C\ ] \ / \ P[\ \text{None in } I(t)] \qquad (5.10)$$

and P[None in I(t)] depends upon the number of objects in C:

$$P[\text{None in } I(t)] = \sum_{k=0}^{\infty} P[\text{None in } I(t) \ \big|\ k \text{ in } C]\ P[\ k \text{ in } C]$$

$$= \sum_{k=0}^{\infty} \{\ p(t)\ \}^{k}\ P[\ k \text{ in } C] \qquad (5.11)$$

But the probability of there being k objects in C is,

$$P([\ k \text{ in } C] \quad = (\lambda\ \pi\ t^2)^{k} \exp\ (\ -\lambda\ \pi\ t^2\ )\ /\ k\ ! \qquad (5.12)$$

Hence on substituting for p(t) from equation (5.9) we obtain

$$H(t) \quad = 1 - \{ \sum_{k=0}^{\infty} [\ A(t)\ /\ \pi\ t^2\ ]^{k}\ (\lambda\ \pi\ t^2)^{k}/\ k\ !\ \}^{-1}$$

$$= 1 - \{ \sum_{k=0}^{\infty} [\ \lambda\ A(t)\ ]^{k}/\ k\ !\ \}^{-1}$$

$$= 1 - \exp(\ -\lambda\ A(t)), \qquad (5.13)$$

the obvious result for a Poisson process.

From this result, combined with the clear-cut results for the remaining 5 sets of objects we obtain the new estimator

$$\hat{G}_3(t) = \frac{\sum_{i=1}^{n} \{\sigma(w_i, t) + [1 - \sigma(w_i, t)][1 - \sigma(t, b_i)]\, H_i(t)\}}{n} \qquad (5.14)$$

where the estimated intensity λ is simply n divided by the area of the window D and $H_i(t)$ is as in $H(t)$, but with X replaced by X_i.

The estimator $\hat{G}_3(t)$ was deduced in the context of a realization of a Poisson process. For a non-random process none of the arguments that permitted the steps between (5.9) and (5.14) will be true. However, in general terms,we could expect the conditional probability $H(t)$ to be a monotonically increasing function of t, and the formula defined in (5.13) ought to continue to provide a reasonable 'score' for the objects falling in set 6. We can expect that the extra stability that results from using all six sets of objects will amply offset any minor bias that has been induced.

5.3 Estimators of F(t)

In this section we are concerned with m points whose positions are known within the window D. The distances from point i to the nearest boundary of D and to the nearest neighbouring object within D are d_i and x_i, respectively. For a given value of t there are, as before, six situations of interest.

5.3.1 Ripley's estimator

Ripley (1977) suggested an estimate of F(t) which we denote as $\hat{F}_1(t)$, defined by

$$\hat{F}_1(t) = \frac{\sum_{i=1}^{m} \sigma(x_i, t)\ \sigma(t, d_i)}{\sum_{i=1}^{m} \sigma(t, d_i)} \qquad (5.15)$$

The estimator $\hat{F}_1(t)$ has about the same disadvantages as $\hat{G}_1(t)$.

5.3.2 Hanisch's analogue

Analogous to $\hat{G}_2(t)$, we define an estimator $\hat{F}_2(t)$ as

$$\hat{F}_2(t) = \frac{\sum_{i=1}^{m} \sigma(x_i, t)\ \sigma(x_i, d_i)\ s(x_i)}{\sum_{i=1}^{m} \sigma(x_i, d_i)\ s(x_i)} \qquad (5.16)$$

5.3.2 The new estimator

Analogous to $\hat{G}_3(t)$, we define a new estimator for $F(t)$ as

$$\hat{F}_3(t) = \frac{\sum_{i=1}^{m} \{\sigma(x_i, t) + [1 - \sigma(x_i, t)][1 - \sigma(t, d_i)]\ H(t)\}}{m} \qquad (5.17)$$

When collecting information for a refined distance analysis using the estimators of $F(t)$, opinions have varied over a suitable choice of m, the number of sampling points. Given that the sampling window contains n objects, we have chosen $m = k^2$, so that k is as defined in equation (2.16). Furthermore, the regular lattice of sampling points used in chapters II and III seemed more stable so far as edge correction go. We

have therefore used the same arrangement of sampling points as in those Chapters.

5.4 G(t) and F(t) for a Poisson process.

The theoretical values of G(t) and F(t) are identical for a Poisson process, since the existence of an object at a particular point a_o say, has no bearing on the distribution of the remaining number of objects in the circle with center a_o and radius t. Thus for this process,

$$G(t) = F(t) = 1 - \exp(-\lambda \pi t^2) \qquad (5.18)$$

Figure 5.1 summarises the results obtained from 500 partial realizations of a Poisson process comprising 20 objects in a unit square. Figure 5.1a shows the dependence of the bias of the estimators of G(t) upon t, with the graphs showing the average values obtained for the 500 trials. It appears that $\hat{G}_2(t)$ slightly overestimates G(t) at large values of t.

Figure 5.1b gives some more insight into the results by plotting the envelopes of the bias obtained with the three estimators. Here the advantage possessed by the new estimator is immediately apparent when one studies the potential for under-estimation that the earlier estimators evince. For most values of t the window for $\hat{G}_1(t)$ is a full unit wide, since, as the number of informative objects decreases, it is almost inevitable that the last valid estimate either takes the form 0/q or q/q for some q.

Figure 5.1c shows the mean squared error for the three estimators. Convergence to 0 at t = 0 and for large values of t is inevitable since these cases correspond to G(t) = 0 and G(t) = 1. For intermediate values of t the smaller envelope for $\hat{G}_3(t)$ from Figure 5.1b translates into an

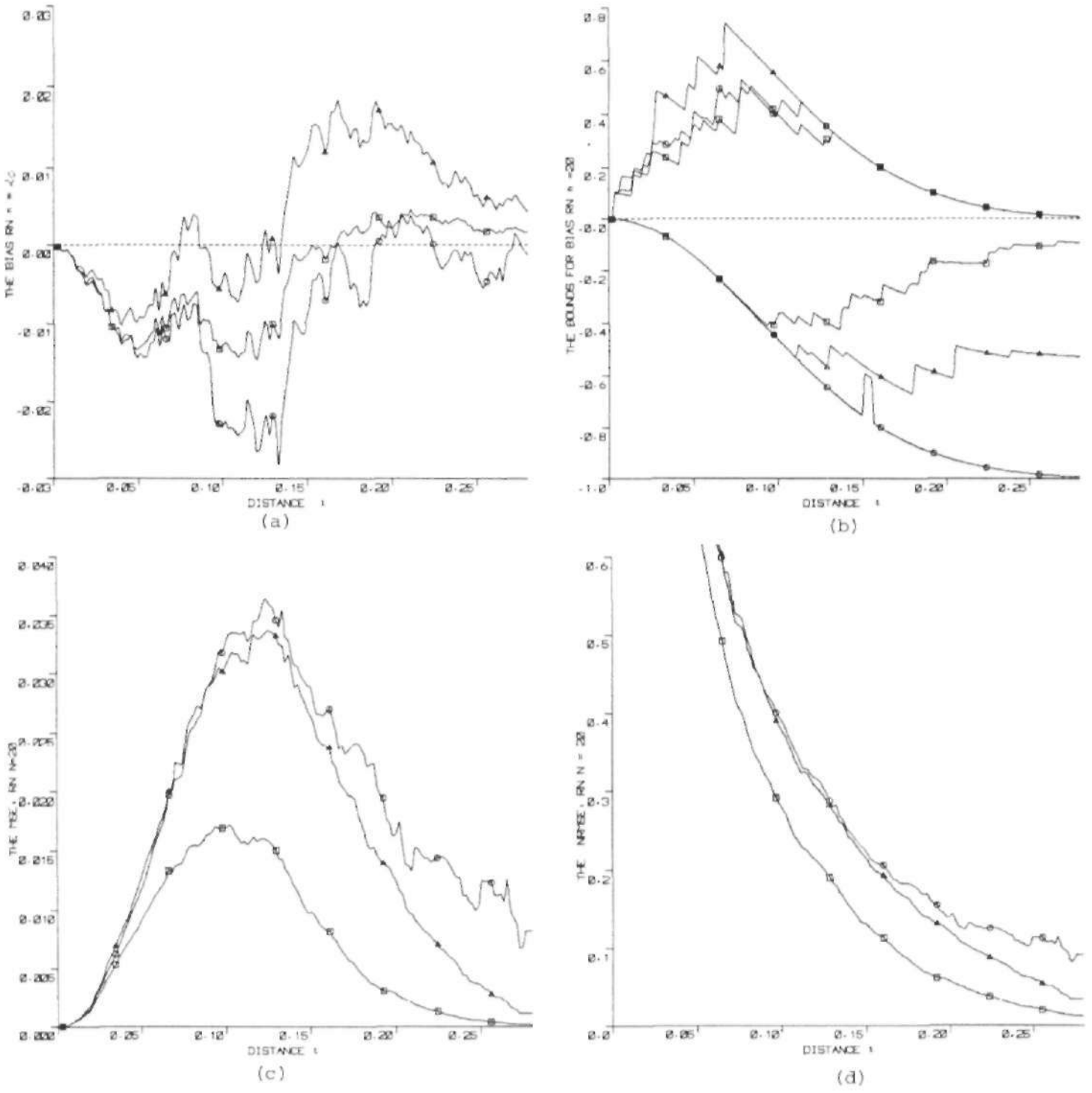


Figure 5.1 : (a) The average bias (b) the envelope of the estimates (c) The mean squared error and (d) the normalized root mean squared error for the estimators of G(t) for a Poisson process.

Key: —○—○—, $\hat{G}_1(t)$; —△—△—, $\hat{G}_2(t)$; —□—□—, $\hat{G}_3(t)$.

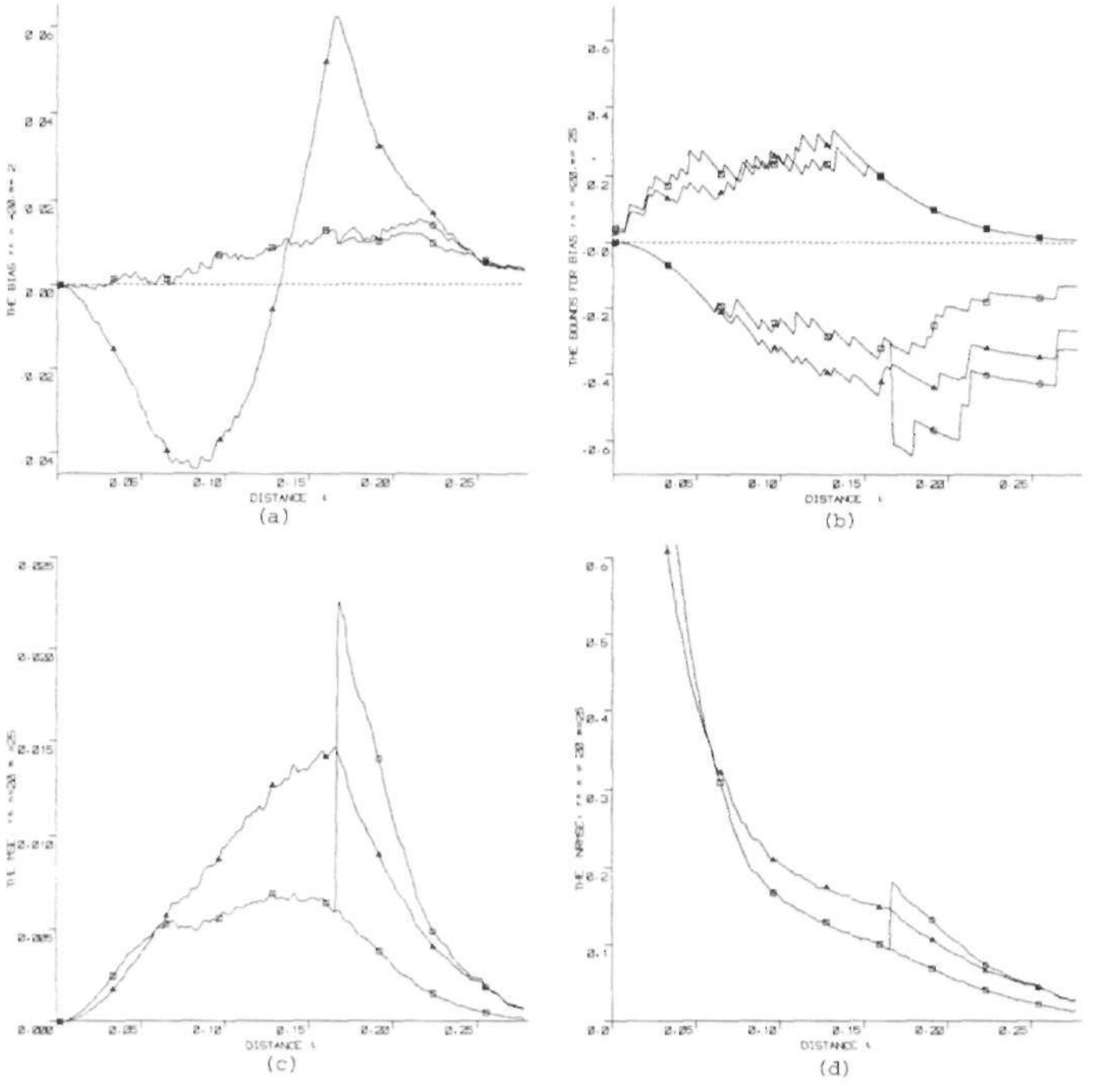


Figure 5.2 : (a) The average bias
(b) The envelope of the estimates
(c) The MSE
(d) The NRMSE for the estimators of F(t) for a Poisson process.

Key: —o—o—, $\hat{F}_1$; —Δ—Δ—, $\hat{F}_2$; —□—□— $\hat{F}_3$.

approximate halving of the mean squared error. This is a consequence of $\hat{G}_3(t)$ using all six sets of objects, whereas the other estimators use only three sets. Note that the bulk of the contribution to the mean squared error is due to the variance of the estimators and not to their bias.

Figure 5.1d shows the normalised root mean squared error (nrmse) defined by,

$$\text{nrmse}\{\hat{G}(t)\} = [\text{mse}\{\hat{G}(t)\}]^{\frac{1}{2}} / G(t)$$

for all the three estimators of G(t). It is clear from this figure, that $\hat{G}_3(t)$ has the smallest NRMSE for all values of t considered, and is therefore preferable.

Figure 5.2 also summarises the results obtained from 500 partial realizations of the Poisson process consisting of n = 20 objects (m = 25 points) in a unit square. Figure 5.2a shows that the estimator $\hat{F}_2(t)$ clearly underestimate F(t) at smaller values of t. Figures 5.2(b to d) suggest that the new estimator $\hat{F}_3(t)$ is much better than its competitors, both in terms of bias and in terms of variability, and is therefore preferable.

There is a striking similarity between $\hat{F}_1$ and $\hat{F}_3$ for values of $t < 0.167$ since for these values of t both $\hat{F}_1$ and $\hat{F}_3$ use the same information. However, for values of $t > 0.167$, a lot of useful information contained in the 16 sampling points (with nearest boundary distances less than 0.167), were not used by $\hat{F}_1(t)$. This resulted in the rapid increase in the variance and the mse of this estimator.

5.5 G(t) and F(t) for a Clustered Process.

A realistic model for aggregated spatial point patterns was provided by Neyman and Scott(1958), Bartlett (1964) and Warren (1971). Here the parents constitute a Poisson process with intensity ρ per unit area. To each parent is attached a number of offspring, the number being realised independently for each parent from a Poisson distribution with mean μ. Each of the offspring is independently, distributed uniformly on the circumference of the circle of radius σ centered on the corresponding parent.

Bartlett (1975) gives general expressions for the distribution functions F(t) and G(t) for this process. If we assume that both the parents and offspring are indistinguishable, then the point-object distance t has the distribution function

$$F(t) = 1 - \exp\{ - \rho\pi (t^2 + 2 \int_t^\infty [1 - P(y,t)] \, y \, dy) \} \qquad (5.19)$$

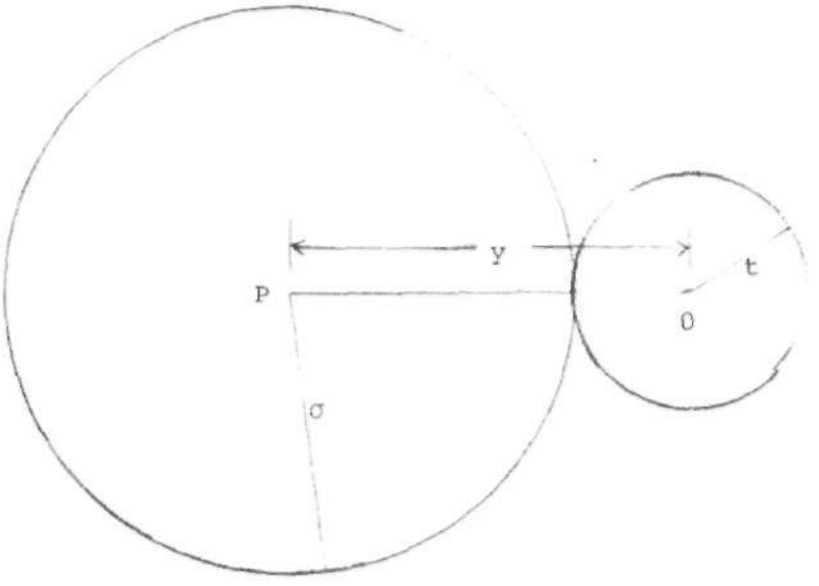
where P(y,t) = P(no offspring is found in the circle centre
the origin and radius t from a parent
a distance y from the origin) (5.20)

The object-to-object distance t also has the distribution function G(t):

$$G(t) = 1 - \{ 1 - F(t) \} P_2(t) \qquad (5.21)$$

where $P_2(t)$ = P(no parent or offspring from the same cluster
as the random sample object is found less than
a distance t from the random sample object) (5.22)

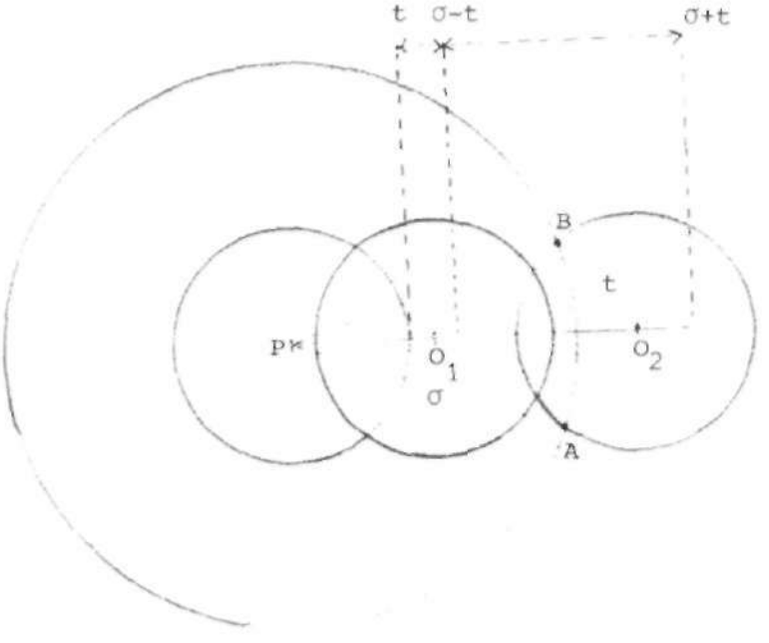
(a)



$y > \sigma + t$

$\Rightarrow P(y,t) = 1$

(b)



Here $t < \sigma/2$

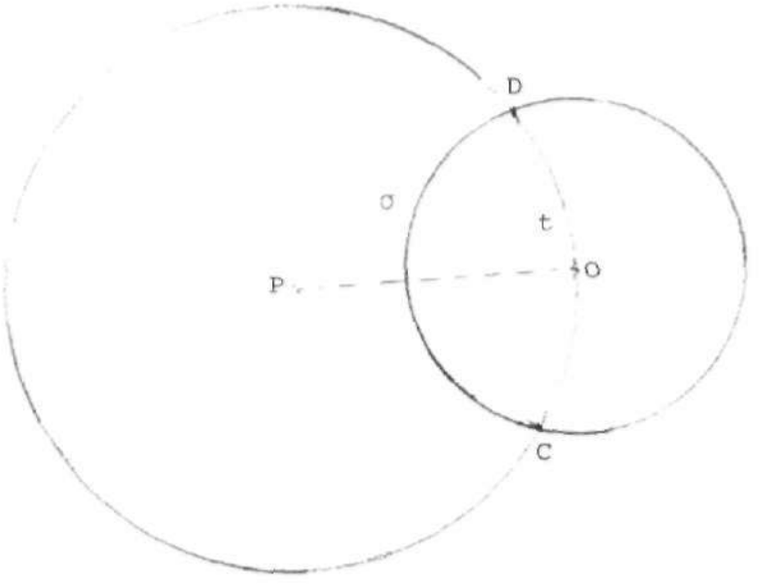
For $t < y < \sigma - t$: $P(y,t) = 1$

For $\sigma - t < y < \sigma + t$:

$P(y,t) = \exp(-\mu\ell/2\pi\sigma)$

where ℓ is the length of the minor arc AB of a circle of radius σ.

(c)



$d(t,\sigma)$ is the length of the minor arc CD of a circle of radius σ.

Figure 5.3 : Interpretation of $P_2(t)$ and $P(y,t)$.

Now consider a semi-deterministic clustering process in which the radial displacement of each offspring relative to its parent is σ. Considering first F(t), we note that $P(y,t) = 1$ for all $y > \sigma+t$ (see Figure 5.3a). For $t < y < t+\sigma$, we should distinguish between two cases:

Case 1: if $t < \sigma/2$, then $P(y,t) = 1$ for all $t \leq y \leq \sigma-t$ (see Figure 5.3b), and for $\sigma-t < y \leq \sigma+t$, P(y,t) is given as

$$P(y,t) = P(\text{ no offspring on minor arc AB of circle of radius } \sigma)$$

$$= \exp\{ - \mu\, l(y,t,\sigma) / 2\pi\sigma \} \qquad (5.23)$$

since the number of offspring on an arc of length $l(y,t,\sigma)$ is Poisson variate with mean $\mu l(y,t,\sigma)/2\pi\sigma$. The function $l(y,t,\sigma)$ is given by the equation,

$$l(y,t,\sigma) = 2\sigma \cos^{-1}\{ [y^2 + \sigma^2 - t^2] / 2\sigma y \} \qquad (5.24)$$

Case 2: If $t > \sigma/2$, then P(y,t) is also given by equation (5.23) for all $t<y<t+\sigma$.

If we now define $f(y,t,\sigma)$ and Q(t) as,

$$f(y,t,\sigma) = 1 - \exp\{ - \mu\, l(y,t,\sigma)/2\pi\sigma \}$$

$$Q(t) = \int_{\max(t,\sigma-t)}^{\sigma+t} f(y,t,\sigma)\, y\, dy$$

then

$$F(t) = 1 - \exp[- \pi\rho\{ t^2 + 2\, Q(t)] \qquad (5.25)$$

If $\sigma = 1$, then these results reduce to the results obtained by Diggle(1975).

For the object-to-object distance t, we may also calculate $P_2(t)$ defined in (5.22) by distinguishing between two cases.

Case 1: With probability $p = \mu\rho/(\rho + \mu\rho)$, the random sample object will be an offspring, whose parent will be σ distance away so that, $P_2(t) = 0$ if $t \geq \sigma$, and $P_2(t) = p_m$, otherwise, where P_m is the probability of no other offspring on minor arc CD of a circle of radius σ (see Figure 5.3c), and is given as

$$p_m = \exp\{ - \mu\, d(t,\sigma)/ 2\pi\sigma \}$$

where $d(t, \sigma) = 2\sigma \cos^{-1}(1 - t^2/ 2\sigma^2)$

Case 2: With probability $q = \rho/(\rho + \mu\rho)$, the random sample plant will be a parent, whose offspring may be a distance σ away, so that, $P_2(t) = p_n$ if $t \geq \sigma$ and $P_2(t) = 1$ otherwise. Here p_n is the probability that there are no offspring on the circumference of a circle of radius σ centred on the corresponding parent. Thus $p_n = \exp(- \mu)$.

Now, combining the two cases, we have:

$$P_2(t) = \begin{cases} q + p \exp\{- \mu d(t,\sigma)/ 2\pi\sigma\} & \text{if } 0 \leq t < \sigma \\ q \exp(-\mu) & \text{if } t \geq \sigma \end{cases} \qquad (5.26)$$

Thus substituting (5.26) and (5.25) in (5.21) we arrive at,

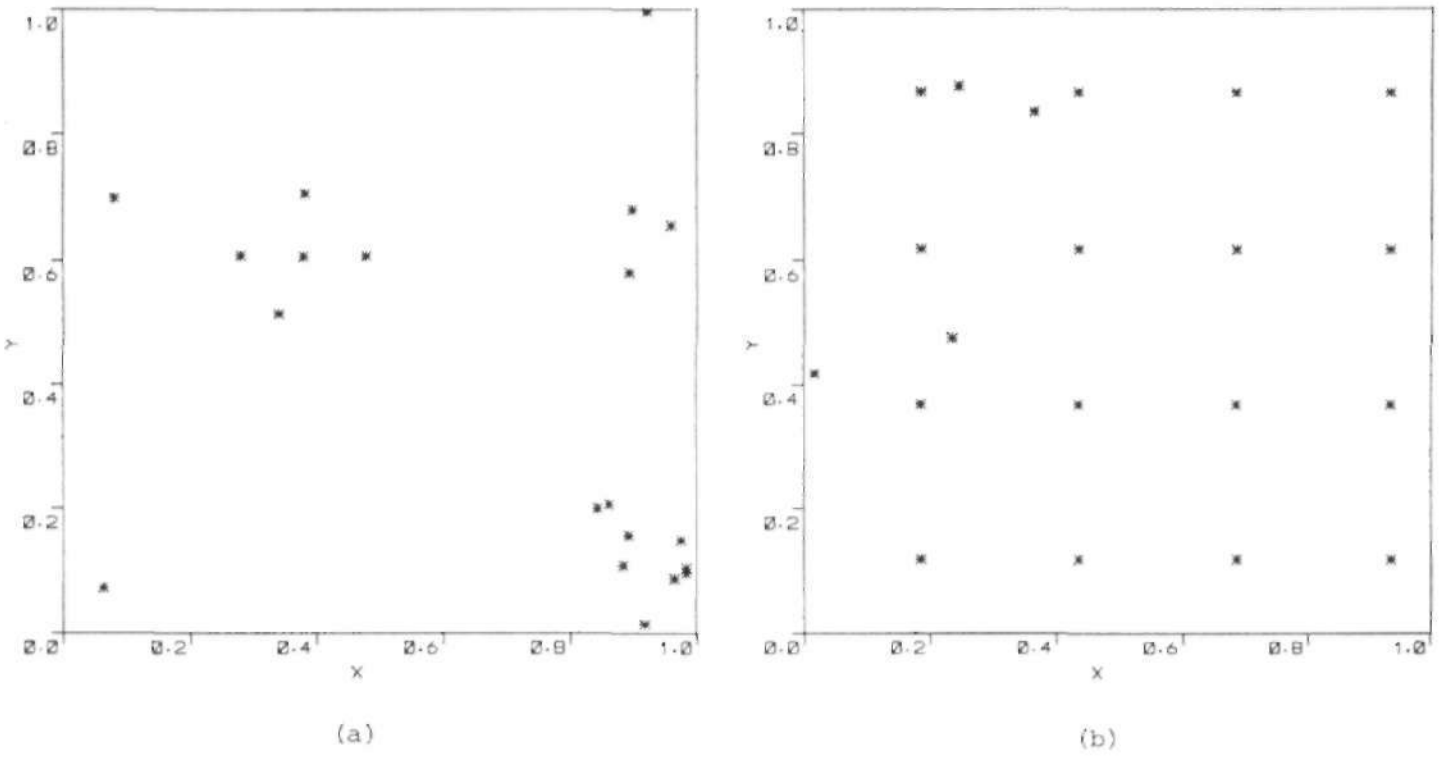


Figure 5.4 : Example realisations of (a) a mother-daughter clustered process, and (b) a superimposed lattice process.

$$G(t) = \begin{cases} 1 - Z(t)[q + p \exp\{ - \mu d(t, \sigma)/2\pi\sigma \}] & \text{if } 0 \leq t < \sigma \\ 1 - q\, Z(t) \exp(-\mu) & \text{if } t > \sigma \end{cases} \qquad (5.27)$$

where $Z(t) = \exp\{ - \pi\rho (t^2 + 2 Q(t))\}$

For our simulations we used the case of five randomly distributed 'mother' objects surrounded by a total of 15 'daughter' objects within a unit square window. The assignment of daughters to mothers was at random, with each daughter being placed at a distance of 0.1 units from its mother, and at an angle generated at random from a uniform distribution on $(0,2\pi)$. In certain cases this resulted in the daughter being initially placed outside the window. In these cases the window was regarded as a toroid and the daughter was appropriately relocated. An example realization of the process is presented in Figure 5.4a.

The fixed mother-daughter distance of 0.1 units implies that G(t) will be close to 1 as t approaches 0.1. In a complete realization of the process inter-object distances of more than 0.1 could only occur if there was an isolated mother having no daughters. In a partial realization it is also possible that a chance positioning of the window could result in an isolated daughter object. All the three estimators show a dramatic reduction in their mean squared errors at $t = 0.1$, to the extent that variations between them cease to be meaningful, and we therefore concentrate on the range of values $0 < t < 0.1$. The average bias, the envelope for the bias, the MSE as well as the nrmse obtained from 500 realizations of the process are illustrated in Figure 5.5. It can be seen from Figure 5.5a that all the three estimators slightly underestimate the true value of G(t), with the magnitude of the bias being somewhat greater than that associated with the estimation of the random process. The MSE and NRMSE for $\hat{G_1}(t)$ and $\hat{G_2}(t)$ are considerably greater than that for $\hat{G_3}(t)$.

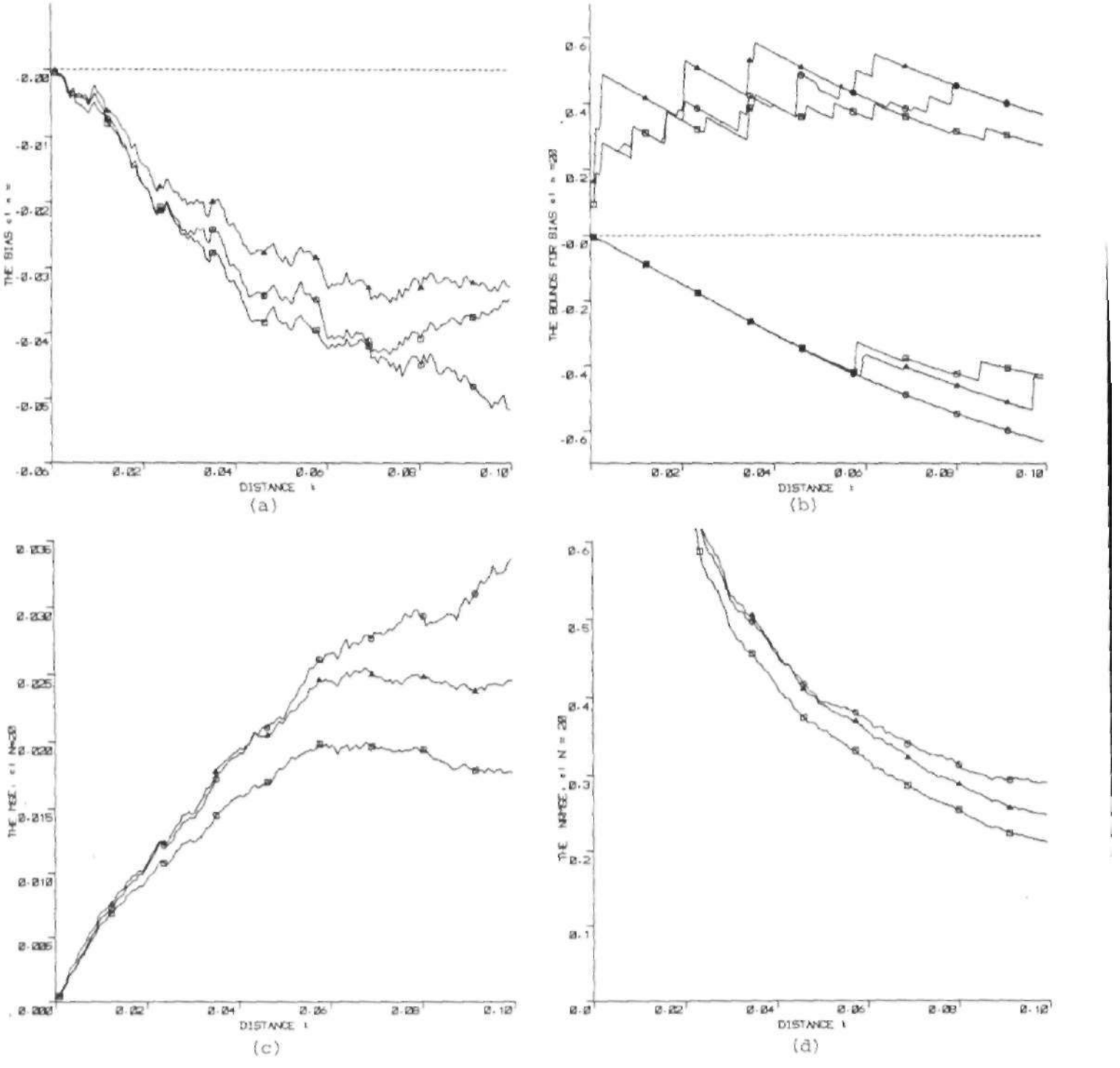


Figure 5.5 : (a) The average bias
(b) The envelope of the estimates
(c) The MSE, and
(d) the NRMSE for the estimators of G(t) for a mother-daughter clustered process.

Key : —o—o—, $\hat{G}_1(t)$; —Δ—Δ—, $\hat{G}_2(t)$; —□—□—, $\hat{G}_3(t)$.

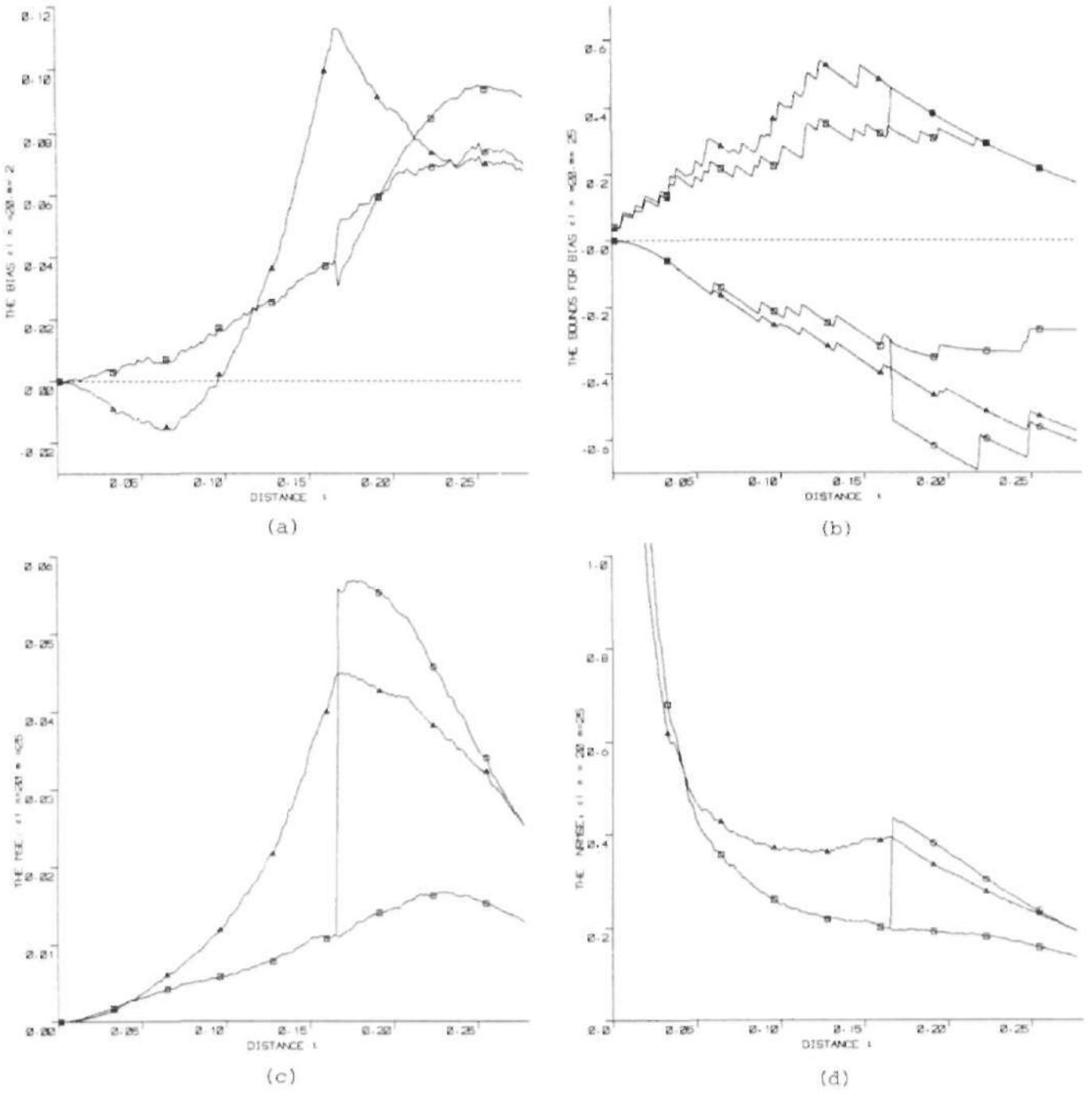


Figure 5.6 : (a) The average bias
(b) The envelopes of the estimates
(c) The MSE, and
(d) The NRMSE for the estimators of F(t) for the mother-daughter clustered process.

Key: —○—○—, $\hat{F}_1$; —△—△—, $\hat{F}_2$; —□—□—, $\hat{F}_3$.

The average bias, envelopes for the bias, MSE and NRMSE for the various estimators of F(t) obtained from 500 realisations (with m = 25) of the process are presented in Figure 5.6. Figure 5.6a shows that all the three estimators of F(t) slightly overestimate the true value of F(t) and this is particularly marked in the case of $\hat{F_2}(t)$. However, as with $\hat{G_3}(t)$, the mse and nrmse graphs of $\hat{F_1}(t)$ and $\hat{F_2}(t)$ are again considerably greater than that for $\hat{F_3}(t)$. This suggests that the new estimator $\hat{F_3}(t)$ is preferable, since it is the variance of these estimators which is the dominating consideration. Note that the explanation given in section 5.4, as to the behaviour of $\hat{F_1}(t)$ also holds for these alternatives.

5.6 G(t) and F(t) for a regular process.

Diggle(1975) suggests superimposing a Poisson process with intensity ρ per unit area upon a deterministic lattice process with intensity L per unit area so as to provide a continuous range of patterns from extreme regularity when ρ is zero, towards complete randomness as ρ tends to infinity.

For a square lattice of side σ, and with an object at each vertex of the regular lattice, a geometrical argument provides the distribution of the point to object nearest neighbour distance t, as

$$D(t) = \begin{cases} \pi t^2/\sigma^2 & \text{if } 0 \leq t < \sigma/2 \\ \{\, 2t^2 \sin^{-1}[\,(\sigma^2 - 2t^2)/2t^2\,)] \\ \quad + \sigma[\,4t^2 - \sigma^2\,]^{\frac{1}{2}}\,\}/\sigma^2 & \text{if } \sigma/2 \leq t < \sigma/\sqrt{2} \\ 1 & \text{if } t \geq \sigma/\sqrt{2} \end{cases} \qquad (5.28)$$

The distribution function of t in a realization of a Poisson process is $B(t) = 1 - \exp(-\rho \pi t^2)$. When the Poisson process is superimposed upon the lattice process, t is the minimum of two random variables, with distribution functions D(t) and B(t), and should therefore have distribution function

$$\begin{aligned} F(t) &= D(t) + B(t) - D(t)\,B(t) \\ &= 1 - \{ 1 - D(t) \} \exp(-\rho \pi t^2) \end{aligned} \qquad (5.29)$$

Now substituting (5.28) in (5.29), we arrive at,

$$F(t) = \begin{cases} 1 - [1 - \pi t^2/\sigma^2] \exp(-\pi\rho t^2) & \text{if } 0 \le t < \sigma/2 \\ 1 - \exp(-\pi\rho t^2)\,[\sigma^2 - \sigma(4t^2-\sigma^2)^{\frac{1}{2}} & \\ \quad -2t^2 \sin^{-1}\{(\sigma^2 - 2t^2)/2t^2\}]/\sigma^2 & \text{if } \sigma/2 \le t < \sigma/\sqrt{2} \\ 1 & \text{if } t \ge \sigma/\sqrt{2}. \end{cases} \qquad (5.30)$$

The object-to-object nearest neighbour distance t will also have the distribution function F(t), conditional on the randomly chosen object being in the realization of the Poisson process, as will occur with probability $p = \rho/(\rho+L)$. Otherwise the randomly chosen object must be a lattice object, as will occur with probability $q = 1 - p$, and the distribution function of t will then be,

$$C(t) = \begin{cases} 1 - \exp(-\rho\pi t^2) & \text{if } t < \sigma \\ 1 & \text{if } t \ge \sigma \end{cases}$$

The distribution function of t in the superimposed process is therefore, given by

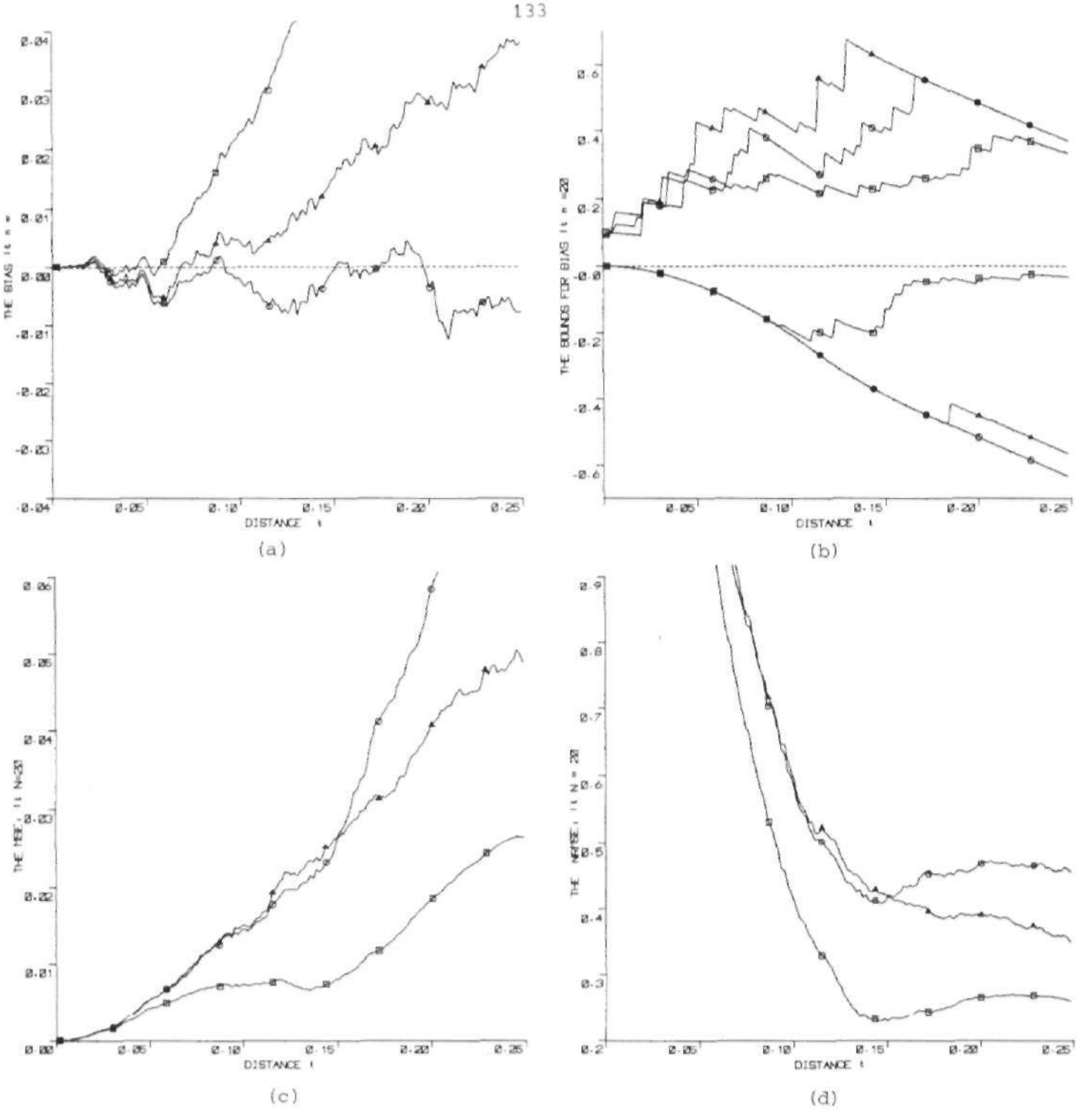


Figure 5.7 : (a) The average bias
(b) The envelope of the estimates
(c) The MSE, and
(d) The NRMSE, for the three estimators of G(t) applied to the superimposed lattice process.

Key: —○—○—, $\hat{G}_1(t)$; —△—△—, $\hat{G}_2(t)$; —□—□—, $\hat{G}_3(t)$.

$$G(t) = p\,F(t) + q\,C(t) \qquad (5.31)$$

Thus substituting the values of F(t) and C(t) in (5.31) gives,

$$G(t) = \begin{cases} p\,\{1 - [\,1 - \pi t^2/\sigma^2]\,\exp(-\rho\pi\,t^2)\} + U(t) & \text{if } 0 \leq t < \sigma/2 \\ p\,\{1 - [\,1 - 2t^2 \sin^{-1}((\sigma^2 - 2t^2)/2t^2)/\sigma^2 \\ \quad -(4t^2-\sigma^2)^{\frac{1}{2}} / \sigma\,\}\,\exp(-\rho\pi\,t^2) + U(t) & \text{if } \sigma/2 \leq t < \sigma/\sqrt{2} \\ p + U(t) & \text{if } \sigma/\sqrt{2} \leq t < \sigma \\ 1 & \text{if } t \geq \sigma \end{cases} \qquad (5.32)$$

where $U(t) = q\{1 - \exp(-\rho\,\pi t^2)\}$.

In our simulations, a lattice of 16 regularly placed objects is randomly located within the unit square window, and a further 4 objects from a Poisson process are added so as to give an element of randomness. A partial realization of this process with $\sigma = 0.25$, is given in Figure 5.4b.

Figure 5.7a shows that the new estimator $\hat{G_3}(t)$ is positively biased. This is undoubtedly due to its treatment of the objects belonging to set 6. Using the overall estimate of density (20 per unit area) and assuming a Poisson process for the unseen exterior portions of the circles centred on the objects results in an overestimation of the number of occasions on which these portions will contain an object. Figure 5.7b shows that there can have been few occasions on which $\hat{G_3}(t) < G(t)$, but it also reveals that the window for the bias shown by $\hat{G_3}(t)$ was much narrower than that for the other estimators, with both $\hat{G_1}(t)$ and $\hat{G_2}(t)$ occasionally giving estimates of 0 or 1 at large values of t.

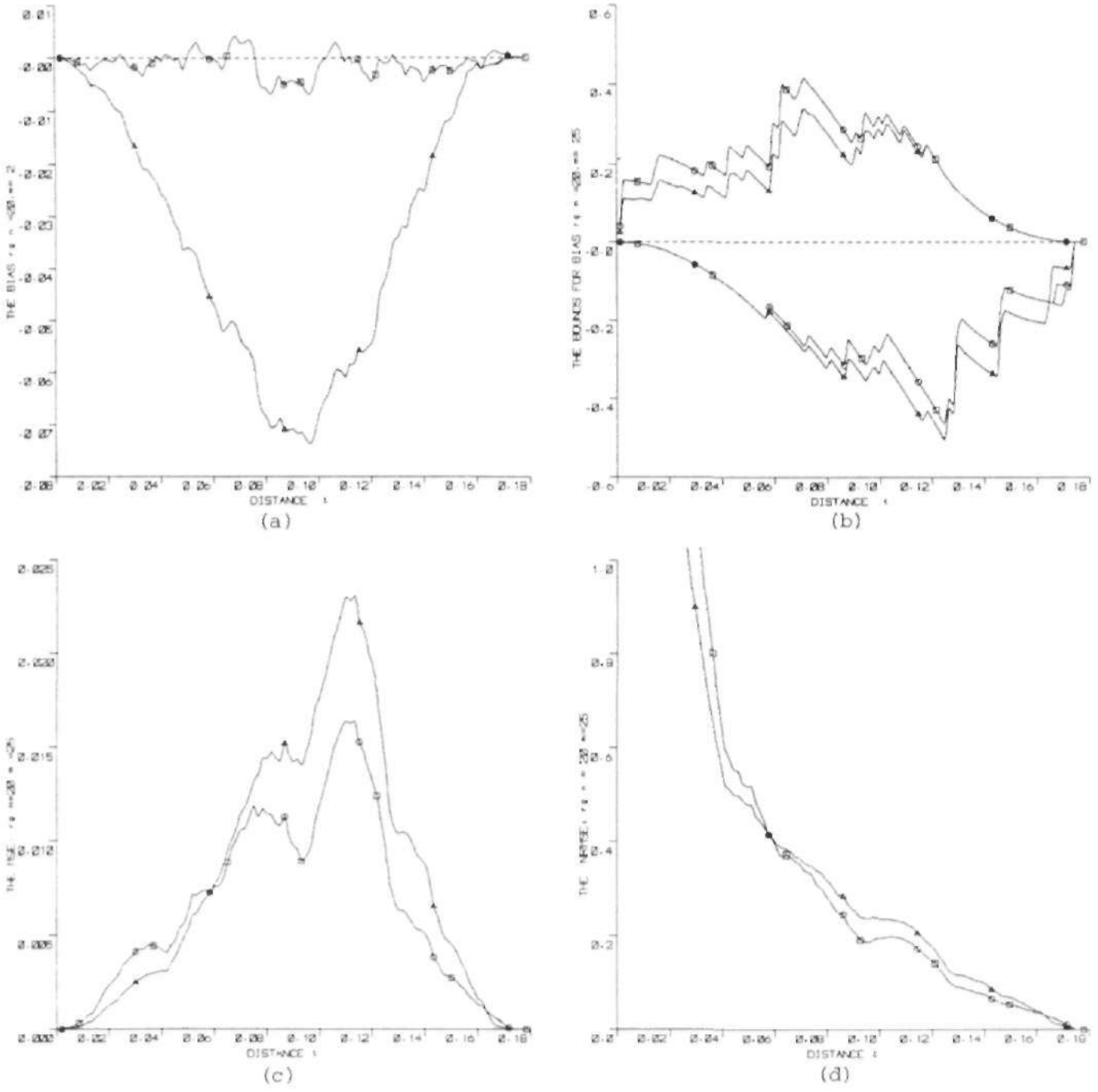


Figure 5.8 : (a) The average bias
(b) The envelope of the estimates
(c) The MSE, and
(d) The NRMSE of the three estimators of F(t) applied to the superimposed lattice process.

Key: —○—○—, $\hat{F}_1(t)$; —△—△—, $\hat{F}_2(t)$; —□—□—, $\hat{F}_3(t)$.

Figure 5.7(c and d) show a repeat of earlier patterns. Despite the increased bias, the reduced variance obtained with $\hat{G}_3(t)$ results in a MSE and NRMSE that is much the smallest over the interesting part of the range of t. This of course suggests that the new estimator is superior to the existing estimators.

Figure 5.8(a to d) shows a repeat performance for the estimators of F(t). The new estimator $\hat{F}_3(t)$, is approximately unbiased for all values of t considered, and has the smallest mse and nrmse. However, the estimator $\hat{F}_2(t)$ is clearly biased.

5.7 Graphical analysis

We shall illustrate by means of some practical examples, the use of graphical methods in the context of preliminary testing, using the 'refined' nearest neighbour analysis. For preliminary testing, some functional description of a spatial point pattern usually provides more information as to the nature of any significant departure from the Poisson forest.

To test for deviations from randomness, Upton and Fingleton (1985) suggest plotting the functions $h_1(t)$ and $h_2(t)$ against t. These functions are defined by

$$h_1(t) = \hat{G}(t) - 1 + \exp(- \lambda\pi t^2) \qquad (5.33)$$

$$h_2(t) = \hat{F}(t) - 1 + \exp(- \lambda \pi t^2) \qquad (5.34)$$

For a random pattern both $h_1(t)$ and $h_2(t)$ would be close to zero. For a clustered pattern, there will be a greater number of small object to object distances than would be the case in a random pattern, and so $h_1(t) > 0$ and

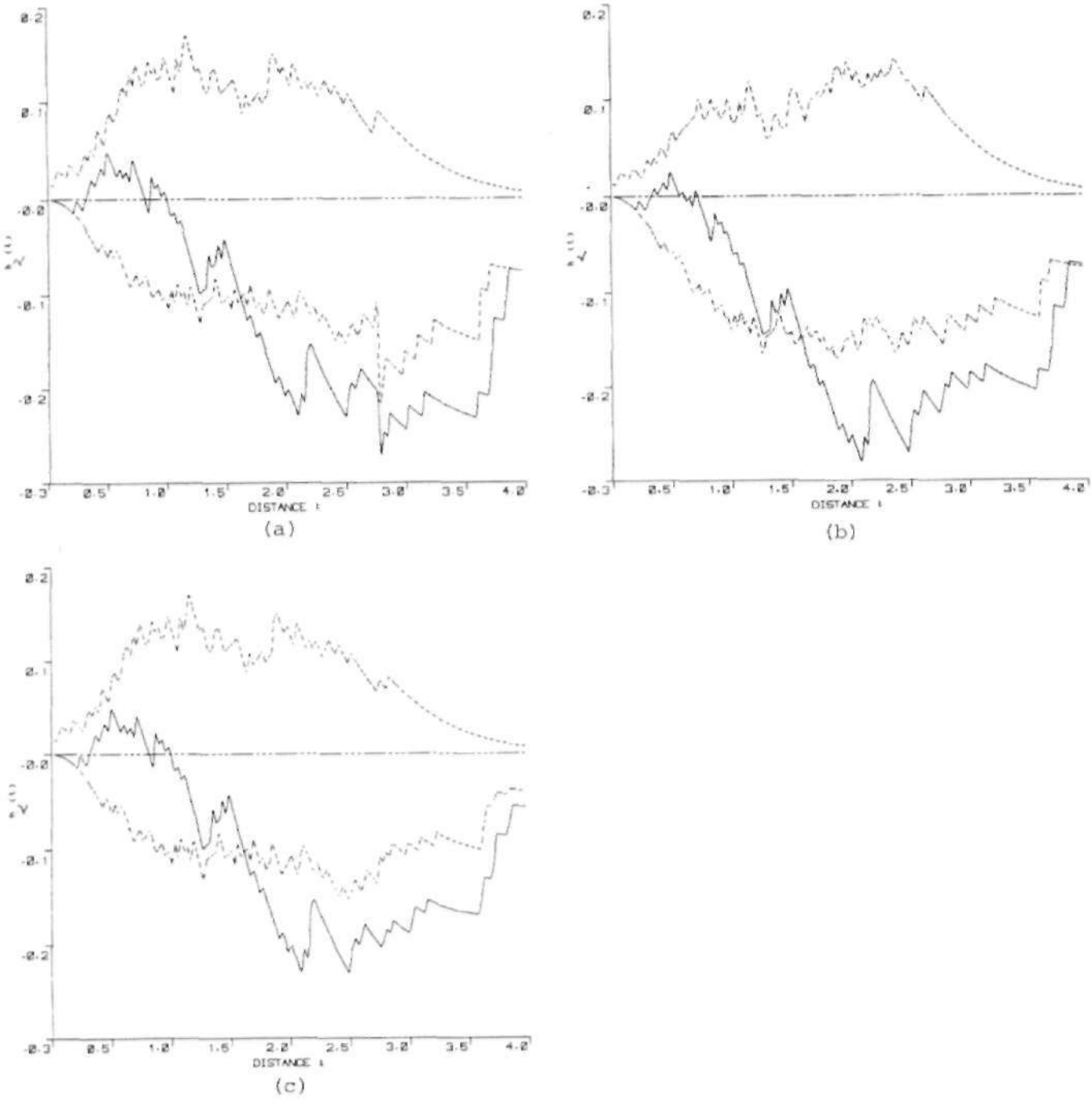


Figure 5.9 : The values of (a) $\hat{F}_1$, (b) $\hat{F}_2$, (c) $\hat{F}_3$ for the redwood seedlings data, together with the corresponding envelope resulting from 99 simulations of a Poisson process of comparable object density.

$h_2(t) < 0$. However for a regular pattern $h_1(t) < 0$ and $h_2(t) > 0$. The power study carried out by Diggle(1979a) suggests that $h_1(t)$ is more appropriate for regular alternatives and $h_2(t)$ for clustered patterns.

To assess the significance or otherwise of the departure from the Poisson forest the conventional approach is to calculate the values of $h_1(t)$ and/or $h_2(t)$ from each of (s-1) independent realizations of the Poisson process consisting of n objects in D and then to obtain the upper and lower simulations envelopes as:

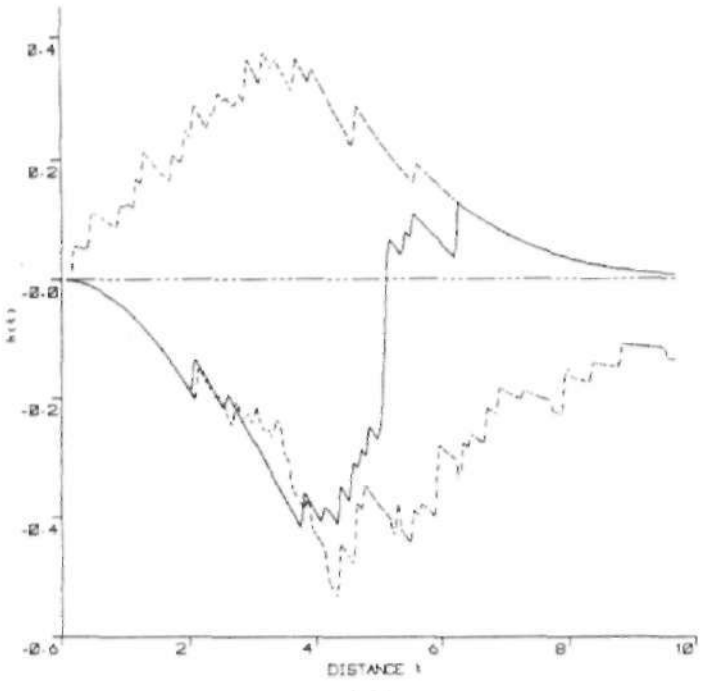
$$U_j(t) = \max_i \{ h_j^{(i)} \}$$
$$L_j(t) = \min_i \{ h_j^{(i)} \} \qquad (5.35)$$

where $j = 1, 2$. These simulation envelopes are intended to help in the interpretation of the plot of $h_j(t)$ against t.

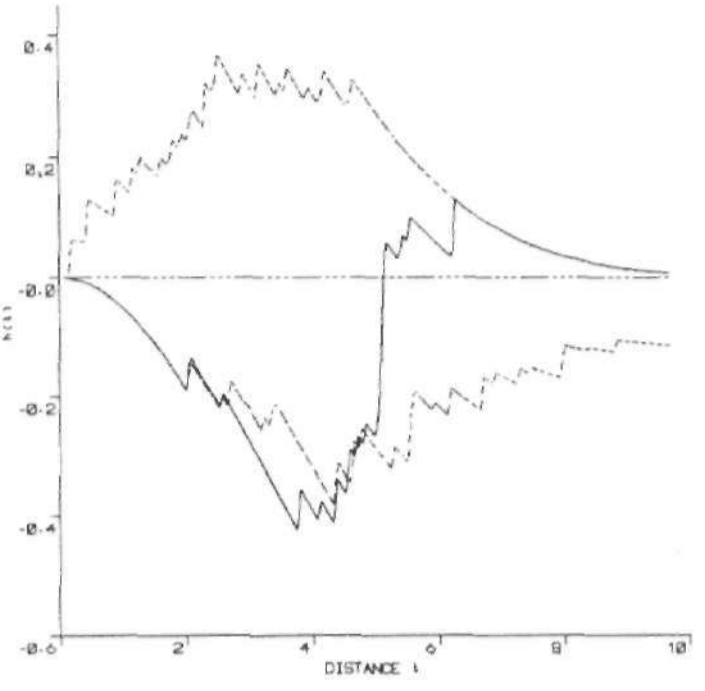
5.7.1 Analysis of redwood seedlings.

In this section we are concerned with the analysis of the redwood seedlings given in Figure 3.5c of Chapter III. Previous analysis of this data suggests a deviation towards aggregation. In order to assess the significance of any departure from the Poisson forest, we first simulate 99 random patterns, using the same object density and same size window. Using the three estimators of F(t), we estimate $h_2(t)$ for each pattern and Figure 5.9 displays dotted lines showing the envelope of these realizations. The envelope for $\hat{F}_3(t)$ is somewhat narrower than those obtained using $\hat{F}_1(t)$ and $\hat{F}_2(t)$ because of the greater precision inherent in the new estimator.

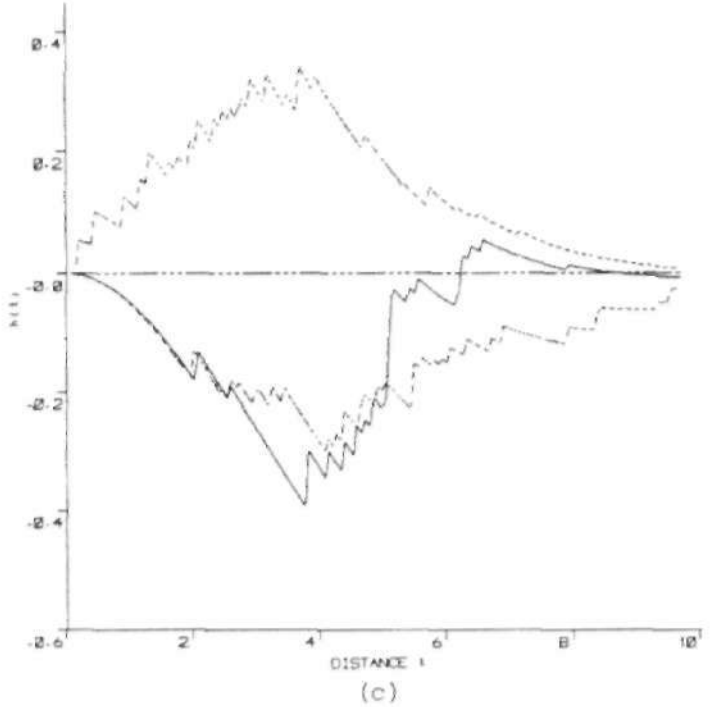
The solid lines in Figure 5.9 indicate the values of $h_2(t)$ obtained for the redwood seedlings. All the three plots suggest that there is a significant clustering for values of $t > 1.6$ m.



(a)



(b)



(c)

Figure 5.10 : The values of (a) $\hat{G}_1(t)$; (b) $\hat{G}_2(t)$ and (c) $\hat{G}_3(t)$ for the waterstriders data, together with the corresponding envelope resulting from 99 simulations of a Poisson process of comparable object density.

5.7.2 Analysis of Waterstriders data.

As an example of the application of the estimators of G(t), we consider some data analysed in Chapter IV, using the second order methods. These data illustrated in Figure 4.7a show the pattern of waterstriders, the fifth larval stage of Limnoporus rufoscutellatus. It is known that in late larval and adult stages, these insects display territorialism and a regular pattern is anticipated.

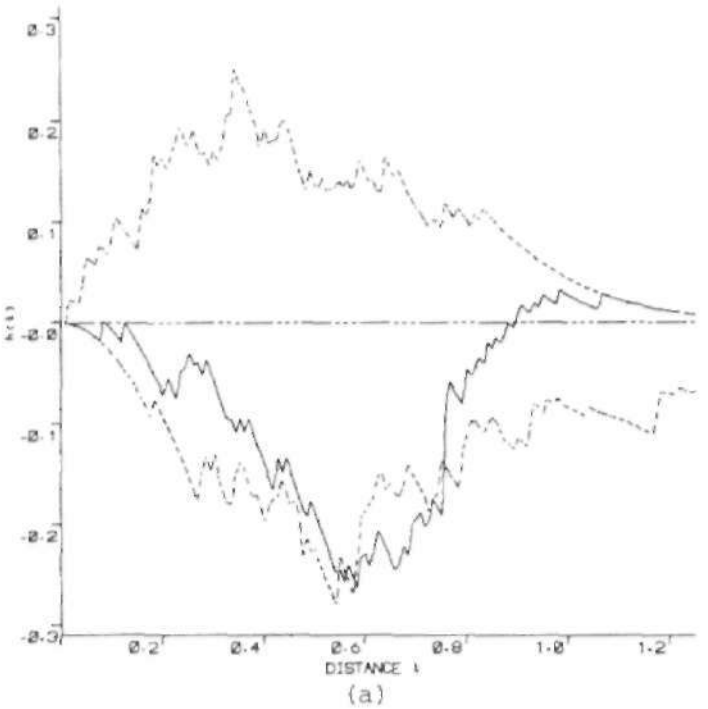
Figure 5.10 displays the dotted lines showing the envelopes of the realizations of the 99 random patterns of similar intensity, as the waterstriders data. As was noted earlier for $\hat{F}_3(t)$, the envelope for $\hat{G}_3(t)$ is much narrower than those obtained using $\hat{G}_1(t)$ and $\hat{G}_2(t)$.

The solid lines in Figure 5.10 indicate the values of $h_1(t)$ obtained for the waterstriders data. These lines quickly penetrate the envelopes, thus providing evidence at the 1% level of significant regularity in the pattern. Clearly at this stage of their development it is unusual to find a pair of waterstriders very close together. The preferred separation appears to be at about 3.5 cm.

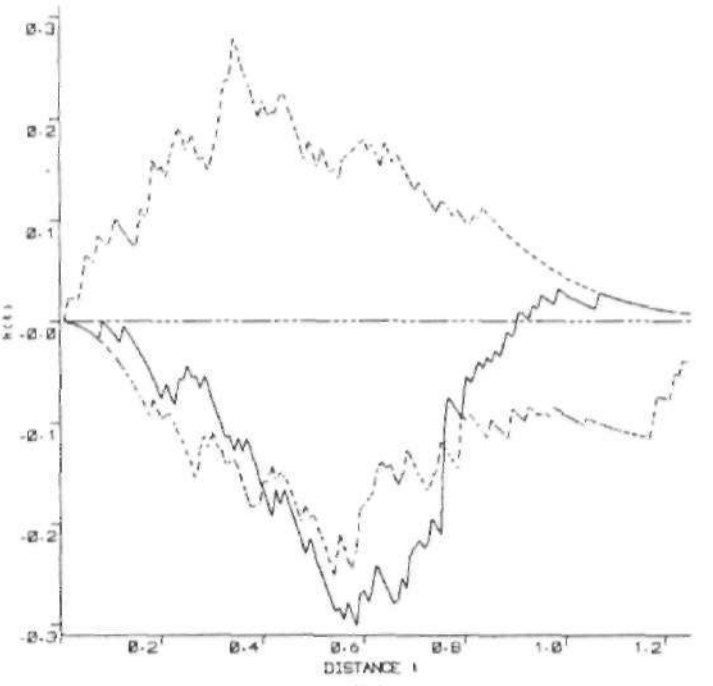
5.7.3 Analysis of a Cellular process.

In Chapter IV, we have used second order methods to analyse the cellular data presented in Figure 4.8a. In this section we shall subject these data to the refine nearest neighbour analysis.

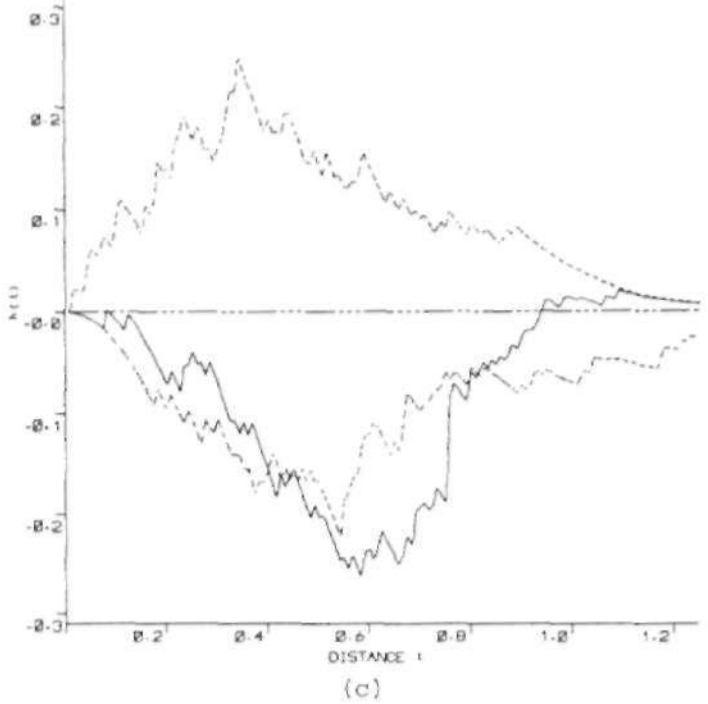
The $h_1(t)$ functions for the cell data, using the various estimators of G(t) together with the envelope for $h_1(t)$ obtained from 99 partial realizations of the Poisson forest of similar intensity are presented in Figure 5.11. Unlike the second order method, the $h_1(t)$ function for the cell data penetrates the 99% envelope for the Poisson realizations at about



(a)



(b)



(c)

Figure 5.11 : The values of (a) $\hat{G}_1(t)$; (b) $\hat{G}_2(t)$ and (c) $\hat{G}_3(t)$ for the cell data, together with the corresponding envelope resulting from 99 simulations of a Poisson process of comparable object density.

t = 0.4 units, thus providing a significant deviation from the random hypothesis towards a regular alternative. Thus while the second order analysis of the cell data has given no reason to reject the Poisson hypothesis, the refined nearest neighbour analysis has led to a different conclusion.

CHAPTER VI

Methods for analysing Multitype Spatial point patterns

6.1 Introduction

Multitype (or multivariate) spatial point patterns arise when the objects in the study region are classified not only by position but also by their type. Many problems occuring in practice involve the analysis of multitype spatial point patterns, particularly in the plane. In most cases however such analysis requires consideration of only two of the types at a time. In this chapter we discuss the extension to two-type patterns, of techniques for dealing with patterns of objects of a unitype discussed in previous chapters.

We are concerned here with the test of the hypothesis that the observed two type patterns are independent. Independence is analogous to spatial randomness for univariate patterns, in that it provides a convenient reference point for the characterization of more interesting two-type structures. For two homogeneous processes, departures from the independence hypothesis might reflect either a direct stochastic interaction between the two types of objects or qualitatively similar but statistically independent reactions to a heterogeneous environment or both. In the event that the hypothesis of independence is rejected we seek to classify the two unitype patterns as positively dependent (attracted to each other) or negatively dependent (repelling each other).

6.2 Multitype Spatial point processes

6.2.1 Processes displaying repulsion

For a process which displays negative dependence, Diggle and Cox(1983) have developed a bivariate sequential process, in which type 1 and type 2 objects are generated in alternating sequence. Each object is provisionally located according to a uniform distribution on the region D, but is retained only if it falls a distance at least σ away from all previously retained objects of the opposite type. Otherwise a new provisional location is generated and the above procedure is repeated. This is a natural two-type analogue of the simple sequential inhibition process described in Chapter I. With this procedure, the inhibition region for one process against the other will be randomly placed and so the combined pattern will appear random, whereas each separate pattern will appear clustered. Figure 6.1 (a and b) shows typical realizations with 49 objects of either type in a unit square, with $\sigma = 0.08$ and $\sigma = 0.15$.

Another two-type model that leads to a simply generated pattern was proposed by Hanisch and Stoyan (1979). They envisaged a two-type pattern, which is subdivided into type 1 and type 2 objects according to the realized remoteness of the generated objects. Specifically a Poisson process is realized and each object of the process is then examined in turn. If an object is found to be at a distance σ or more from all the surrounding objects, then this object is deemed to belong to type 2, and otherwise is deemed to belong to type 1. It is evident that the type 1 objects must display clustering while the type 2 objects will display regularity of the hard core type.

A softer variant of the two-type sequential process was also proposed by Diggle and Cox(1983). They used a two parameter generalisation and introduced a survival function

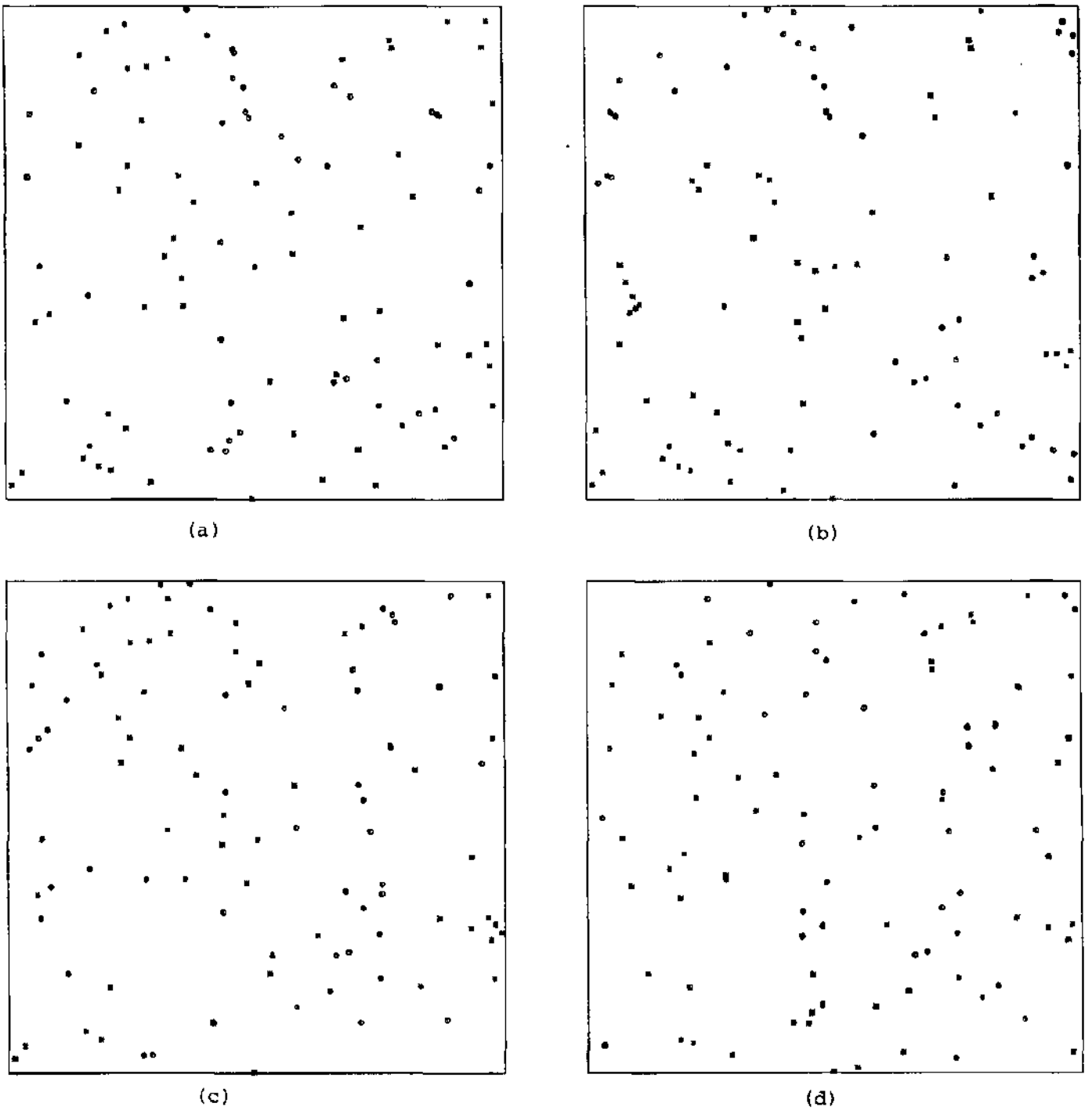


Figure 6.1 : (a) and (b) - realizations of a bivariate simple inhibition process with σ=0.08 and σ=0.15 respectively.

(c) and (d) - realizations of a soft-core bivariate simple inhibition process with σ=0.08, β=1.0 and σ=0.15 and β=1.0 respectively all in a unit square.

$$p(d) = \begin{cases} (d / \sigma)^{\beta} & \text{if } d < \sigma \\ 1 & \text{if } d \geq \sigma \end{cases} \qquad (6.1)$$

which operates as follows. The two types of objects are generated in alternating sequence according to a uniform distribution in D, but now the provisional location of the $(m+1)^{st}$ type i object is retained, with probability,

$$P_{i,m+1} = \prod_{k=1}^{m} p(d_{m+1,k}) \qquad (6.2)$$

where the $d_{m+1,k}$ denote the distances from the potential new $(m+1)^{st}$ object of type i, to the m previously retained objects of type j. Figure 6.1 (c and d) shows typical realization with 49 objects of either type in a unit square with $\sigma = 0.08$, $\beta = 1.0$ and with $\sigma = 0.15$, $\beta = 1.0$.

6.2.2 Processes displaying attraction

Following Diggle and Milne (1983), we denote by $\Lambda(x,y)$ a stationary, isotropic random field within a tiny region centred on the position (x, y). For a Poisson process, the intensity is everywhere the same and so

$$\Lambda(x,y) = \lambda \text{ for all } (x,y) \qquad (6.3)$$

The general Cox process with varying intensity is then defined by

$$\Lambda(x,y) = \lambda(x,y) \qquad (6.4)$$

where $\lambda(x,y)$ is a function of the location (x,y). For a two-type point process, we have two object intensities, $\Lambda_1(x,y)$ and $\Lambda_2(x,y)$. If

$\Lambda_1(x,y) = \lambda$ and $\Lambda_2(x,y) = \mu$, then this would imply that both individual patterns were bivariate Poisson with overall intensity $\mu + \lambda$.

Consider the case where the two point patterns are generated by link attractions. In this case we might have,

$$\Lambda_1(x,y) = c\,\Lambda_2(x,y) \qquad (6.5)$$

where c is an arbitrary constant. Diggle and Milne (1983) refer to this process as a linked Cox process. If $\Lambda_1(x,y) = \Lambda_2(x,y) = \lambda$, this process degenerates into a linked-pairs process. Diggle and Cox (1983) model the linked-pairs process by assuming that the type 1 object has an associated type 2 object whose relative position is described by a radially symmetric Gaussian distribution . That is , the orientation of the type 2 object with respect to the type 1 object is uniform on $(0, 2\pi)$ and their distance apart is described by the distribution function F(t).

To obtain the distribution function F(t), consider an arbitrary type 1 object as the origin and its associated type 2 object as (x_1 , y_1), which are r distance apart. Since x_1 and y_1 are from $N(0,\sigma^2)$, then

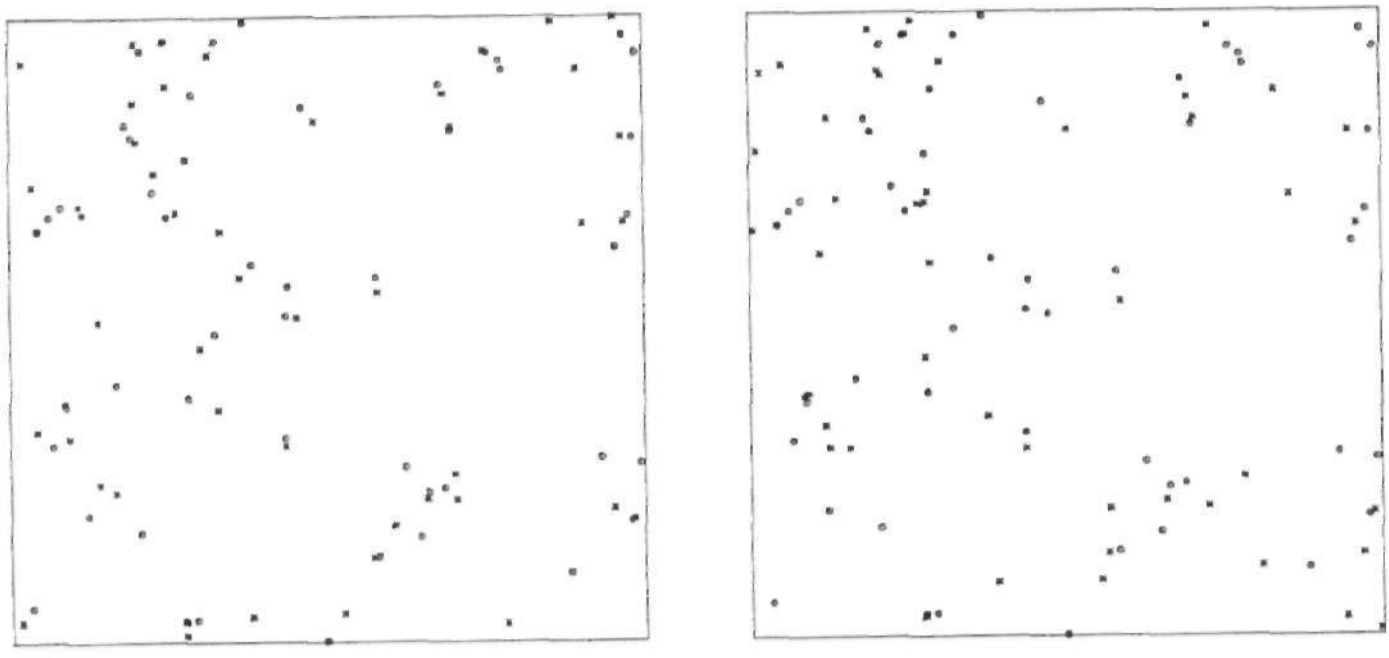
$$F(t) = P(r \leq t)$$

$$= P\{ x_1^2 + y_1^2 \leq t^2 \}$$

$$= P\{ x_1^2/\sigma^2 + y_1^2/\sigma^2 \leq t^2/\sigma^2 \}$$

But $\{x_1/\sigma\}^2$ is Chi-squared distributed with one degree of freedom. Similarly $\{y_1/\sigma\}^2$ has the same distribution. Therefore

$$F(t) = P\{ \chi_2^2 \leq t^2/\sigma^2 \}$$



(a) (b)

Figure 6.2 : Realizations of a 'linked pairs' process :
(a) σ=0.05; (b) σ=0.10 in a unit square.

$$= \quad G\ (\ t^2 / \sigma^2)$$

where $\quad G(y) \quad = \quad 1 - \exp(\ -\ y/2\ )$

Whence $\quad F(t) \quad = \quad 1 - \exp(\ -\ t^2/\ 2\sigma^2\ ) \qquad (6.6)$

Figure 6.2 (a and b) shows a partial realisation of a link pairs process with 49 objects of either type on the unit square, with $\sigma = 0.05$ and $\sigma = 0.10$ respectively.

6.3 Conditional Monte Carlo tests.

We have considered the use of Monte Carlo tests for hypotheses about spatial point processes in previous chapters. For multitype processes however, we have to preserve the separate object distributions in their observed form, since that form represents the entirety of our certain knowledge concerning their pattern. The restriction on preserving the separate observed patterns led Lotwick and Silverman (1982) to consider a conditional Monte Carlo test. This test provides a test of independence for data in a square or rectangular region D, conditional on the observed marginal structure as follows:

(1) the region D is converted into a torus,

(2) the value of μ_1, which is any suitable statistic that measures the dependence in the observed pattern, is calculated,

(3) define a random toroidal shift to be a translation of every type 2 object x to x + v, where v is a realisation from the uniform distribution on the torus, and compute the value μ_2 for the resulting bivariate pattern,

(4) repeat (3) using further independent random toroidal shifts to obtain μ_3 , μ_4 , ..., μ_s ,

(5) order the $\{\mu_k\}$ to give $\mu_{(1)} < \mu_{(2)} < \mu_{(3)} \ldots < \mu_{(s)}$.

The stationarity and independence of the patterns imply that,

$$P[\ \mu_1 = \mu_{(k)}\ ] = 1/s, \quad k = 1, 2, \ldots, s.$$

and the rank of μ_1 provides the basis of a conditional Monte Carlo tests. Thus rejection of the independence hypothesis on the basis that μ_1 ranks r largest or higher gives an 'exact' one sided test of size $\alpha = r/s$.

Table 6.1 : Notation for a two-type presence/absence cross classification

		Type 2 objects: Present	Type 2 objects: Absent	Total
Type 1 objects	Present	a	b	m
	Absent	c	d	n
	Total	r	s	N

6.4 Quadrat counts method

An alternative procedure for detecting possible attraction or repulsion involves noting, for each quadrat, whether an object of type i, i = 1, 2, ..., k is present or absent in that quadrat. The resulting categorical data can then be summarized in a 2^k contingency table. For a two-type pattern, k = 2 and the resulting 2 x 2 table of frequencies for a total of N quadrats is presented in Table 6.1. From this table, it is clear that the estimated chance of a quadrat containing a type 1 object is $\hat{p}_1 = m/N$, while the chance of a quadrat containing a type 2 object is

$\hat{p}_2 = r/N$. If the locations of the two types were independent of one another, then the proportion of quadrats that would be found to contain both types would be $\hat{p}_1\hat{p}_2$. The expected number that would contain both types would be estimated by $N\hat{p}_1\hat{p}_2$. Similarly, the estimates of the remaining expected frequencies under the assumption of independence of locations of the two types would be ms/N, nr/N and ns/N.

In order to compare the observed frequencies with the corresponding expected frequencies, we use the statistic

$$\chi^2 = N (ad - bc)^2 / m n r s \qquad (6.7)$$

Under the independence hypothesis χ^2 is closely approximated by the continuous χ^2_1 distribution. However this approximation may be improved by making a slight continuity correction to the formula (6.7). Upton and Fingleton (1985) suggest that improved tests can be provided by using

$$\chi^2_p = (N - 1) \{ | ad - bc | - N / 2 \}^2 / m n r s \qquad (6.8)$$

provided that the entire region has been divided into N quadrats and these are found to contain m quadrats in which type 1 objects are present and r quadrats in which type 2 objects are present.

Table 6.2: The presence/absence table for the linked-pairs process.

		Type 2 objects: Present	Type 2 objects: Absent	Total
Type 1 objects	Present	21	0	21
	Absent	0	4	4
	Total	21	4	25

In order to demonstrate the applicability of the quadrat count statistic (6.8) we used a simulated realization of a linked-pairs process, consisting of 49 objects of either type in a unit square window. This realization is illustrated in Figure 6.2 a. Table 6.2 gives the presence/absence cross classification for this realisation, using N = 25 quadrats to partition the unit square. From this table, and using equation (6.8) we obtain a value of χ^2_p as 17.39. Since the upper 1% point of a χ^2_1 distribution is 6.63, it is clear that the presence/absence Table 6.2 displays a significant departure from independence. However, the number of quadrats used to partitioned the sampling window would have some effect on the statistic defined in (6.8). For example Table 6.3 presents the values of this statistic for various values of N. For N = 15 or 20 the value of this statistic does not suggest a significant departure from the independent hypothesis.

Table 6.3: Effects of changing the number of quadrats on χ^2_p

N	χ^2_p
15	1.163
20	1.778
25	17.389
30	10.819
36	10.275
49	12.974
64	13.928
81	31.018
100	30.575
121	27.949

Upton and Fingleton (1985) suggest that a more informative analysis could be obtained by considering the actual quadrat counts $\{x_i\}$ for type 1 objects and $\{y_i\}$ for type 2 objects, with $i = 1, 2, \ldots, N$. In the case of attraction we would expect to have a positive correlation between X and Y, with negative correlation for repulsion. The product-moment correlation coefficient is given by the equation

$$r = \frac{\sum_{i=1}^{n} x_i y_i / n - \bar{x}\,\bar{y}}{\sqrt{\{\sum_{i=1}^{n} x_i^2/n - \bar{x}^2\}\{\sum_{i=1}^{n} y_i^2/n - \bar{y}^2\}}} \qquad (6.9)$$

To test the significance of r, we shall require knowledge of its probability distribution under the null hypothesis of independence. This distribution is summarised in cumulative form in Table 6.4

Table 6.4. The cumulative distribution of r for the linked-pairs process, based on 99 random toroidal shifts of the type 2 objects.

Value of r:	- 0.34306	- 0.31421	- 0.25190	- 0.06654
Freq > r :	99	98	95	60
Value of r:	0.04399	0.35812	0.65251	0.69901
Freq > r :	30	5	2	1

Using Figure 6.2a, with n = 25 quadrats, we find $\sum x_i y_i = 134$, $\sum x_i^2 = 147$, $\sum y_i^2 = 145$. This means that r = 0.760. Since from Table 6.4, the upper 1% point of the distribution of r is equal to 0.699, we have highly significant evidence of a positive association or attraction between

the two object distributions. Table 6.5 summarizes the effect of changing the number of quadrats to partitioned the study area, upon our interpretation of the simulated data. The values of $r_{0.01}$ are at the 1% level, obtained using independent random toroidal shifts of the type 2 objects. Note that even for n = 20, the corresponding value of r is still significant at the 1% level. Also note that the values of r for all the quadrats are positive, indicating spatial affinity between the two object patterns.

Table 6.5 : The effect of changing the number of quadrats on the apparent correlation.

N	$\sum x_i y_i$	$\sum x_i^2$	$\sum y_i^2$	r	$r_{0.01}$
15	196	209	219	0.669	0.755
20	145	155	159	0.676	0.671
25	134	147	145	0.760	0.699
30	136	143	149	0.849	0.737
36	110	127	119	0.771	0.448
49	87	105	99	0.718	0.685
64	72	95	91	0.622	0.571
81	62	81	79	0.643	0.419
100	56	89	69	0.592	0.535
121	46	77	71	0.484	0.447

6.5 The average nearest neighbour distance method

Suppose that we have a two-type spatial point pattern in which the separate point patterns are independent with intensities λ_1 and λ_2. Let W be the distance between an arbitrary type 1 object and its nearest type 2 neighbour. The proportion of the two types are then given by

$p_j = \lambda_j / (\lambda_1 + \lambda_2)$, $j = 1, 2$. When one object is randomly selected as the centre of a circle with radius w, the probability that the circle contains exactly X objects of the type different from the central object is shown by Lee (1979) to be a product of two terms:

(1) the proportion factor and

(2) the function f(.).

The proportion factor provides the probability that one object of a certain type is selected and the function f(.), gives the probability of finding X objects of the other type within the circle b(o,w). Thus

$$P\{ N[b(o,w)] = X \} = p_1 f(\lambda_2) + p_2 f(\lambda_1) \qquad (6.10)$$

where

$$f(c) = (c \pi w^2)^x \exp(- c \pi w^2) / x !$$

The probability that the circle b(o,w) contains no objects of the type different from the central object is given by

$$F(W > w) = P \{ N[b(o,w) = 0 \}$$

$$= p_1 \exp(-\lambda_2 \pi w^2) + p_2 \exp(-\lambda_1 \pi w^2)$$

Whence $F(w) = 1 - F(W > w)$, and differentiating F(w) with respect to w gives the probability density function of w as,

$$f(w) = \lambda_2 p_1 f (w, \lambda_2) + \lambda_1 p_2 f (w, \lambda_1) \qquad (6.11)$$

where

$$f (w, \lambda_k) = 2\pi w \exp(- \lambda_k \pi w^2)$$

Now

$$E (W) = \int_0^\infty w f(w) dw$$

$$= \sum_{k=1}^{2} \lambda_k \; p_{3-k} \int_0^{\infty} w \; f(w, \lambda_k) \, dw$$

$$= \sum_{k=1}^{2} p_{3-k} \; / \; 2\sqrt{\lambda_k} \qquad (6.12)$$

The result (6.12) is exact for an independent infinite two- type process but an approximation for a bounded region. If the value of the statistic

$$R_{\omega} = \bar{w} \; / \; \{ \sum_{k=1}^{2} p_{3-k} \; / \; 2\sqrt{\lambda_k} \; \} \qquad (6.13)$$

for the observed two-type patterns is less than 1, this would indicate positive dependence between the two patterns and a value of R_{ω} greater than unity will indicate repulsion between the two separate patterns. To test the significance of this departure, we used the conditional Monte Carlo approach with

$$L_{\omega} = | \; \bar{w} - E(W) \; | \qquad (6.14)$$

as a suitable statistic.

Table 6.6. The cumulative distribution of L_{ω} for the link-pairs process, based on 99 random toroidal shifts of the type 2 objects.

Value of L_{ω}	: 0.00047	0.00076	0.00175	0.00786
Freq > L_{ω}	: 99	98	95	60
Value of L_{ω}	: 0.01188	0.02583	0.02780	0.03079
Freq > L_{ω}	: 30	5	2	1

Applying the statistics R_ω and L_ω to our linked-pairs data of Figure 6.2a, we obtain $\bar{w} = 0.0343$ as the observed mean nearest neighbour distance. Using equation 6.13 this leads to $R_\omega = 0.4804$, which is less than 1, and hence implies a departure from independence towards positive dependence. The observed value of the statistic L_ω is 0.0372. To interpret this value, we shall require knowledge of its probability distribution under the null hypothesis of independence. This distribution is summarized in cumulative form in Table 6.6

The value for the two - type link pairs process, was the most extreme value calculated and is clearly significant.

6.6 Refined nearest-neighbour methods

In the univariate case, we considered the empirical distribution functions $\hat{G}(w)$ and $\hat{F}(x)$: the observed distribution functions of the object-to-object nearest neighbour distances and the point-to-object distances respectively. With two types of objects of intensities λ_1 and λ_2, we need to extend our notation from that used in Chapter Five.

We shall define the distribution functions $G_{ij}(w)$ and $F_{oj}(x)$ as,

$$G_{ij}(w) = P(\text{Circle of radius } w, \text{ centred on the arbitrary type } i \text{ object contains at least one type } j \text{ object}) \quad (6.15)$$

and

$$F_{oj}(x) = P(\text{Circle of radius } x, \text{ centred on an arbitrary point contains at least one type } j \text{ object}) \quad (6.16)$$

where $i = 1,2$, and $j = 3 - i$. Goodall (1965) observed that if the two types are stationary and isotropic and are distributed independently of one another, then whatever the type of distribution of the type j objects, it

Applying the statistics R_ω and L_ω to our linked-pairs data of Figure 6.2a, we obtain $\bar{w} = 0.0343$ as the observed mean nearest neighbour distance. Using equation 6.13 this leads to $R_\omega = 0.4804$, which is less than 1, and hence implies a departure from independence towards positive dependence. The observed value of the statistic L_ω is 0.0372. To interpret this value, we shall require knowledge of its probability distribution under the null hypothesis of independence. This distribution is summarized in cumulative form in Table 6.6

The value for the two - type link pairs process, was the most extreme value calculated and is clearly significant.

6.6 Refined nearest-neighbour methods

In the univariate case, we considered the empirical distribution functions $\hat{G}(w)$ and $\hat{F}(x)$: the observed distribution functions of the object-to-object nearest neighbour distances and the point-to-object distances respectively. With two types of objects of intensities λ_1 and λ_2, we need to extend our notation from that used in Chapter Five.

We shall define the distribution functions $G_{ij}(w)$ and $F_{oj}(x)$ as,

$$G_{ij}(w) = P(\text{Circle of radius } w, \text{ centred on the arbitrary type } i \text{ object contains at least one type } j \text{ object}) \quad (6.15)$$

and

$$F_{oj}(x) = P(\text{Circle of radius } x, \text{ centred on an arbitrary point contains at least one type } j \text{ object}) \quad (6.16)$$

where $i = 1,2$, and $j = 3 - i$. Goodall (1965) observed that if the two types are stationary and isotropic and are distributed independently of one another, then whatever the type of distribution of the type j objects, it

should appear just the same when viewed from arbitrary sampling points as when viewed from arbitrary objects of type i. This would imply that

$$F_{oj}(t) = G_{ij}(t) \qquad (6.17)$$

The relationship defined in (6.17) suggests using as test statistics, the quantities $H_1(t)$ and $H_2(t)$ defined by

$$H_j(t) = F_{oj}(t) - G_{ij}(t) \qquad (j=1, 2) \qquad (6.18)$$

For processes that display positive dependence the $G_{ij}(t)$ values would be much greater than would be expected for an independent pattern, whereas the $F_{oj}(t)$ values would be much smaller than would be expected. This will therefore imply a negative value of $H_j(t)$ for most t. For processes that display negative dependence, the converse is of course true. This would mean a positive value of $H_1(t)$ and $H_2(t)$ for most t.

Another function of interest, is the distribution function $F_o(t)$ defined as,

$F_o(t)$ = P(Circle of radius t, centred on an arbitrary point contains at least one object of type i or type j) (6.19)

This function $F_o(t)$ is the distribution function of the distance from an arbitrary point to the nearest object of unspecified type. The independence of the two types implies that,

$$[\ 1 - F_o(t)\ ] = [\ 1 - F_{oi}(t)\ ]\ [\ 1 - F_{oj}(t)\ ] \qquad (6.20)$$

Diggle (1983) suggests using the function $E_2(t)$ defined as,

$$E_2(t) = [\, 1 - F_o(t) \,] - \prod_{j=1}^{2} [\, 1 - F_{oj}(t) \,] \qquad (6.21)$$

as a measure of the near-neighbour dependence between the two types. A positive value of $E_2(t)$ indicates positive dependence in the sense that neighbouring type 1 and type 2 objects are, probabilistically speaking, closer together than in the case of independent patterns. Similarly a negative value of $E_2(t)$ indicates negative dependence or spatial avoidance between the two types. In order to test the independence hypothesis using the refined nearest-neighbour method, we can use any of the three summary statistics, $H_1(t)$, $H_2(t)$ or $E_2(t)$.

6.6.1 Estimators of $G_{ij}(t)$

Let (w_{ik}, b_{ik}), $k = 1, 2, \ldots, n_i$ denote the distances from each object of type i to the nearest object of type j in D and to the nearest point on the boundary of D. By analogy with Diggle's estimator given by (5.1), we have,

$$\hat{G}^1_{ij}(t) = \frac{\sum_{k=1}^{n_i} \sigma(w_{ik}, t)\, \sigma(t, b_{ik})}{\sum_{k=1}^{n_i} \sigma(t, b_{ik})} \qquad (6.22)$$

where $\sigma(y,z) = 1$ if $y \leq z$ and $\sigma(y,z) = 0$, otherwise. Similarly by analogy with Hansich's and the new estimator given by (5.6) and (5.14), we have:

$$\hat{G}^2_{ij}(t) = \frac{\sum_{k=1}^{n_i} \sigma(w_{ik}, t)\quad \sigma(w_{ik}, b_{ik})\, s(w_{ik})}{\sum_{k=1}^{n_i} \sigma(w_{ik}, b_{ik})\, s(w_{ik})} \qquad (6.23)$$

and

$$\hat{G}_{ij}^{3}(t) = \frac{\sum_{k=1}^{n_i} \{\sigma(w_{ik},t)+[1-\sigma(w_{ik},t)]\,[1-\sigma(t,b_{ik})]\,r_k(t)\}}{n_i} \qquad (6.24)$$

where

$$s(t) = [(a-2t)(b-2t)]^{-1}$$

$$r_k(t) = 1 - \exp\{-\lambda_j A(t)\}$$

and A(t) is given in (5.8). Note however that both $\hat{G}_{ij}^{1}(t)$ and $\hat{G}_{ij}^{2}(t)$ are not defined whenever

$$\sum_{k=1}^{n_i} \sigma(t, b_{ik}) = 0$$

and

$$\sum_{k=1}^{n_i} \sigma(w_{ik}, b_{ik}) = 0$$

6.6.2 Estimators of $F_{oj}(t)$

To estimate $F_{oj}(t)$, let (x_{jk}, e_{jk}), j=1, 2 and k = 1, 2,...., n_i,where i = 3-j denote the distances from each of the n_i sample points to the nearest object of type j in D and to the nearest point on the boundary of D. By analogy with Ripley's , Hanisch's and the new estimators defined in equations (5.15), (5.16) and (5.17) we have,

$$\hat{F}_{oj}^{1}(t) = \frac{\sum_{k=1}^{n_i} \sigma(x_{jk},t)\,\sigma(t,e_{jk})}{\sum_{k=1}^{n_i} \sigma(t,e_{jk})} \qquad (6.25)$$

$$\hat{F}_{oj}^{2}(t) = \frac{\sum_{k=1}^{n_i} \sigma(x_{jk},t)\ \sigma(x_{jk},e_{jk})\ s(x_{jk})}{\sum_{k=1}^{n_i} \sigma(x_{jk},e_{jk})\ s(x_{jk})} \qquad (6.26)$$

$$\hat{F}_{oj}^{3}(t) = \frac{\sum_{k=1}^{n_i} \{\sigma(x_{jk},t) - [1-\sigma(x_{jk},t)][1-\sigma(t,e_{jk})]\ r_k(t)\}}{n_i} \qquad (6.27)$$

respectively. Note also that $\hat{F}_{oj}^{1}(t)$ and $\hat{F}_{oj}^{2}(t)$ are not defined for values of t, for which,

$$\sum_{k=1}^{n_i} \sigma(t, e_{jk}) = 0$$

and

$$\sum_{k=1}^{n_i} \sigma(x_{jk},e_{jk}) = 0$$

6.6.3 Estimators of $F_o(t)$

To estimate $F_o(t)$, let (x_k, e_k) denote the distances from each of m sample points to the nearest object of unspecified type in D and to the nearest point on the boundary of D. Then the estimators of $F_o(t)$, namely $\hat{F}_o^{1}(t)$, $\hat{F}_o^{2}(t)$ and $\hat{F}_o^{3}(t)$ corresponding to Ripley's, Hanisch's and the new estimator are as given in (5.15), (5.16) and (5.17) respectively. However, the intensity λ in r(t) is replaced by $\lambda_1+\lambda_2$ for the case of the new estimator.

In order to use the function $E_2(t)$ defined in equation (6.21), the functions $F_{oj}(t)$, j = 1, 2, should be estimated from the same point locations used in the estimation of $F_o(t)$. We therefore replace n_i in

(6.25), (6.26) and (6.27) by m, and the values of $\{x_k\}$ corresponding to $F_o(t)$ are easily obtained using the relation

$$x_k = \text{Min}\ (\ x_{ik}\ ,\ x_{jk}\ ),\quad i \neq j$$

where x_{zk} is the distance between the k^{th} sampling point and the nearest object of type z (z =1 ,2) in D.

6.6.4 Graphical analysis

To assess the significance or otherwise of departures from the null hypothesis of independence, the conventional approach would be to find the sampling distributions of

$$H_j^m(t) = \hat{F}_{oj}^m(t) - \hat{G}_{ij}^m(t)$$

and

$$E_2^m(t) = [\ 1 - \hat{F}_o^m(t)\ ] - \prod_{j=1}^{2} [\ 1 - \hat{F}_{oj}^m(t)\ ]$$

where j = 1, 2; i = 3-j and m = 1, 2, 3, under the null hypothesis of independence.

We calculate the $H_j^m(t)$, r = 2,..,s from each of s-1 independent random toroidal shifts of the type j objects in the region D, and define the upper and lower envelope,

$$U_j^m(t) = \underset{2\leq r\leq s}{\text{Max}}\ \{\ H_{j(r)}^m(t)\ \}$$

$$L_j^m(t) = \underset{2\leq r\leq s}{\text{Min}}\ \{\ H_{j(r)}^m(t)\ \}$$

The stationarity and independence of the patterns imply that for each t,

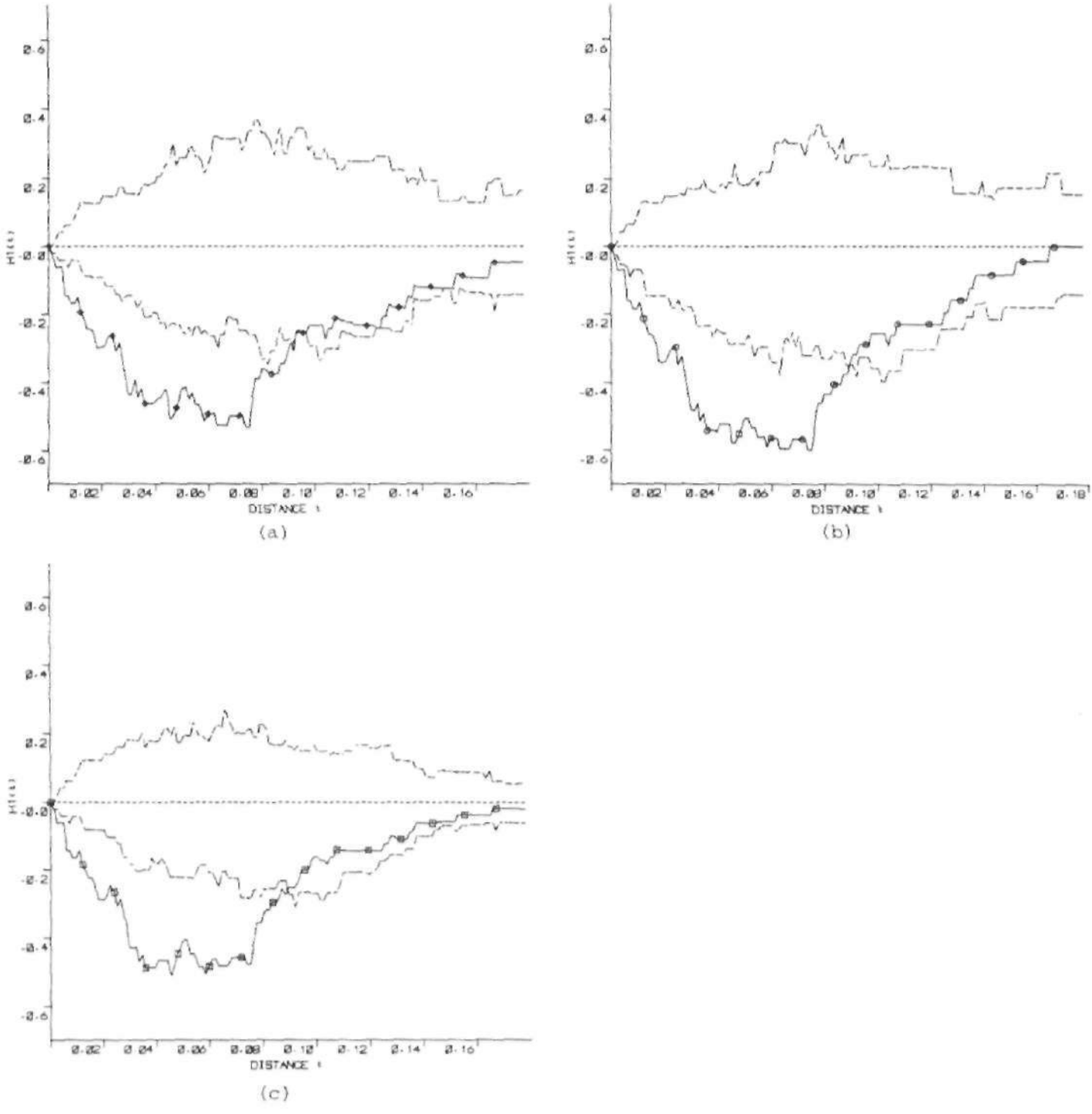


Figure 6.3 : Comparisons of $\hat{H}_1(t)$ (solid line) for the linked pairs process, with the envelope (dashed lines) formed using 99 toroidal shifts.

Key: (a) $\hat{H}_1^{\,1}(t)$; $\hat{H}_1^{\,2}(t)$; $\hat{H}_1^{\,3}(t)$

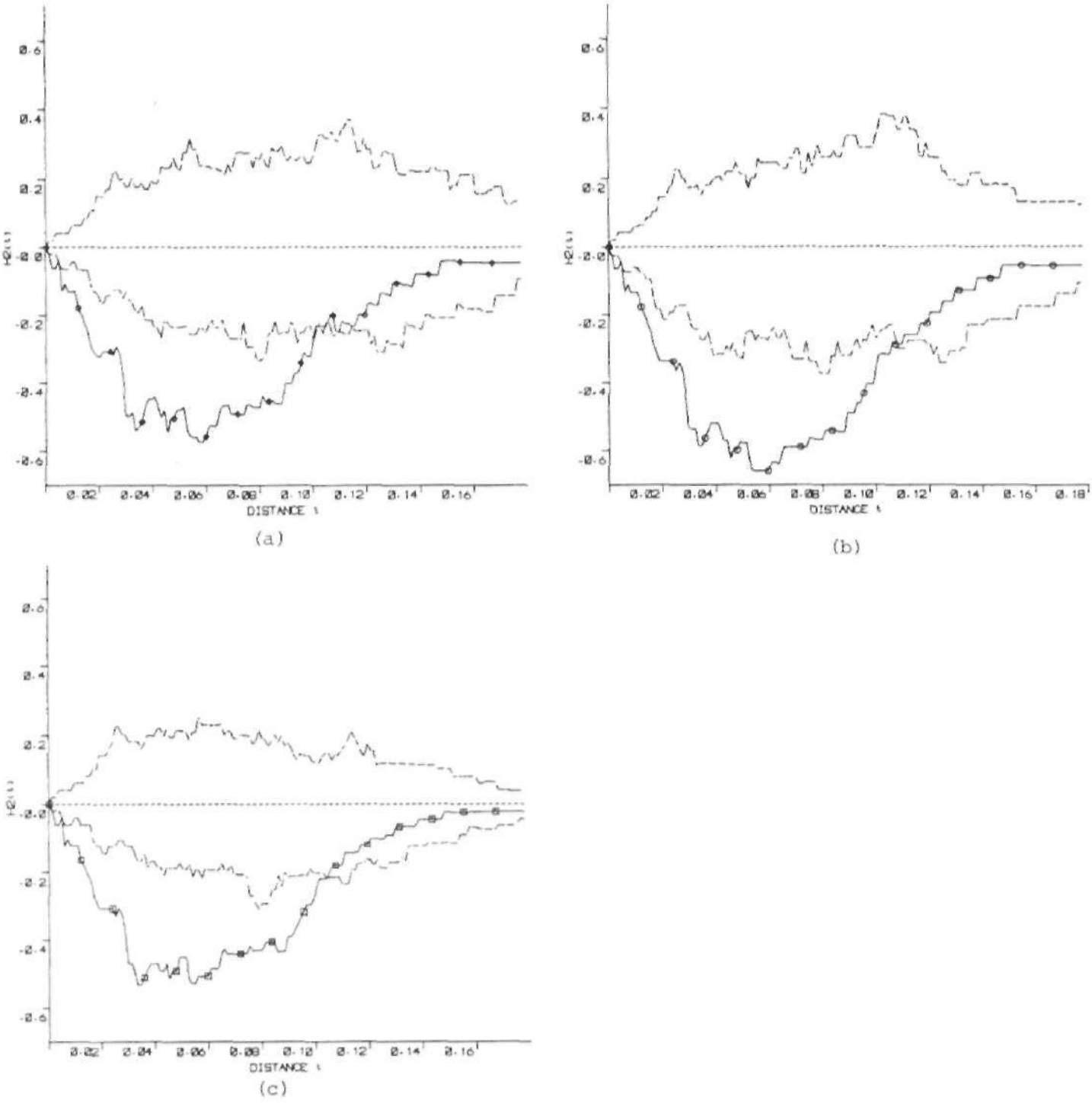


Figure 6.4 : Comparison of $\hat{H}_2(t)$ (solid line) for the linked pairs process, with the envelope (dashed line) formed using 99 toroidal shifts.

Key: (a) —◇—◇— $\hat{H}_2^{\,1}(t)$; —○—○— $\hat{H}_2^{\,2}(t)$; —□—□— $\hat{H}_2^{\,3}(t)$

$$P\{ H_{j(1)}^{m}(t) > U_j^{m}(t) \} = P\{ H_{j(1)}^{m}(t) < L_j^{m}(t) \} = 1/s$$

These envelopes are intended to help in the interpretation of the plot of $H_{j(1)}^{m}(t)$ against t. Similarly the same method can be used to obtain the envelopes for $E_2^{m}(t)$.

We illustrate the techniques described in this Section, with an artificial realization of a linked-pairs process with 49 objects of either type in a unit square window. This realisation is given in Figure 6.2a. The graph of $H_1(t)$ against t, together with the envelope formed from 99 simulations derived using toroidal shifts is presented in Figure 6.3. This graph suggests that there is a significant attraction for distances of less than 0.1 units. Similarly the graph of $H_2(t)$ against t with the envelope formed from 99 simulations derived using toroidal shift is illustrated in Figure 6.4. The same conclusion is arrived at using the $H_2(t)$ statistic. Note that the simulation envelopes for $H_j^{3}(t)$ is much narrower than those for $H_j^{2}(t)$ and $H_j^{1}(t)$, suggesting that the former is less variable.

Figure 6.5 shows the graph of $E_2(t)$ against t with the envelope formed from 99 simulations derived using independent random toroidal shifts of the type 2 objects. The values of $E_2(t)$ for the linked-pairs process is greater than zero for all values of t considered. However significance departure from the independence hypothesis occurs for values of t between 0.05 to about 0.12 units.

The use of the statistics $H_1(t)$, $H_2(t)$ and $E_2(t)$ in the analysis of the link pairs process led to the rejection of the independent hypothesis in favour of positive dependence between the two type patterns.

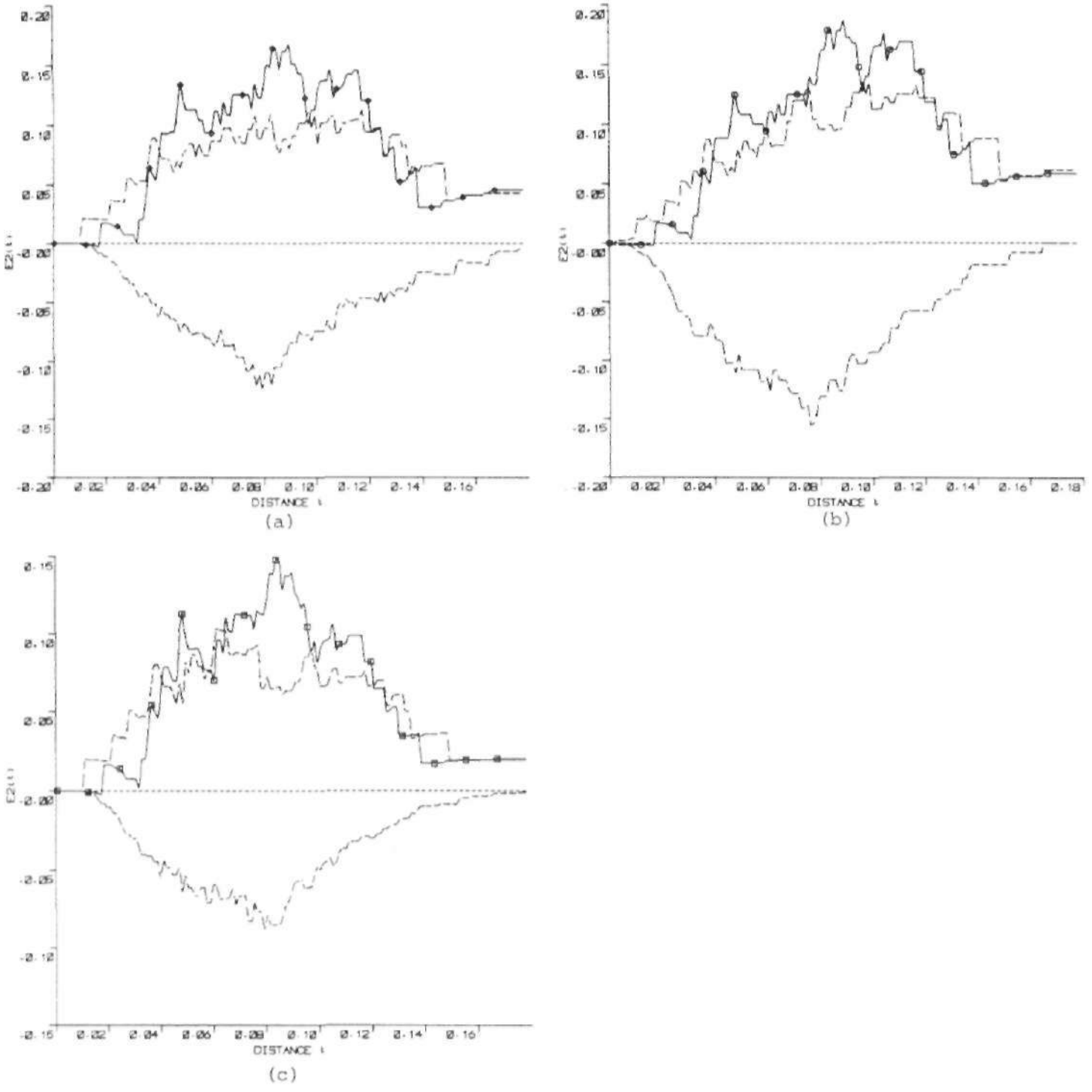


Figure 6.5 : Comparison of $\hat{E}_2(t)$ for the linked pairs process, with the envelope formed using 99 random toroidal shifts.

Key: (a) $\hat{E}_2^{\,1}(t)$; $\hat{E}_2^{\,2}(t)$; $\hat{E}_2^{\,3}(t)$.

6.7 The second order methods

Second order methods for the analysis of point processes have been considered in Chapter IV. In this section we shall extend the methods to multitype spatial point patterns.

Given a multitype pattern of k types of objects which is stationary under rigid motions of the plane, let λ_j, for j = 1, 2, ..., k be the intensity of the objects of type j. Then a natural extension of the K(t) function suggested by Hanisch and Stoyan (1979) is obtained as,

$$\lambda_j K_{ij}(t) = E \{ \text{number of objects of type j within distance t of an arbitrary object of type i} \} \qquad (6.28)$$

For the two-type process, however, i=1, 2; j = 3-i. The individual point processes are characterised by the functions $K_{ii}(t)$ and $K_{jj}(t)$ defined by

$$\lambda_i K_{ii}(t) = E \{ \text{number of other type i objects within distance t of an arbitrary type i object} \} \qquad (6.29)$$

If objects of type j with intensity λ_j are placed at random with respect to objects of type i, then the expected number of objects of type j lying within a distance t of an object of type i is $\lambda_j \pi t^2$ and so if the two processes are independent, we shall have,

$$K_{ij}(t) = \pi t^2 \qquad (6.30)$$

with

$$L_{ij}(t) = t - \{ K_{ij}(t)/\pi \}^{\frac{1}{2}} \qquad (6.31)$$

A large positive value of $L_{ij}(t)$ will indicate negative dependence or repulsion between the two processes at a value of t, whereas a large negative value is an indication of positive dependence or attraction

between the two processes. The individual object processes may be classified as regular, random or clustered depending upon the numerical value of $L_{ii}(t)$.

6.7.1 The estimators of $K_{ij}(t)$ and $K_{ji}(t)$

The theoretical values of $K_{ij}(t)$ and $K_{ji}(t)$ are identical but in practice the realised values of their separate estimators may differ. Suppose that the region D contains N_i objects of type i, of which $N_i(t)$ lie outside the 'null region' corresponding to the distance t, with a corresponding notation for the numbers of the type j objects.

Assuming that the various object intensities will require estimation, we have by analogy with Ripley's estimator defined in (4.9):

$$\tilde{K}_{ij}^{3}(t) = \frac{A \sum_{k=1}^{N_i} \sum_{\ell=1}^{N_j} 1_{k\ell} S_{k\ell}}{N_i \quad N_j} \qquad (6.32)$$

where $1_{k\ell} = 0$ if the distance from the k^{th} object of type i to the ℓ^{th} object of type j is more than t and equals unity, otherwise and $S_{k\ell}$ is defined by,

$$S_{k\ell}^{-1} = \text{The proportion of the perimeter of the circle centred on object } x_k \text{ of type i and passing through object } x_\ell \text{ of type j that lies within D)} \qquad (6.33)$$

By analogy with Ohser's estimator given by (4.11):

$$\tilde{K}_{ij}^{4}(t) = \frac{A \sum_{k}^{N_i(t)} \sum_{\ell}^{N_j} 1_{k\ell} S_{k\ell}}{N_i(t) \; N_j} \qquad (6.34)$$

where $S_{k\ell}$ is defined in (6.33). Similarly from Stoyan and Ohser's estimator defined in (4.16) :

$$\tilde{K}_{ij}^{5}(t) = \frac{A \sum_{k}^{N_i} \sum_{\ell}^{N_j} 1_{k\ell} S_{k\ell}}{N_i \; N_j} \qquad (6.35)$$

where

$$S_{k\ell}^{-1} = \gamma_D(r_{k\ell}) / A \qquad (6.36)$$

and $r_{k\ell}$ is the distance between the k^{th} object of type i and the ℓ^{th} object of type j. For a rectangular sampling window $\gamma_D(r)$ is defined in (4.14).

By analogy with the Vere-Jones estimator, $\hat{K}_6(t)$ and the new estimator, $\hat{K}_7(t)$ defined in (4.19) and (4.21) we have:

$$\tilde{K}_{ij}^{6}(t) = \frac{A \sum_{k}^{N_i} \sum_{\ell}^{N_j} 1_{k\ell}}{N_j \sum_{k=1}^{N_i} \{ r_k(t) \}^{-1}} \qquad (6.37)$$

and

$$\tilde{K}_{ij}^{7}(t) = \frac{A \sum_{k}^{N_i(t)} \sum_{\ell}^{N_j} 1_{k\ell}\, r_k(t)}{N_i(t)\ N_j} \qquad (6.38)$$

respectively. The weight function $r_k(t)$ is defined by

$\{r_k(t)\}^{-1}$ = The proportion of the area of the circle centred on object x_k of type i and radius t that lies within the sampling window D (6.39)

An optimal estimate of the common value of $K_{ij}(t)$ and $K_{ji}(t)$ is given by Lotwick and Silverman (1982) as,

$$\hat{K}_{ij}^{m}(t) = \frac{N_j\, \tilde{K}_{ij}^{m}(t) + N_i\, \tilde{K}_{ji}^{m}(t)}{N_i + N_j} \qquad (6.40)$$

and

$$\hat{K}_{ij}^{n}(t) = \frac{N_j(t)\, \tilde{K}_{ij}^{n}(t) + N_i(t)\ \tilde{K}_{ji}^{n}(t)}{N_i(t) + N_j(t)} \qquad (6.41)$$

where m = 3, 5 and 6, and n = 4 and 7.

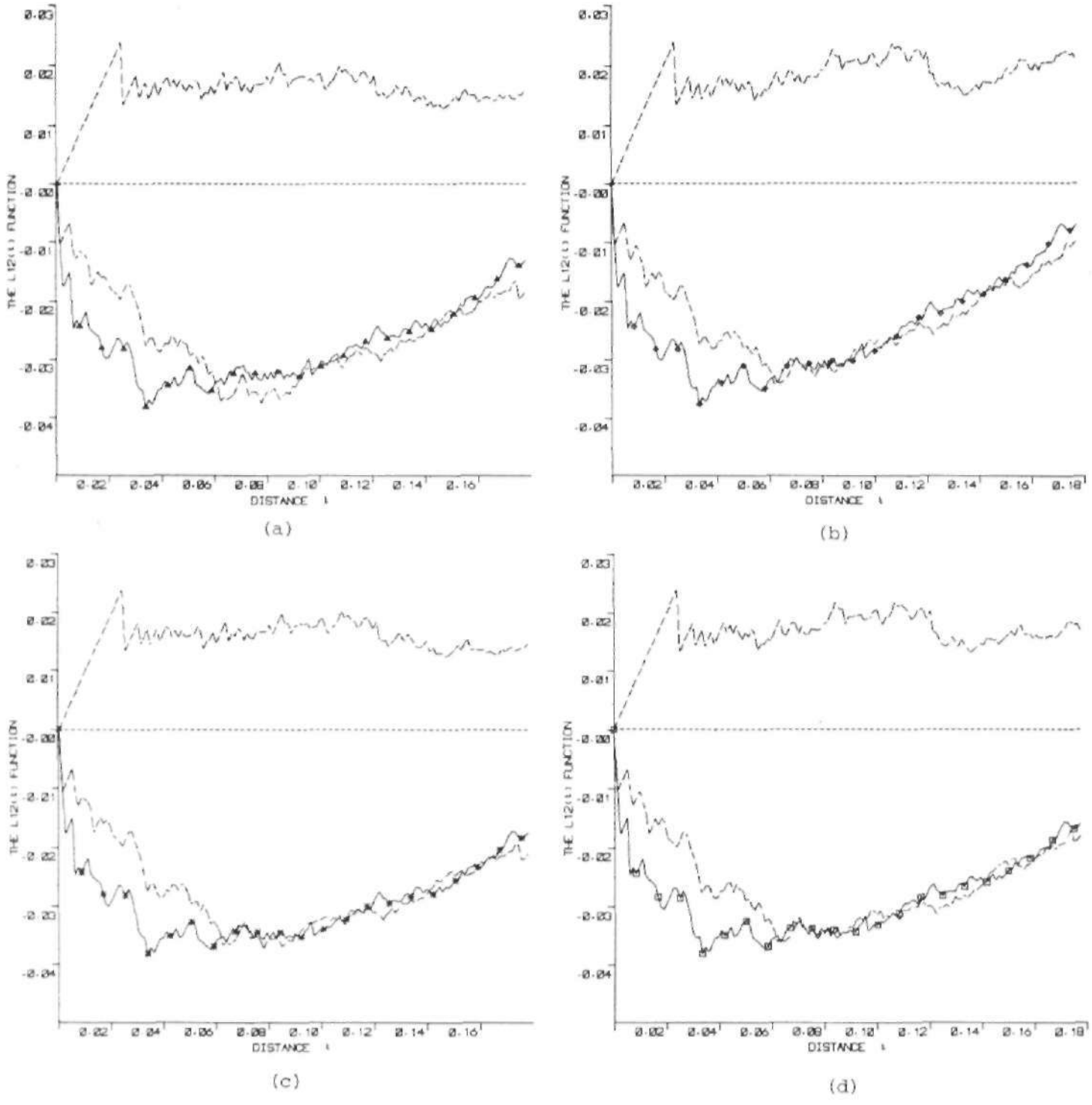


Figure 6.6 : Comparison of $\hat{L}_{12}(t)$ functions for the linked-pairs process, with the envelopes formed using 99 toroidal shifts.

Key: (a) $\hat{K}_{12}^{3}(t)$, (b) $\hat{K}_{12}^{5}(t)$, (c) $\hat{K}_{12}^{7}(t)$, (d) $\hat{K}_{12}^{6}(t)$.

6.7.2 Graphical analysis

To assess the significance of any departure from the independence hypthesis, the usual approach would be to find the sampling distribution of $\hat{L}_{ij}(t)$ defined in (6.28) under the independence hypothesis. We calculate the $\hat{L}_{ij}(t)$, from each of s-1 independent random toroidal shifts of the type j objects and define the upper and lower simulation envelopes:

$$\hat{U}(t) = \max_{\text{all } s-1} \{ \hat{L}_{ij}(t) \}$$

$$\hat{L}(t) = \min_{\text{all } s-1} \{ \hat{L}_{ij}(t) \}$$

The stationarity and independence of the patterns imply that, for each t

$$P\{ \hat{L}_{ij}(t) > \hat{U}(t) \} = P\{ \hat{L}_{ij}(t) < \hat{L}(t) \} = 1/s.$$

To test the effectiveness of the various estimators of $K_{ij}(t)$, we have considered the linked-pairs process with 49 objects of either type in a unit square. A partial realisation of this process is presented in Figure 6.2a.

Figure 6.6 shows the plots of the interaction statistic $\hat{L}_{12}(t)$ for the linked-pairs process, together with the envelopes formed from 99 simulations derived using toroidal shifts, for the various estimators of $K_{12}(t)$. In this Figure, the $\hat{L}_{12}(t)$ functions were calculated at each of 150 equi-spaced values of t between 0.0 and $1.25/\sqrt{\lambda_1}$. The plots obtained using the various estimators of $K_{12}(t)$ (Figure 6.6) are almost identical and show positive dependence at short ranges ($t < 0.06$) very clearly.

CHAPTER VII

Summary and Conclusions

The average point-object nearest neighbour distance, $\bar{X}$, is defined for a set of objects, to be the mean of the distances from each of the m regular grid points to the nearest object of the process. Simulations were performed of n random objects in various circular, square and rectangular regions of the plane. It was found that both the mean and variance of $\bar{X}$ could be corrected for edge-effects and these corrections resulted in the point object analogue of the Clark-Evans statistic, M, being approximately normally distributed with mean zero and unit variance.

A comparative study was performed, using the edge-corrected statistic M, the edge-corrected Clark-Evans statistic CE and some other statistics, which inevitably take about the same degree of effort to perform. The results of the power study suggests that the statistic M is a powerful detector of departures from randomness in the clustered direction.

Ripley (1976,1977) introduced a cumulative function K(t), that combines some of the advantages of quadrat counting methods with those of distance based measures. Alternative estimation procedures for K(t) as well as a new estimation procedure were considered. The bias and the mse of the various estimators were estimated from simulated realizations of three different processes: the Poisson process, the Poisson cluster process and the Matern static inhibition process, representing a random, a clustered and a regular pattern respectively.

The bias and mse of the various estimators of L(t) were evaluated for small values of t, since the useful information contained in $\hat{L}(t)$, however calculated is confined to these values of t.

The mse of the various estimators of L(t), suggest that the Ohser-Stoyan estimator is inferior to Ripley's estimator, Vere-Jones estimator and the new estimator for most values of t, and that for all values of t considered, the new estimator was marginally preferable, for all the three different processes considered.

As expected all the four estimators were almost unbiased for the Poisson process and it was obvious that the major contribution to the mse comes from the variance of the estimators. For the non-random processes however, the bias of the new estimator was very similar to the Vere-Jones estimator, but was marginally preferable to it. Both the new estimator and the Vere-Jones estimator outperformed the Ohser-Stoyan estimator. The Ripley estimator displayed an unexpected behaviour, performing well for the Matern static process, but very poorly for the Poisson cluster process. Repeated simulations, varying the parameters of these processes produced very similar results.

The relatively poor performance of the Ohser-Stoyan estimator reflects the fact that it does not rely on the assumption of isotropy, but was in this thesis, applied to isotropic processes. However, it is still the only estimator available in the case of anisotropic processes.

For stationary and isotropic processes, one does not know whether a process is regular, clustered or random. Therefore, one needs a dependable estimator and the results presented in this thesis, suggested that, at least for small distances and with moderate numbers of objects the new estimator is preferable to the existing estimators.

Four different patterns were analysed using the new estimator, and all, but the cellular process, were differentiated from the Poisson process. Thus the $\hat{L}(t)$ function was unable to distinguish the differences between the cellular process and the Poisson process. This was because both processes have identical second order properties. In view of this, Getis and Franklin (1987) introduced the second order neighbourhood function $S_i(t)$ that could be used to provide information as to the pattern membership characteristics of a given object i. Furthermore, the $S_i(t)$ function could be used to produce maps of pattern density at a given scale. However, the $S_i(t)$ function could still not be used for testing whether the mapped pattern is consistent with the hypothesis of a Poisson process.

Variants of the $S_i(t)$ function were introduced for such a purpose. These variants were able to distinguish those processes that have identical second order properties as the Poisson process. A power study was performed using various tests originating from the inter-object distances. A new test statistic g was introduced. This statistic was found to be a powerful detector of departures from randomness towards regular alternatives.

Roder(1975) and Diggle(1979) introduced the cumulative distribution function G(w) of the distance from an arbitrary object and its nearest neighbour. Ripley(1977) suggested considering the analogous distribution F(x) for point-nearest-object distances. These two functions provide tests of randomness and serve as additional summary descriptions for spatial point processes.

Various estimation procedures have been proposed for estimating G(w) and F(x). A new estimation procedure was proposed for estimating G(w) and F(x). The new estimation method makes more complete use of the information available, especially for small and moderate sample sizes. In order to estimate the errors associated with the various estimation procedures, we

have used a small sample size of $n = 20$ objects, and $m = 25$ sampling points. Simulations were performed of the Poisson process, the Matern cluster process and the Diggle superimposed lattice process, representing a random, a clustered and a regular pattern respectively. As with the $K(t)$ function, these processes were chosen because the theoretical values of $G(w)$ and $F(x)$ could easily be evaluated. The bias and mse were estimated from these simulated realizations. The results of our simulations showed a dramatic reduction of the mse associated with the new estimation procedure, to about one half of that of the existing alternatives. All the estimators of $G(w)$ were negligibly biased for all the three processes considered, whereas the Hanisch analogue for $F(x)$ was clearly biased for the various alternative processes considered.

Most of our estimation procedures, in particuler those of $K(t)$, $G(w)$ and $F(x)$ functions were extended to multitype patterns for testing the independence hypothesis. A simulated link-pairs process data was analysed using the various procedures.

REFERENCES

1 Baddeley, A.J. and Silverman, B.W.(1984). A cautionary example on the use of second order methods for analysing point patterns. Biometrics 40, 1089-1093.

2 Barnard, G.A.(1963). Contribution to the discussion of Professor Bartlett's paper. Journal of the Royal Statistical Society, B25, 294.

3 Bartlett, M.S.(1964). The spectral analysis of two-dimensional point processes. Biometrika 51, 299-311.

4 Bartlett, M.S.(1975). The Statistical Analysis of Spatial Pattern. Chapman and Hall, London.

5 Besag, J. and Diggle, P.J.(1977). Simple Monte Carlo tests for Spatial pattern. Applied Statistics 26, 327-333.

6 Brown, D.(1975). A test of randomness of nest spacing. Wildfowl 26, 102-103.

7 Brown, D. and Rothery, P.(1978). Randomness and local regularity of points in a plane. Biometrika 65, 115-122.

8 Clapham, A.R.(1936). Over-dispersion in grassland communities and the use of statistical methods in plant ecology. Journal of Ecology, 24, 232-251.

9 Clark, P.J. and Evans, F.C.(1954). Distance to nearest neighbour as a measure of Spatial relationship in populations. Ecology 35, 445-453.

10 De Vos, S.(1973). The use of nearest neighbour methods. Tijdschrift voor Economische en Sociale Geografie 64, 307-319.

11 Dice, L.R.(1952). Measuring of Spacing between individuals within a population. Contrib. Lab. Vert. Biol. Univ. Mich, 55, 1-23.

12 Diggle, P.J.(1975). Robust density estimation using distance methods. Biometrika 62, 39-48.

13 Diggle, P.J.(1979a). On parameter estimation and goodness-of-fit testing for spatial point patterns. Biometrics 35, 87-101.

14 Diggle, P.J.(1979b). Statistical methods for Spatial point patterns in ecology. In Spatial and Temporal Analysis in Ecology(R.M. Cormack and J.K. Ords, eds). Finland: International Co-operative Publishing House, pp 95-150.

15 Diggle, P.J.(1983). Statistical Analysis of Spatial point Patterns. Academic Press: London.

16 Diggle,P.J., Besag, J. and Gleaves, J.T.(1976). Statistical analysis of spatial point patterns by means of distance methods. Biometrics, 32, 659-667.

17 Diggle, P.J. and Cox, T.F.(1983). Some distance based tests of independence for sparsely-sampled multivariate spatial point patterns. International Statistical Review, 51, 11-23.

18 Diggle, P.J. and Milne, R.K.(1983). Bivariate Cox processes: Some models for bivariate spatial point patterns. Journal of the Royal Statistical Society, B 45, 11-21.

19 Doguwa, S.I. and Upton, G.J.G.(1988a). On edge corrections for the mean and variance of the point-event analogue of the Clark-Evans statistic. To appear in Biometrical Journal.

20 Doguwa, S.I. and Upton, G.J.G.(1988b). Simulations to determine the mean and variance of the point-object analogue of the Clark-Evans statistic. To appear in Biometrical Journal.

21 Doguwa, S.I. and Upton, G.J.G.(1988c). Edge-corrected estimators for the reduced second moment measure of point processes. To appear in Biometrical Journal

22 Doguwa, S.I.(1988). On second-order neighbourhood analysis of mapped point patterns. To appear in Biometrical Journal.

23 Donnelly, K.P.(1978). Simulations to determine the variance and edge effects of total nearest neighbour distance. In Simulation methods in Archaeology. I. Hodder, Ed. Cambridge University Press, London.

24 Eberhardt, L.L.(1967). Some developments in "distance sampling". Biometrics 23, 207-216.

25 Fisher, R.A; Thornton, H.G and Mackenzie, W.A.(1922). The accuracy of the plating method of estimating the density of bacterial populations with particular reference to the use of Thornton's agar medium with soil samples. Annals of Applied Biology 9, 325-359.

26 Getis, A. and Franklin, J.(1987). Second order neighbourhood analysis of mapped point patterns. Ecology 68, 473-477.

27 Goodall, D.W.(1965). Plot-less tests of inter-specific association. Journal of Ecology 53, 197-210.

28 Greig-Smith, P.(1952). The use of random and contiguous quadrats in the study of the structure of plant communities. Annals of Botany 16, 293-316.

29 Hanisch, K.H. and Stoyan, D.(1979). Formulas for the second-order analysis of marked point processes. Mathematische Operationsforschung und Statistik; Series Statistics 10, 555-560.

30 Hanisch, K.H.(1984). Some remarks on the estimation of the distribution of the nearest neighbour distance in stationary spatial point patterns. Mathematische Operationsforschung und Statistik; Series Statistics 15, 409-412.

31 Hermans, M; Rasson, J.P; and Weverbergh D. (1987). Some new tests of randomness for Point patterns. To appear in the Journal of the American Statistical Association.

32 Hoel, P.G.(1943). On indices of dispersion. Annals of Mathematical Statistics 14, 155-162.

33 Hope, A.C.A.(1968). A simplified Monte Carlo Significance test procedure. Journal of the Royal Statistical Society B 30, 582-598.

34 Isham, V.(1984). Multitype Markov point processes: Some approximations. Procedings of the Royal Society of London A 391, 39-53.

35 Jolivet, E.(1978). Caracterisation et test du caractere agregatif des processus ponctuels stationnaires sur R^2. Lecture notes in Mathematics. 636, 1-25.

36 Kelly, F.P. and Ripley, B.D.(1976). A note on Strauss's model for clustering. Biometrika 63, 357-360.

37 Kathirgamatamby, N.(1953). Note on the Poisson index of dispersion. Biometrika 40, 225-228.

38 Keuls, M., Over, H.J., and de Wit, C.T.(1963). The distance method for estimating densities. Statistica Neerlandica. 17, 71-91.

39 Lee, Y.(1979). A nearest neighbour spatial association measure for the analysis of firm interdependence. Environment and Planning, Series A 11, 169-176.

40 Liebetrau, A.M.(1977). Tests for randomness in two dimensions. Communications in Statistics, Theory and Methods, Series A 6, 1367-1383.

41 Liebetrau, A.M. and Rothman, E.D.(1977). A classification of spatial distributions based upon several cell sizes. Geographical Analysis 9, 14-28.

42 Lotwick, H.W. and Silverman, B.W.(1982). Methods of analysing spatial processes of several types of points. Journal of the Royal Statistical Society. Series B 44, 406-413.

43 Marriott, F.H.C.(1979). Monte Carlo tests: how many simulations ? Applied Statistics 28, 75-77.

44 Matern, B.(1960). Spatial Variation. Meddelanden Statens fran Skogsforsknigsinstutut Stockolm. 49, 1-144.

45 Matern, B.(1971). Doubly stochastic Poisson process in the plane, pp 195-213 in Statistical Ecology (Patil, G.P., Pielou, E.C., and Waters, W.E,. Eds). Vol 1 Pennsylvania State University Press: College Town, Pennsylvania.

46 Mead, R.(1974). A test for spatial pattern at several scales using data from a grid of contiguous quadrats. Biometrics 30, 295-307.

47 Morisita, M.(1959). Measuring of the dispersion and analysis of distribution patterns. Memoires of the Faculty of Science. Kyushu University, Series E, Biology 2, 215-235.

48 Neyman, J. and Scott, E.L.(1952). A theory of the Spatial distribution of the galaxies. Astrophysics Journal 116, 144-163.

49 Neyman, J. and Scott, E.L.(1958). Statistical approach to problems of cosmology. Journal of the Royal Statistical Society, Series B20, 1-43.

50 Numata, M.(1961). Forest vegetation in the vicinity of Choshi, Coastal flora and vegetation at Choshi, Chiba Prefecture IV. Bulletin of the Choshi Marine Laboratory, Chiba University 3, 28-48.

51 Ohser, J.(1983). On estimators for the reduced second moment measure of point processes. Mathematische Operationsforschung und Statistik; Series Statistics 14, 63-71.

52 Ohser, J. and Stoyan, D.(1981). On the second order and orientation analysis of planar stationary point processes. Biometrical Journal 23, 522-533.

53 Ohser, J., Stoyan, D. and Ripley, B.D.(1985). On the efficiency of edge correction for spatial point processes.

54 Payandeh, B.(1970). Comparison of methods for assessing spatial distributions of trees. Forestry Sciences 16, 312-317.

55 Penttinen, A.(1984). Modelling Interactions in Spatial Point Patterns: Parameter Estimation by the Maximum Likelihood Method, in Jyvaskyla, Finland: University of Jyvaskyla.

56 Perry, J.N. and Mead, R.(1979). On the power of the dispersion test to detect spatial pattern. Biometrics 35, 613-622.

57 Ripley, B.D. and Kelly, F.P.(1977). Markov point processes. Journal of the London Mathematical Society 15, 188-192.

58 Ripley, B.D. and Silverman, B.W.(1978). Quick test for spatial regularity. Biometrika 65, 641-642.

59 Ripley, B.D.(1976). The second-order analysis of stationary point process. Journal of Applied Probability, 13, 255-266.

60 Ripley, B.D.(1977). Modelling spatial patterns (with discussion). Journal of the Royal Statistical Society B 39, 172-212.

61 Ripley, B.D.(1979b). Simulating spatial patterns: Dependent samples from a multivariate density. Applied statistics 28, 109-112.

62 Ripley, B.D.(1979a). Tests of "randomness" for spatial point patterns. Journal of the Royal Statistical Society B41, 368-374.

63 Ripley, B.D.(1981). Spatial Statistics, Wiley: New York.

64 Ripley, B.D.(1982). Edge effects in Spatial point processes. In Statistics in Theory and Practice: Essays in Honour of Bertil Matern ed. B. Ranneby, Swedish University of Agricultural Sciences, 247-262.

65 Roder, W.(1975). A procedure for assessing point patterns without reference to area or density. The Professional Geographer 27, 432-440.

66 Silverman, B.W. and Brown, T.(1978). Short distances, flat triangles and Piosson limits. Journal of Applied Probability 15, 815-825.

67 Upton, G.J.G.(1984). On Mead's test for pattern. Biometrics 40, 759-766.

68 Upton, G.J. and Fingleton, B.(1985). Spatial Data Analysis by Example. Volume 1: Point pattern and Quantitative Data. Chichester: Wiley.

69 Vere-Jones, D.(1978). Space time correlations for microearthquackes - A pilot study. Supplement Advances in Applied Probability. 10, 73-87.

70 Warren, W.G.(1971). The center-satellite concept as a basis for ecological sampling, in Statistical Ecology (Patil, G.P., Pielou, E.C., and Walters, W.E., Eds) Vol 2. Pennsylvania State University Press: College Town, Pennsylvania.